



Chemistry and Biology Studies on Anti-inflammatory Bile Acid Derivatives

A thesis submitted to the University of Dublin, Trinity College Dublin
for the degree of Master by Research in Pharmaceutical Sciences

By

Su Liu, B.Sc.

Under the supervision of Professor John Gilmer, PhD

School of Pharmacy and Pharmaceutical Sciences

Trinity College Dublin

March 2019

Declaration

I confirm that this submission that I submit to Trinity College Dublin is as a result of my original research. This dissertation has not been submitted by anyone for obtaining credit or degree. To the best of my knowledge, I ensure that my work dose not breach the Irish Copyright Legislation and all the publish and unpublished work was taken from others has been cited in the thesis. Besides, I would like to deposit this dissertation in the University Open Access Institutional Repository.

Su Liu

March, 2019

Abstract

The objective of the dissertation is to clarify the potency, cytotoxicity and metabolism of novel steroidal anti-inflammatory compounds in the treatment inflammatory bowel disease (IBD). Biochemical methods with the purpose of understanding the relationship among chemical structure, potency and adverse effects.

In the first chapter, there is a discussion in relation to bile acids (BAs) structure, function, metabolism and their effect on maintaining health in general circumstances and their role in causing enterohepatic disease under pathological conditions. In chapter two, there is a discussion on the physiology and diseases of colon and the potential role of bile acids in colorectal disease. This chapter also presents some studies into the effect of some endogenous BAs on cell death and on cytoprotection in the intestinal epithelial cell line Caco-2.

The third Chapter reviews the medicinal chemistry and biological activities of ursodeoxycholic acid (UDCA). This Chapter describes the design and synthesis of novel UDCA derivatives including an amide, a triazole and a sulfonamide. The anti-inflammatory effect of these derivatives and their ability to activate the glucocorticoid receptor (GR) were examined in order to find a structural prototype with better potency/efficacy. The cytotoxicity in liver and colon cells of these compounds was also assessed in order to find a derivative with cell protection ability. Their evaluation in different cells reveals different levels of activity especially on NF- κ B activity and the related secretion of proinflammatory cytokines IL-6 and IL-8.

Acknowledgements

I would like to express my sincere gratitude to my supervisor Professor John Gilmer for giving me a chance to work on this project and providing the support and guidance throughout my Master study and research. His patience, enthusiasm and loyalty motivated me whenever I have a question and ran into a trouble spot and he always provided useful inspection to steer me in the right direction. I have learnt a lot from him, not only research capability but also working approach and I am really grateful for that.

Thanks to Dr. Maria Therese Pigott who provided huge amount of help patiently every day through the first year of this project. Thanks for her patience, assistance and kind supervision given to me over that period.

Thanks to Dr. Gloria Ana and Yin Lu for help with the chemistry synthesis, Associate Professor Carlos Medina Martin and Hante Nadhim Kamil help with zymography, Dr. Anne-Marie Byrne help with immunofluorescence, Dr. Vanesa Martinez help with PBMCs isolation, Miriam Lyons help with chemical order, general things in the lab and sharing her bench with me, Kate O'Donnell help with general things in Trinity Translational Medicine Institute. I would like to thank all the members in research group for building a friendly working environment where I can get a help whenever I need.

Thanks to my parents for giving me a chance to study abroad. Their patience, support and understanding inspired me when I felt frustrated.

Finally, thanks to my close friends Aleksandra Pavlenkova, Zhen Lao and Paloma Ortiz Botella, for supporting, encouraging and helping me during my postgraduate study.

Abbreviations

AP Alkaline phosphatase

APAF1 Apoptotic protease activating factor

BA Bile acid

BSA Bovine serum albumin

CA Cholic acid

CDCA Chenodeoxycholic acid

CDCl₃ Deuterated chloroform

CD Crohn's disease

CYP27A1 mitochondrial sterol 27-hydroxylase

CYP8B1 C-12 position hydroxylation of the microsomal sterol 12 α -hydroxylase

DCA Deoxycholic acid

DCM Dichloromethane

DMEM Dulbecco's Modified Eagle's Medium

DMPU 1,3-Dimethyl-3,4,5,6-tetrahydro-2(1H)-pyrimidinone

DMSO-d₆ Deuterated dimethyl sulfoxide

DSS Dextran sulfate sodium

EGFR Epidermal growth factor receptor

ELISA Enzyme-linked immunosorbent assay

ERK Extracellular signal-regulated kinase

EtOAc Ethyl acetate

EtOH Ethanol

FBS Fetal bovine serum

FGF19 Fibroblast growth factor 19

FKBP52 FK506-binding protein 52

FXR Farnesoid X receptor

GC Glucocorticoid

GR Glucocorticoid receptor

GREs Glucocorticoid response elements

GPCRs G protein-coupled receptors

HCl Hydrochloric acid

HClO₄ Perchloric acid

HPLC High performance liquid chromatography

HSP 70 Heat shock protein 70

HSP 90 Heat shock protein 90

IBD Inflammatory bowel disease

IL Interleukin

IKK IκB kinase

LCA Lithocholic acid

MAPKs Mitogen-activated protein kinases

MeOD Deuterated Methanol

MEM Minimum essential media

MeOH Methanol

MgSO₄ Magnesium sulfate

MMPs Matrix metalloproteinases

MOA Mechanism of action

MTT 3-(4,5-Dimethylthiazol-2-yl)-2,5-diphenyltetrazolium bromide

Na₂SO₄ Sodium sulfate

NaHCO₃ Sodium bicarbonate

NaN₃ Sodium azide

NaOH Sodium hydroxide

NEMO NF-κB essential modulator

NF-κB Nuclear factor kappa beta

NLS Nuclear localization signal

NMR Nuclear magnetic resonance

OPG Osteoprotegerin

PBS Phosphate buffered saline

Pd/C Palladium on carbon

PFA Paraformaldehyde

PMA Phorbol myristate acetate
PPh₃ Triphenylphosphine
RANKL Receptor activator of nuclear factor (NF)-κB-ligand
ROS Reactive oxygen species
RHD Rel homology domain
SEAP Secreted alkaline phosphatase
TEA Triethylamine
TFA Trifluoroacetic acid
TGF Transforming growth factor
TGR5 Transmembrane G-protein receptor 5
TLC Thin layer chromatography
TLR Toll-like receptor
TNF Tumor necrosis factor
TUDCA Tauroursodeoxycholic acid
UC Ulcerative colitis
UDCA Ursodeoxycholic acid
μM Micromolar

Table Of Contents

Chapter 1. BAs in health and in diseases of colon and liver	1
1.1 Structure and function of the BAs.....	1
1.2 Synthesis of BAs from cholesterol and their conjugation, storage, release and recirculation.....	2
1.3 Receptors for BAs and their role in health and disease with focus on FXR and TGR.....	5
Chapter 2. BAs in modulating apoptosis in the colonic epithelium	7
2.1 Structure, function and physiology of the colon.....	7
2.2 Inflammatory diseases of the colon	9
2.3 Role of apoptosis in the inflammatory disease of the colon.....	10
2.4 Role of BAs in causing or preventing colorectal epithelial cell death.....	11
2.5 Aims and objectives of the work in this Chapter	13
2.6 Results for TNF- α , IFN- γ and BAs in causing bile acid induced cell death in colorectal cell lines.....	14
2.6.1 Results for TNF- α , IFN- γ effect on proliferation.....	14
2.6.2 Results for effect of secondary BA on Caco-2 cell proliferation	18
2.6.3 Results for LCA derivatives effects on Caco-2 cell viability in the MTT assay.....	20
2.6.4 Result for treatment with DCA and combination with TNF- α	22
2.6.5 Studies into the potential cytoprotective effect for 3 α -hydroxy-7 β -(methanesulfonamido)-5 β -cholanoate (35) with DCA induced cell death as a model of pathophysiological epithelial apoptosis.....	23
2.6.6 Discussion	25
Chapter 3. UDCA analogues as anti-inflammatory agents in cholestatic disease	29
3.1 Glucocorticoids (Natural and Synthetic GCs).....	29
3.2 Side effect of GCs.....	32
3.3 GR Signaling Pathway.....	32
3.4 NF- κ B Signaling Pathway.....	34
3.5 Dissociated Steroids.....	36
3.6 Structure of UDCA, its chemical and clinical properties and effects	38
3.7 Evidence for UDCA activation of GR	40
3.8 Aims and objectives.....	42
3.9 Design and Synthesis of UDCA derivatives.....	43
3.9.1 Synthesis of 3 α -(benzamido)-7 β -hydroxy-5 β -cholanoate (15) and 3 α -(4-chlorobenzamido)-7 β -hydroxy-5 β -cholanoate (17).....	44
3.9.2 Synthesis of 3 β -(benzamido)-7 β -hydroxy-5 β -cholanoate (23) and 3 β -(4-chlorobenzamido)-7 β -hydroxy-5 β -cholanoate (24).....	47
3.9.3 Synthesis of N-cyclohexylbenzamide (25).....	49
3.9.4 Synthesis of 3 α -hydroxy-7 β -(1H-1,2,3-triazol-1-yl)-5 β - cholanoate (33) and 3 α -hydroxy-7 β -(methanesulfonamido)-5 β - cholanoate (35).....	49
3.10 Effect of BAs derivatives on cell viability by MTT and Alamar blue.....	50
3.10.1 MTT Assay.....	50
3.10.2 Alamar Blue Assay	51
3.10.3 Cytotoxicity studies on the Caco-2 cell line.....	52

3.10.4 Cytotoxicity studies on the Huh 7 cell line	58
3.10.5 Cytotoxicity studies on the THP 1-Blue cell line using the MTT assay	58
3.11 Effect of BAs on THP1-Blue stimulated with TNF- α	60
3.11.1 QUANTI-Blue Assay (The THP1-Blue reporter assay for NF- κ B)	60
3.11.2 Result of BAs effect on THP 1-Blue stimulated with TNF- α	60
3.12 Effect of the compounds on IL-8 stimulated by inflammatory promoters in Caco-2, PBMC and Huh7 cell lines.....	71
3.12.1 IL-8 estimation for BA derivatives effect on Caco-2 cells	72
3.12.2 IL-8 estimation for BA derivatives on PBMCs.....	73
3.12.3 IL-8 estimation for BA derivatives on Huh7.....	79
3.12.4 IL-6 estimation for BA derivatives on Huh7.....	80
3.13 Discussion.....	81
Chapter 4. Methodology.....	85
4.1 Chemistry.....	85
4.1.1 General synthetic method.....	85
4.1.2 Procedure for the 3 α -, 3 β -amides formation	85
4.1.3 Procedure for the 7 β -amides formation.....	86
4.1.4 Synthesis of UDCA derivatives.....	87
4.2 Cell Culture.....	91
4.2.1 Counting	91
4.2.2 Cryopreserve and revival cells	91
4.2.3 Caco-2.....	92
4.2.4 HT-29.....	92
4.2.5 THP1-Blue.....	93
4.2.6 Huh-7	93
4.2.7 PBMCs.....	94
4.3 Biology.....	94
4.3.1 QUANTI-Blue Assay	94
4.3.2 MTT Assay.....	95
4.3.3 Flow Cytometry	95
4.3.4 Alamar Blue Assay	96
4.3.5 ELISA	96
4.3.6 GR translocation.....	97
Chapter 5. References	99

Table of Figures

Figure 1. The relationship between CA and BAs	1
Figure 2. Two pathways of BA synthesis^[21] <i>There are two ways of generating the primary BAs, DCA and LCA. One way is the classic pathway, the other, the alternative pathway.</i>	4
Figure 3. Colonic cells structure^[43]	8
Figure 4. Cell proliferation and cell death regulation by BAs^[79]	13
Figure 5. MTT result of TNF-α <i>Caco-2 cells were treated with different concentrations of TNF-α for 24 h in the 37°C incubator. The vehicle was 1% H₂O. Values of TNF-α were expressed as fold different to the vehicle as mean \pm SEM of triplicate experiments, ns $P > 0.05$ was determined by oneway ANOVA with Dunnett's post-hoc correction.</i>	14
Figure 6. MTT result of IFN-γ <i>Caco-2 cells treated with different concentrations of IFN-γ for 24 h in the 37°C incubator. The vehicle was 1% H₂O. Values of IFN-γ were expressed as fold different to the vehicle as mean \pm SEM of triplicate experiments, ns $P > 0.05$ was determined by oneway ANOVA with Dunnett's post-hoc correction.</i>	15
Figure 7. MTT result of mixture of TNF-α and IFN-γ <i>Caco-2 cells treated with different concentrations of TNF-α and IFN-γ for 24 h in the 37°C incubator. The vehicle was 1 % H₂O. Values of TNF-α & IFN-γ were expressed as fold different to the vehicle as mean \pm SEM of triplicate experiments, ****$P < 0.0001$ was determined by oneway ANOVA with Dunnett's post-hoc correction.</i>	16
Figure 8. MTT result of TNF-α and IFN-γ <i>HT-29 cells were treated with different concentrations of TNF-α and IFN-γ for 24 h in the 37°C incubator. The vehicle was 1 % H₂O. Values were expressed as fold difference compared to the vehicle as mean \pm SEM of triplicate experiments, **$p < 0.01$, *** $p < 0.001$, ****$P < 0.0001$ was determined by oneway ANOVA with Dunnett's post-hoc correction and by t test.</i>	17
Figure 9. MTT result of DCA <i>Caco-2 cells were treated with different concentrations of DCA for 24 h in the 37°C incubator. The vehicle was 1 % DMSO. Values of DCA were expressed as fold different to the vehicle as mean \pm SEM of triplicate experiments, ****$P < 0.0001$ was determined by oneway ANOVA with Dunnett's post-hoc correction.</i>	19
Figure 10. MTT result for LCA <i>Caco-2 cells were treated with different concentrations of LCA for 24 h in the 37°C incubator. The vehicle was 1% DMSO. Values of DCA were expressed as fold different to the vehicle as mean \pm SEM of triplicate experiments, ****$P < 0.0001$ was determined by oneway ANOVA with Dunnett's post-hoc correction.</i>	19
Figure 11. MTT result of sodium TLCA <i>Caco-2 cells were treated with different concentrations of sodium TLCA for 24 h in the 37°C incubator. The vehicle was 1 % DMSO. Values of TLCA were expressed as fold different to the vehicle as mean \pm SEM of triplicate experiments, *$P < 0.05$ was determined by oneway ANOVA with Dunnett's post-hoc correction.</i>	20

Figure 12. MTT result of LCA 3-sulfate	<i>Caco-2 cells were treated with different concentrations of 3-sulfate LCA for 24 h in the 37 °C incubator. The vehicle was 1 % DMSO. Values of LCA 3-sulfate were expressed as fold different to the vehicle as mean ± SEM of triplicate experiments, *** p<0.001, ****P <0.0001 was determined by oneway ANOVA with Dunnett's post-hoc correction.</i>	21
Figure 13. MTT result of TLCA 3-sulfate	<i>Caco-2 cells were treated with different concentrations of TLCA 3-sulfate for 24 h in the 37 °C incubator. The vehicle was 1 % DMSO. Values of TLCA 3-sulfate were expressed as fold different to the vehicle as mean ± SEM of triplicate experiments, *** p<0.001, ****P <0.0001 was determined by oneway ANOVA with Dunnett's post-hoc correction.</i>	22
Figure 14. MTT result of cocktail of DCA and TNF-α	<i>Caco-2 cells were treated with different concentrations of DCA with 200 ng/mL TNF-α for 24 h in the 37 °C incubator. The vehicle was 0.5 % DMSO. Values were expressed as fold difference to the vehicle as mean ± SEM of triplicate experiments, ** p<0.01, was determined by oneway ANOVA with Dunnett's post-hoc correction.</i>	23
Figure 15. MTT assay result of 3α-hydroxy- 7β-(methanesulfonamido)-5β-cholanoate (35)	<i>Caco-2 cells were treated with different concentrations of compound and 35 for 24 h in the 37 °C incubator. The vehicle was 0.5 %DMSO. Values were expressed as fold difference to the vehicle as mean ± SEM of triplicate experiments, *p<0.05, was determined by oneway ANOVA with Dunnett's post-hoc correction.</i>	24
Figure 16. MTT assay result of DCA and 3α-hydroxy-7β-(methane sulfonamido)-5β-cholanoate (35)	<i>Caco-2 cells were treated with 250 μM 35 for 24 h followed by adding different concentrations of DCA. The vehicle is 1% DMSO.</i>	25
Figure 17. Interconversion between cortisol and cortisone		29
Figure 18. Clinical synthetic GCs Dexamethasone (3) and prednisolone (4)		31
Figure 19. GR Signaling Pathway ^[115, 116]		33
Figure 20. Key NF-κB Signaling pathways ^[134]	<i>This figure includes the canonical and non-canonical NF-κB signaling pathway. The enzyme IκB kinase (IKK) or NF-κB-inducing kinase (NIK) is activated by various extracellular signals and then and triggers a serial of reactions.</i>	36
Figure 21. Chemical structure of dissociated steroids RU24858		37
Figure 22. Chemical structure of dissociated steroids AL-438		38
Figure 23. Structure of UDCA		39
Figure 24. Chemical structure of TUDCA		40
Figure 25. Novel GR chemical structure		41
Figure 26. MTT Assay ^[159]	<i>MTT Assay is an enzyme-based method that is used widely in cell toxicity and cell viability through coloring reagent and dehydrogenase. In the figure, nicotinamide adenine dinucleotide (NADH) consists of nicotinamide adenine dinucleotide (NAD) + hydrogen (H). It is essential in the energy generation reaction in all living cells.</i>	51
Figure 27. MTT assay		51
Figure 28. Alamar Blue Assay ^[160]	<i>The assay relies on the metabolic activity in the</i>	

mitochondria of cells. It is a fluorometric method that is based on the reduction reaction transforming blue resazurin to resorufin.....52

Figure 29. Alamar blue assay.....52

Figure 30. Alamar Blue assay result of 3 α -(4-chlorobenzamido)-7 β -hydroxy-5 β -cholanoate (17) Caco-2 cells were treated with different concentrations of 3 α -(4-chlorobenzamido)-7 β -hydroxy-5 β -cholanoate (17) for 24 h in the 37 °C incubator. The vehicle was 0.5 % DMSO. Values were expressed as fold difference compared to the vehicle as mean \pm SEM of triplicate experiments, *** $p < 0.001$, **** $P < 0.0001$ was determined by oneway ANOVA with Dunnett's post-hoc correction.....53

Figure 31. A comparison of the effect of 3 α -(benzamido)-7 β -hydroxy-5 β -cholanoate (15) and 3 β -(benzamido)-7 β -hydroxy-5 β -cholanoate (23) Caco-2 cells were treated with different concentrations of 3 α -(benzamido)-7 β -hydroxy-5 β -cholanoate (15) and 3 β -(benzamido)-7 β -hydroxy-5 β -cholanoate (23) for 24 h. The vehicle was 0.5 % DMSO. Values were expressed as fold difference compared to the vehicle as mean \pm SEM of triplicate experiments, *** $P < 0.001$, was determined by oneway ANOVA with Dunnett's post-hoc correction.....54

Figure 32. MTT assay result of 3 β -(4-chlorobenzamido)-7 β -hydroxy-5 β -cholanoate (24) Caco-2 cells were treated with different concentrations of compound 24 for 24 h. The vehicle is 0.5 %DMSO. Values were expressed as fold difference compared to the vehicle as mean \pm SEM of triplicate experiments, ** $p < 0.01$, *** $p < 0.001$, **** $P < 0.0001$ was determined by oneway ANOVA with Dunnett's post-hoc correction.....55

Figure 33. A comparison of the effect of 3 α -(4-chlorobenzamido)-7 β -hydroxy-5 β -cholanoate (17) and 3 β -(4-chlorobenzamido)-7 β -hydroxy-5 β -cholanoate (24) Caco-2 cells were treated with different concentrations of 3 α -(4-chlorobenzamido)-7 β -hydroxy-5 β -cholanoate (17) and 3 β -(4-chlorobenzamido)-7 β -hydroxy-5 β -cholanoate (24) for 24 h. The vehicle was 0.5 % DMSO. Values were expressed as fold difference compared to the vehicle as mean \pm SEM of triplicate experiments, *** $P < 0.001$, was determined by oneway ANOVA with Dunnett's post-hoc correction.....56

Figure 34. MTT assay result of 3 α -hydroxy-7 β -(1H-1,2,3-triazol-1-yl)-5 β -cholanoate(33) and 3 α -hydroxy-7 β -(methanesulfonamido)-5 β -cholanoate (35) Caco-2 cells were treated with different concentrations of compound 33 and 35 for 24 h in the 37 °C incubator. The vehicle is 0.5 %DMSO. Values were expressed as fold difference compared to the vehicle as mean \pm SEM of triplicate experiments, * $p < 0.05$, ** $p < 0.01$, *** $p < 0.001$, **** $P < 0.0001$ was determined by oneway ANOVA with Dunnett's post-hoc correction and by t test..57

Figure 35. MTT Assay result of bile acid derivatives Huh 7, a hepatocarcinoma cell line, was treated with different concentrations (50, 100 μ M respectively) of six BAs analogues for 24 h. The vehicle control is 0.5 %DMSO. Values were expressed as fold difference compared to the vehicle as mean \pm SEM of triplicate experiments, * $p < 0.05$, ** $p < 0.01$, was determined by oneway ANOVA with

<i>Dunnett's post-hoc correction</i>	58
Figure 36. MTT Assay result of bile acid derivatives on THP 1-Blue <i>Peripheral blood mononuclear cells (PBMCs) were treated with different concentrations of BA analogues for 24 h. The following procedures are the same. The vehicle control is 0.5 % DMSO. Values were expressed as fold difference compared to the vehicle as mean ± SEM of triplicate experiments, *p<0.05, ***p<0.001, was determined by oneway ANOVA with Dunnett's post-hoc correction.</i>	59
Figure 37. QUANTI-Blue Assay <i>The SEAP is secreted into cell supernatant different with intracellular reporters. QUANTI-Blue Assay, colorimetric assay, determines the SEAP activity in cell supernatant.</i>	60
Figure 38. QUANTI-Blue assay result of TNF-α <i>In the negative group THP 1-Blue cells were treated with 0.5 % DMSO cell medium (RPMI-1640 Medium) alone for 24h. THP 1-Blue cells were treated with 10 ng/ml TNF-α in 0.5 % DMSO cell medium for 24h in the positive group.</i>	61
Figure 39. QUANTI-Blue assay result of dexamethasone <i>THP1-Blue cells were treated with 10 ng/ml TNF-α and different concentrations of dexamethasone for 24 h. Values were expressed as fold difference compared to the vehicle as mean ± SEM of triplicate experiments, *p<0.05, **p<0.01, was determined by oneway ANOVA with Dunnett's post-hoc correction.</i>	62
Figure 40. QUANTI-Blue assay result of TUDCA (7) <i>THP-1 Blue cells were treated with 10 ng/ml TNF-α and different concentrations of TUDCA for 24 h. The vehicle is 0.5 %DMSO. The dexamethasone concentration is 1 μM. Values were expressed as fold difference compared to the vehicle as mean ± SEM of triplicate experiments, **p<0.01, ****P <0.0001 was determined by oneway ANOVA with Dunnett's post-hoc correction and by t test.</i>	63
Figure 41. QUANTI-Blue assay result of 3α-(4-chlorobenzamido)-7β–hydroxy-5β–cholanoate (17) <i>THP1-Blue cells were treated with different concentrations of 3α-(4-chlorobenzamido)-7β-hydroxy-5β-cholanoate (17) and 10ng/ml TNF-α for 24 h. The vehicle is 0.5 %DMSO. The dexamethasone concentration is 1 μM. Values were expressed as fold difference compared to the vehicle as mean ± SEM of triplicate experiments, **p<0.01, ****P <0.0001 was determined by oneway ANOVA with Dunnett's post-hoc correction and by t test.</i>	64
Figure 42. Comparison of the QUANTI-Blue assay result of 3α-(benzamido)-7β-hydroxy-5β-cholanoate(15) and 3α-(4-chlorobenzamido)-7β-hydroxy-5β- cholanoate (17) <i>THP1-Blue cells were treated with 10 ng/ml TNF-α and different concentrations of either 3α- (benzamido)-7β-hydroxy-5β-cholanoate (15) or 3α- (4-chlorobenzamido)- 7β- hydroxy-5β-cholanoate (17) for 24 h. The vehicle is 0.5 %DMSO. Values were expressed as fold difference as mean ± SEM of triplicate experiments, **p<0.01, *** p<0.001, was determined by t test.</i>	65
Figure 43. Comparison of the QUANTI-Blue assay result of 3β-(benzamido)-7β-hydroxy-5β-cholanoate (23) and 3α-(benzamido)-7β-hydroxy-5β-cholanoate (15) <i>THP1-Blue cells were treated with 10 ng/ml TNF-α and different concentrations of either 3β-(benzamido)</i>	

-7 β -hydroxy-5 β -cholanoate (**23**) or 3 α -(benzamido)-7 β -hydroxy-5 β - cholanoate (**15**) for 24 h. The vehicle is 0.5 %DMSO. Values were expressed as fold difference compared to the vehicle as mean \pm SEM of triplicate experiments, ** $p < 0.01$, *** $p < 0.001$, **** $P < 0.0001$ was determined by t test.66

Figure 44. QUANTI-Blue assay result of 3 β -(4-chlorobenzamido)-7 β -hydroxy-5 β -cholanoate (24**)** THP1-Blue cells were treated with 10ng/ml TNF- α and different concentrations of 3 β -(4-chlorobenzamido)-7 β -hydroxy-5 β -cholanoate (**24**) for 24 h. The vehicle is 0.5 %DMSO. The dexamethasone concentration is 1 μ M. Values were expressed as fold difference compared to the vehicle as mean \pm SEM of triplicate experiments, ns $P > 0.05$, **** $P < 0.0001$ was determined by oneway ANOVA with Dunnett's post-hoc correction and by t test. 67

Figure 45. Comparison of the QUANTI-Blue assay result of 3 β -(benzamido)-7 β -hydroxy-5 β -cholanoate (23**) and 3 β -(4-chlorobenzamido)-7 β -hydroxy-5 β -cholanoate (**24**)** THP1-blue cells were treated with 10 ng/ml TNF- α and different concentrations of these compounds for 24 h. The vehicle is 0.5 %DMSO. Values were expressed as fold difference as mean \pm SEM of triplicate experiments, **** $P < 0.0001$ was determined by t test.67

Figure 46. QUANTI-Blue assay result of 3 α -hydroxy-7 β -(methane sulfonamido)-5 β -cholanoate (35**)** THP1-Blue cells were treated with different concentrations of compound **35** with 10 ng/ml TNF- α for 24 h. The vehicle is 0.5 %DMSO. The concentration of dexamethasone is 1 μ M. Values were expressed as mean \pm SEM of triplicate experiments, ns $p > 0.05$, was determined by t test.68

Figure 47. QUNATI-Blue assay results for UDCA-based triazole **33.** THP1-Blue cells were treated with different concentrations of 3 α -hydroxy-7 β -(1H-1,2,3-triazolo-1-yl)-5 β -cholanoate (**33**) with 10 ng/ml TNF- α for 24 h. The vehicle is 0.5 %DMSO. The concentration of dexamethasone is 1 μ M. Values were expressed as mean \pm SEM of triplicate experiments, ** $p < 0.01$, was determined by t test.69

Figure 48. Comparison of the QUANTI-Blue assay result of UDCA-based triazole (33**) and UDCA-based sulfonamide (**35**)** THP1-Blue cells were treated with 10 ng/ml TNF- α and different concentrations of compound **33** and **35** for 24 h. The vehicle is 0.5 % DMSO. The dexamethasone concentration is 1 μ M. Values were expressed as mean \pm SEM of triplicate experiments, ns $p > 0.05$, was determined by t test.70

Figure 49. QUANTI-Blue assay results for 4-chloro-N-cyclohexyl benzamide (25**)** THP1-Blue cells were treated with different concentrations of 4-chloro-N-cyclohexylbenzamide (**25**) and 10 ng/ml TNF- α for 24 h. The vehicle is 0.5 %DMSO. The dexamethasone concentration is 1 μ M. Values were expressed as fold difference compared to the vehicle as mean \pm SEM of triplicate experiments, *** $p < 0.001$, **** $P < 0.0001$ was determined by t test.70

Figure 50. ELISA ^[165, 166] In the assay, the antigen immobilization has direct and indirect way including absorption to the plate and attaching to an antibody. Also, the antigen is detected by the primary antibody conjugated with enzyme or by the

<i>unlabeled primary antibody and secondary antibody.....</i>	<i>72</i>
Figure 51. ELISA from one of the IL-8 assay.....	72
Figure 52. IL-8 result of BAs TNF-α and IFN-γ stimulation <i>Caco-2 were treated with 100 ng/mL TNF-α and 300 ng/mL IFN-γ for 30 min and then bile acid analogue solution (final concentration is 100 μM) was added into each well before 24 h incubation. 50 μL cell supernatant was used to do the ELISA. The vehicle control is 0.5 % DMSO. Values were expressed as fold difference as mean \pm SEM of triplicate experiments.</i>	<i>73</i>
Figure 53. LPS stimulation on experiment 1 <i>PBMCs were treated with 1 μg/mL LPS for 30 min and then bile acid analogues solution (final concentration is 50 μM) for 24 h incubation. Values were expressed as mean \pm SEM of one experiment compared to PBMCs treated with LPS, ns $p > 0.05$, was determined by t test.</i>	<i>74</i>
Figure 54. LPS stimulation on experiment 2 <i>PBMCs were treated with 1 μg/mL LPS for 30 min and then bile acid analogues solution (final concentration is 50 μM) for 24 h incubation. Values were expressed as mean \pm SEM of one experiment compared to PBMCs treated with LPS, ns $p > 0.05$, was determined by t test.</i>	<i>74</i>
Figure 55. LPS stimulation on experiment 3 <i>PBMCs were treated with 1 μg/mL LPS for 30 min and then bile acid analogues solution (final concentration is 50 μM) for 24 h incubation. Values were expressed as mean \pm SEM of one experiment compared to PBMCs treated with LPS, ns $p > 0.05$, was determined by t test.</i>	<i>75</i>
Figure 56. TNF-α stimulation on experiment 1 <i>PBMCs were treated with 10 μg/mL TNF-α for 30 min and then bile acid analogues solution (final concentration is 50 μM) for 24 h incubation. Values were expressed as mean \pm SEM of one experiment compared to PBMCs treated with TNF-α, * $p < 0.05$, was determined by t test.</i>	<i>75</i>
Figure 57. TNF-α stimulation experiment 2 <i>PBMCs were treated with 10 μg/mL TNF-α for 30 min and then bile acid analogues solution (final concentration is 50 μM) for 24 h incubation. Values were expressed as mean \pm SEM of one experiment compared to PBMCs treated with TNF-α, **$p < 0.01$, was determined by t test.</i>	<i>75</i>
Figure 58. TNF-α stimulation on experiment 3 <i>PBMCs were treated with 10 μg/mL TNF-α for 30 min and then bile acid analogues solution (final concentration is 50 μM) for 24 h incubation. Values were expressed as mean \pm SEM of one experiment compared to PBMCs treated with TNF-α, ns $p > 0.05$, was determined by t test.</i>	<i>76</i>
Figure 59. PMA stimulation on experiment 1 <i>PBMCs were treated with 50 μg/mL PMA for 30 min and then bile acid analogues solution (final concentration is 50 μM) for 24 h incubation. Values were expressed as mean \pm SEM of one experiment compared to PBMCs treated with PMA, * $p < 0.05$, was determined by t test.</i>	<i>76</i>
Figure 60. PMA stimulation experiment 2 <i>PBMCs were treated with 50 μg/mL PMA for 30 min and then bile acid analogues solution (final concentration is 50 μM) for 24 h incubation. Compound 5 is UDCA. Values are expressed as mean \pm SEM of one experiment compared to PBMCs treated with PMA, * $p < 0.05$, **$p < 0.01$, was determined by t test.</i>	<i>77</i>

Figure 61. PMA stimulation on experiment 3	<i>PBMCs were treated with 50 µg/mL PMA for 30 min and then bile acid analogues solution (final concentration is 50 µM) was added into each well before 24 h incubation. 50 µL cell supernatant was used to do the ELISA. The positive control is 0.5 % DMSO. Values were expressed as mean ± SEM of one experiment compared to PBMCs treated with PMA, ns p> 0.05, was determined by t test.</i>	77
Figure 62. DCA stimulation on experiment 1	<i>PBMCs were treated with 200 µM DCA for 30 min and then bile acid analogues solution (final concentration is 50 µM) was added into each well before 24 h incubation. Values were expressed as mean ± SEM of one experiment compared to PBMCs treated with DCA, ns p> 0.05, was determined by t test.</i>	77
Figure 63. DCA stimulation experiment 2	<i>PBMCs were treated with 200 µM DCA for 30 min and then bile acid analogues solution (final concentration is 50 µM) was added into each well before 24 h incubation. Values were expressed as mean ± SEM of one experiment compared to PBMCs treated with DCA, ns p> 0.05, was determined by t test.</i>	78
Figure 64. DCA stimulation on experiment 3	<i>PBMCs were treated with 200 µM DCA for 30 min and then bile acid analogues solution (final concentration is 50 µM) was added into each well before 24 h incubation. Values were expressed as mean ± SEM of one experiment compared to PBMCs treated with DCA, ns p> 0.05, was determined by t test.</i>	78
Figure 65. DCA stimulation, mean of three experiments	<i>PBMCs were treated with 200 µM DCA for 30 min and then bile acid analogues solution (final concentration is 50 µM) was added into each well before 24 h incubation. Values were expressed as mean ± SEM of one experiment compared to PBMCs treated with DCA, ns p> 0.05, was determined by t test.</i>	79
Figure 66. IL-8 estimation of bile acid derivatives	<i>Huh7 cells were treated with different agonists for 30 min and then bile acid analogues solution (final concentration is 50 µM) was added into each well before 24 h incubation. Values were expressed as fold difference as mean ± SEM of triplicate experiments.</i>	79
Figure 67. IL-6 secretion in response to stimuli and bile acid derivatives	<i>Huh7 cells, were treated with different agonists for 30 min and then bile acid analogues solution (final concentration is 50 µM) was added into each well before 24 h incubation. 100 µL cell supernatant was used to do the ELISA. The vehicle control is 0.5 % DMSO. Values were expressed as fold difference as mean ± SEM of triplicate experiments.</i>	80
Figure 68. IL-6 following PMA stimulation	<i>Huh7 cells were treated with 50 µg/mL PMA for 30 min and then bile acid analogues solution was added into each well before 24 h incubation. Aliquots of 100 µL cell supernatant was obtained for ELISA. The vehicle was 0.5 % DMSO. Values were expressed as mean ± SEM of triplicate experiments compared to PBMCs treated with DCA, ns p> 0.05, was determined by t test.</i>	81

Table of Tables

Table 1. Cell type and function in the colon^[44]	8
Table 2. Flow cytometry result of TNF-α and IFN-γ <i>HT-29 cells were treated with different concentrations of TNF-α and IFN-γ at around 80% confluency for 24 h in the 37°C incubator before fixing and staining with PI. The vehicle was PBS. Values were expressed as mean \pm SEM of one experiment.</i>	18

Table of Schemes

Scheme 1. Synthesis of 3α-azide of UDCA	45
Scheme 2. Formation of 3 α-benzamido and 3α-chlorobenzamido of UDCA	46
Scheme 3. Synthesis of 3β-azide of UDCA	47
Scheme 4. Formation of 3β-benzamido of UDCA	48
Scheme 5. Formation of 3 β-chlorobenzamido of UDCA	48
Scheme 6. Formation of N-cyclohexylbenzamide (25)	49
Scheme 7. Formation of 3α-hydroxy-7β-(1H-1,2,3-triazol-1-yl)-5β- cholanoate (33) and 3α-hydroxy-7β-(methanesulfonamido)-5β- cholanoate (35)	50

Chapter 1. BAs in health and in diseases of colon and liver

1.1 Structure and function of the BAs

BAs (Bile acids), the principal components of bile, is an umbrella term for alkyl-derivative of 24-carbon cholic acid (CA) in humans^[1,2]. The term includes primary BAs and secondary BAs. Primary BAs are synthesized directly in the liver from cholesterol. Indeed, this is the main elimination pathway for cholesterol. Secondary BAs are a product of bacterial metabolism of BAs that make it to the bowel during enterohepatic circulation/elimination. BAs can be found conjugated with glycine and taurine^[3-5], the former being more common in humans, the latter in mice.

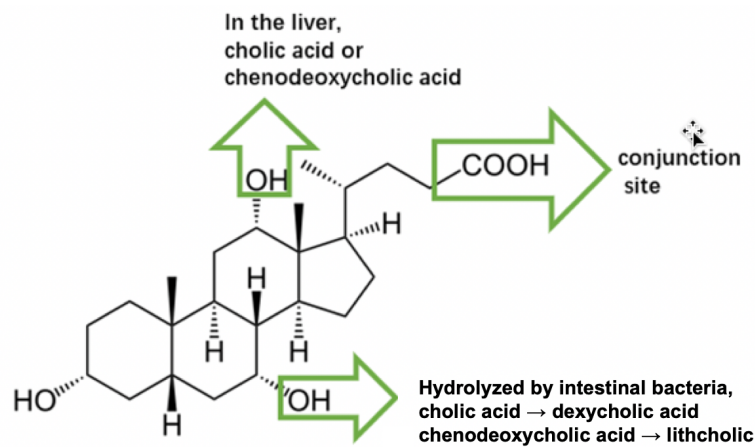


Figure 1. The relationship between CA and BAs

BAs improve fats and fat-soluble vitamin digestion and absorption because they are amphipathic substances which include a hydrophilic group such as a hydroxyl^[6, 7], carboxyl or sulfonic acid group and hydrophobic hydrocarbon and methyl groups. The asymmetric distribution of hydrophobic and hydrophilic groups is the reason why BAs have strong interfacial activity enabling them to reduce surface tension between oil phase and water phase in order to promote fat and lipid emulsification^[6]. Simultaneously, BAs can increase lipase interface

with ester droplets in the digestive tract following a meal, thus accelerating ester breakdown to more easily absorb or more soluble substances. BAs also have a role to play in preventing gallstone formation^[8]. It is well known that cholesterol is insoluble in water, a property which makes cholesterol easily precipitate out as crystalline form which can accumulate forming so-called gallstones. BAs, in combination with lecithin, can form mixed micelles which helps cholesterol travel from bile ducts to small intestine without separating out.

1.2 Synthesis of BAs from cholesterol and their conjugation, storage, release and recirculation

Primary BAs derived from cholesterol are generated in the liver and there are two pathways of production termed the classic and alternative pathways^[9].

The classic pathway is called the neutral way because the percentage of neutral sterols are high in the intermediates for bile acid synthesis in this pathway^[10]. It is regarded as the main pathway for bile acid production and cholesterol elimination in humans. In the first step, cholesterol is converted to 7 α -hydroxycholesterol catalyzed by the cholesterol 7 α -hydroxylase (CYP7A1). Then 3 β -hydroxy-27-steroid (3 β -HSD), the microsomal dehydrogenase/isomerase, converts 7 α -hydroxycholesterol into 7 α -hydroxy-4-cholestane-3-one as an intermediate. Finally, through the C-12 position hydroxylation of the microsomal sterol 12 α -hydroxylase (CYP8B1) and modification by CYP27A1, 7 α -hydroxy-4-cholestene-3-one is converted to CA. The enzyme, CYP8B1, participates as a catalyst in the classic pathway of BA synthesis (**Figure 2**)^[11].

Around 10 % of bile acid synthesis will be regulated through the alternative pathway which takes place in the extrahepatic sites mainly. The alternative pathway begins with the mitochondrial sterol 27-hydroxylase (CYP27A1) which

converts cholesterol into 27-hydroxycholesterol^[12]. It is hydroxylated and converted to chenodeoxycholic acid (CDCA) through 7 α -hydroxylase (CYP7B1)^[13, 14]. Besides, CYP27A1 also converts 7 α -hydroxy-4-cholestene-3-one into CDCA.

After primary BAs are synthesized in the liver, they are conjugated with amino acids taurine and glycine in hepatocytes^[15]. The acidity of these conjugated BAs is stronger (pKa decreases) and the solubility increases. On the one hand this helps form micelles in the acid environment of the duodenum preventing conjugated BAs from being resorbed in the biliary tract and the small intestine. Conjugation which reduces lipid solubility also reduces toxicity and, in general, conjugated BAs are less prone to causing cell damage than free BAs. Approximately 50 % of newly synthesized BAs are transported to the intestine; the rest are stored in the gall bladder awaiting secretion postprandially. After BAs are released to the intestine leading to improved transportation of lipids and absorption in the bowel, they are reabsorbed to the liver in the terminal jejunum and ileum in a highly efficient active process. This overall process is called enterohepatic circulation^[16], which can compensate for the lack of BAs produced by the liver and make the limited amount of BAs exert biggest impact in emulsification^[17, 18]. Therefore, this process of BA reabsorption means they can be reused and improve the digestion and emulsification of fat and lipid soluble vitamins.

Around 95 % of the BA pool is intestinally retrieved. This, along with the BAs freshly synthesized by the liver, are transported to the biliary tract again and most of the BAs are stored in the gall bladder^[19]. The same process is repeated after a meal, indeed depending on the length of the meal several enterohepatic cycles are possible.

In the upper intestine, bile acids are associated with fat digestion and absorption. In the ileal mucosa, 95 % of BAs are reabsorbed and returned to the liver via the portal vein. Around 5% of luminal bile acid transits to the large bowel or colon^[20]. Conjugated BAs are hydrolyzed to unconjugated primary BAs by bacteria in the upper part of ileum and colon. Then the primary BAs, CA and CDCA, maybe be converted to secondary BAs, DCA and LCA, through 7 α - dehydroxylation by intestinal bacteria enzymes. Free secondary BAs may passively diffuse from the colon returning to the liver where they may undergo further metabolism and conjugation. Only 5% of that is unabsorbed and converted to cholanic acid derivatives by the intestinal bacteria action which are excreted from the body in the faeces.

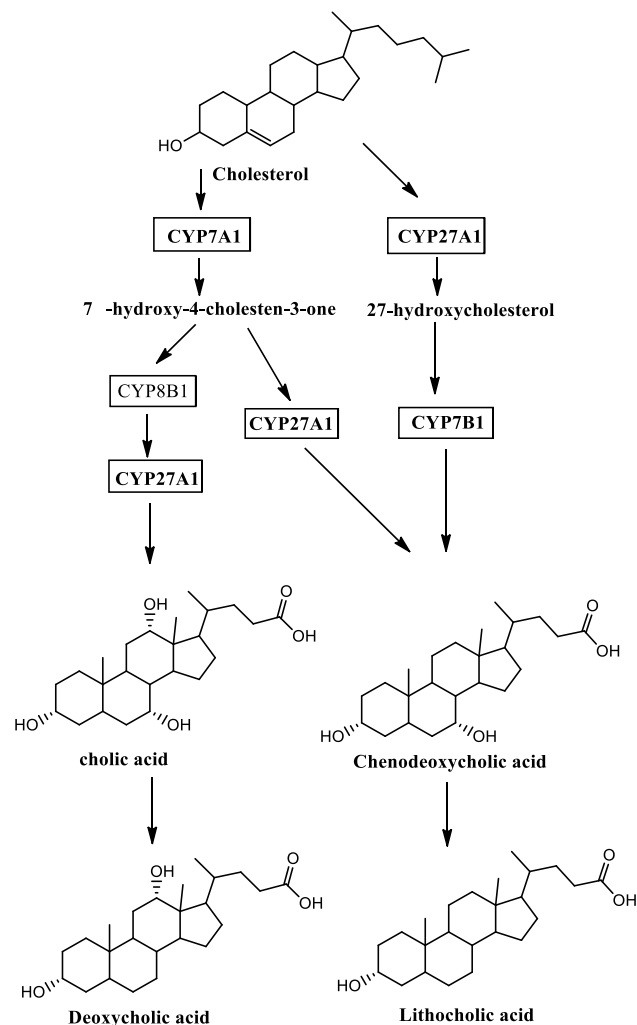


Figure 2. Two pathways of BA synthesis^[21] There are two ways of generating the primary BAs, DCA and LCA. One way is the classic pathway, the other, the

alternative pathway.

1.3 Receptors for BAs and their role in health and disease with focus on FXR and TGR

Two specific receptors have been assigned to BAs. These are the farnesoid X receptor (FXR)^[22] and a G-protein-coupled receptor or GPCR known as GPBAR1 or TGR5^[23]. These play an important role in physiological processes and immune homeostasis. BAs interact with myriad other receptors including the vitamin D receptor (VDR), pregnane X receptor (PXR), muscarinic GPCRs, and constitutive androstane receptor (CAR). However, at present FXR and TGR5 are the assigned bile acid receptors because BAs are the prototypical endogenous ligands for these.

During enterohepatic circulation, BAs synthesis is regulated by FXR on several levels^[24]. Activation of ileal FXR causes upregulation and secretion of Fibroblast Growth Factor 15/19 (FGF 15/19)^[25]. This diffuses to the liver and negatively regulates transcription of cholesterol 7 α -hydroxylase (CYP7A1)^[26], the rate-limiting enzyme for primary BAs synthesis from cholesterol in the classic pathway. This process acts as a negative feedback on bile acid synthesis in response to bile acid retrieval from the intestinal tract postprandially.

BAs are retrieved from portal blood by several highly efficient important proteins including Na⁺-taurocholate cotransporting polypeptide (Ntcp)^[27]. In hepatocytes they bind to the FXR causing an indirect inhibition of CYP7A1 transcription. So FXR activation at ileal and hepatocyte levels negatively regulates bile acid synthesis in response to BAs, for which it acts as a kind of sensor.

Apart from the above physiological function, in regulation of their own formation, BAs also regulate immune homeostasis. BAs exert effects on inflammation

through immune cells and activation of BA sensitive receptors including the FXR and TGR5. Under pathologic conditions, neutrophils are stimulated by BAs to induce inflammation. But BAs have a suppressive influence on Kupffer cells which secrete pro-inflammatory cytokines in animal model of obstructive cholestasis^[28]. Therefore, BAs can have either anti-inflammatory or inflammatory effects depending on different immune cells. On the other hand, activation of dedicated bile acid receptors appears to exert anti-inflammatory effects. FXR has anti-inflammatory effects on the liver and bowel through the interaction with NF- κ B signalling^[29, 30]. Under the combined effects of FXR and TGR5, BAs play a role in controlling inflammatory responses by decreasing immunocyte infiltration^[31]. Besides, BAs themselves such as CDCA, CA and UDCA have direct toxic effect on the intestinal epithelial cells. That is to say, mucosal barrier function is compromised and the intestinal permeability increases, which induces local inflammation. In recent years, clinical observation has indicated that an alteration of BA pool, including a decline in secondary form concentration and an increase in sulfate forms and BAs malabsorption is associated with inflammatory activity in IBD^[32, 33]. For example, studies show a decline in secondary BA concentrations and a rise in the sulfate form of LCA in patients with Crohn's disease (CD) and ulcerative colitis (UC)^[34]. Even though there is link between the alteration of BAs and IBD, there is not much evidence that BAs directly lead to or cause IBD^[35]. There is substantial contradictory evidence that increases in colorectal secondary bile acids associated with changes in diet or in the colorectal microflora, can negatively impact gut health and lead to inflammation and its more sinister long term consequence, cancer. Further work is needed to clarify the effects of the secondary BAs on cell viability and signalling in the colon.

Chapter 2. BAs in modulating apoptosis in the colonic epithelium

2.1 Structure, function and physiology of the colon

The large intestine is anatomically divided into four main regions: the cecum, the colon, the rectum, and the anus^[36]. The colon begins from the end of the small intestine and extends down to the rectum, consisting of six sections: ascending colon, the right colic flexure (hepatic flexure), transverse colon, the left colic flexure (splenic flexure), descending colon, and the sigmoid colon^[37]. It is a 2.5-inch diameter, 5-feet long hollow tube, framing the jejunum and ileum on three sides (**Figure 3**)^[38].

From the inside to the outside, the histological structure of the colon is mucosa, submucosa, muscularis, and serosa. The mucosa is in the innermost layer composing of three cell layers including the epithelium, the lamina propria, and the muscularis mucosae. The last two layers of the mucosa support the epithelium. In the submucosa, lymphatic vessels and blood vessels supply nutrients to the colon^[39]. The muscle contractions in the muscularis make a 36-h peristalsis process. The outmost layer is the serosa^[40].

The mucosal layer is simple columnar epithelium composed of a single layer of cells that forms the wall of the large intestine. The vital functions of the intestinal epithelium are to absorb nutrients and act as a barrier against the harmful waste matter. The renewal process of epithelial cells takes 4–5 days and this process is completed by crypt cells which are the fundamental unit of the colon function^[41]. The stem cells that reside at the crypt base form various new cells including enteroendocrine cells, colonocytes, goblet cells, paneth cells, microfold cells, cup cells, and tuft cells (**Figure 3**). These new cells migrate up,

out of the crypt and renew the colonic epithelium^[42]. Each type of cell has different function and it is listed in the following table (**Table 1**).

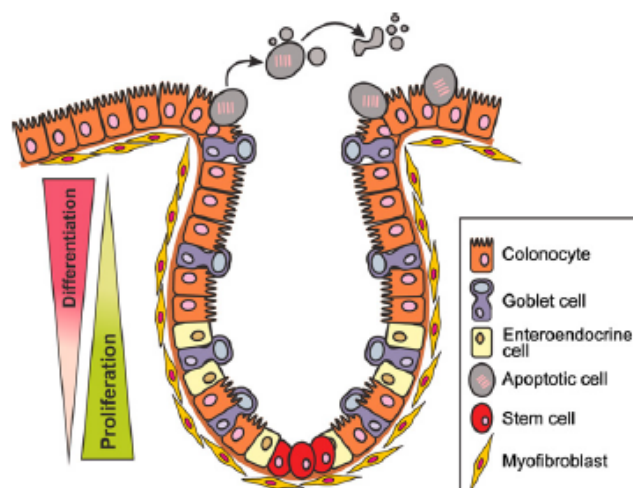


Figure 3. Colonic cells structure^[43]

Cell type	Function
Stem cell	Proliferate and differentiate into other type of cells
Goblet cell	Secrete mucus to protect the mucosa layer
Enteroendocrine cell	Secrete different gut hormones
Paneth cell	Secrete host defense peptides
Microfold cell	Sample antigens
Cup cell	Unknown
Tuft cell	Immune response

Table 1. Cell type and function in the colon^[44]

Though the large intestine is the end of alimentary tract, it does not have digestion functions itself. That is to say, the colon does not play as important a role as the small intestine in nutrient absorption. However, the colon is still a significant organ with many vital functions including absorption, secretion,

bacterial digestion and peristaltic mechanical digestion of food. The water and fat-soluble nutrients are reabsorbed from food residue that passed through the colon. Other unabsorbed wastes are fermented by microorganisms and bacteria^[45]. Goblet cells in the colonic mucosa secrete alkaline liquid to protect the mucosa layer of the colon and moisten faeces to ensure a good bowel movement. Even though the colon does not produce enzymes and digest food, gut bacteria digest cellulose and synthesize various vitamins depending on what vitamins the body needs. The role of the colon is to extract the water, maintain water balance, generate vitamins such as vitamin K, vitamin B1, vitamin B2 and so on, provide a site for flora-aided fermentation and to store the waste in sigmoid.

2.2 Inflammatory diseases of the colon

IBD, being chronic, recurrent inflammation conditions in the intestine, are caused by the aberrant response to microbes in the bowel^[46] and probably results from a complex set of factors such as environment, genetic and immune^[47, 48]. The term IBD includes two distinct diseases, UC and CD, whose cause is unknown. The two diseases affect different parts of the colon. For UC, the surface of the mucosal layer has inflammation and it readily bleeds into the colon. Generally, up to 20% of patients whose entire large intestine is affected while in 30% of patients the disorder affects the rectum^[49]. The whole gastrointestinal tract is affected by CD and the bowel wall inflammation through all layers. These disease sites are interspersed with the normal bowel. Compared with UC, there is 20% of patients with inflammation confined in the colon while its presence in the small intestinal is more common^[49]. IBD becomes more and more common globally^[50]. The factor of diet plays a significant role in the incidence of IBD because several substances have an influence on microbiota composition in the gut. It is also found that restricted diet has a good

effect on childhood CD^[51].

It is common that hepatobiliary diseases and IBD coexist in patients. Among them, the most common one is primary sclerosing cholangitis (PSC)^[52] and the uncommon one is the primary biliary cirrhosis (PBC). PSC is a chronic progressive disease which is characterised by inflammation and fibrosis in bile ducts which resulted in multi-focal biliary duct narrowing (strictures) and hardening (sclerosis). It is associated with IBD with both diseases present together in many patients^[53]. It is reported that the percentage of UC patients with concomitant PSC is 2.4-7.5% and PSC is the most common hepatobiliary disease in the UC patients^[54-58]. The progression of colitis is independent of PSC coexistence^[57]. PBC has some symptoms, such as fatigue and itching, that are similar to PSC but they affect different parts of the hepatobiliary system^[59]. PBC is an autoimmune liver disease characterized by long-term cholestasis and it also results in liver fibrosis and cirrhosis^[60, 61]. As mentioned above, according to clinical history IBD does not have a close association with PBC and the incidence of PBC in IBD patients is rare ^[62, 63] As such it is not certain whether there is some relationship between PBC and IBD^[62].

2.3 Role of apoptosis in the inflammatory disease of the colon

Apoptosis is referred to as programmed cell death regulated at a genetic level^[64]. Programmed or regulated cell death allows injured, senescent or useless cells to be removed without causing inflammation and damage to the microenvironment. It is essential for microenvironment balance, various physiological functions of tissues and pathological reactions^[65].

In human physiology, immature stem cells located in the basement of colon crypts turn into new epithelial cells migrating upward along the microvillus axis

of crypt^[66]. Abnormal colon epithelial cells which reside in the colonic mucosa are eliminated through apoptosis, in such a way that the colon can maintain its turnover and homeostasis^[67]. Under pathophysiological conditions, epithelial cells follow a sequence of proliferation-differentiation-apoptosis along the microvillus axis of crypt^[68].

Under IBD conditions, abnormal apoptosis of intestinal mucosal tissues' cells, such as excessive apoptosis of intestinal epithelial cells and apoptosis of immature stem cells of colonic crypt, break the balance between intestinal epithelial cells' proliferation and apoptosis^[69]. That is to say, the speed of apoptosis is faster than cell compensatory proliferation leading to the damage of epithelial tissue and gut mucosal barrier breakdown. On the other hand, T cells resist apoptosis^[70] in gut mucosa resulting in T cell aggregation which leads to immunological responses targeting intestinal tissues. Collectively these observations indicate that apoptosis plays an important role in IBD. Interactions of BAs, especially secondary BAs with this phenomenon is interesting for understanding disease pathogenesis and progression and opportunities for therapy.

2.4 Role of BAs in causing or preventing colorectal epithelial cell death

As described already here, BAs are synthesized from cholesterol in the liver and secreted to the intestine postprandially, facilitating digestion and absorption of lipids^[71]. In addition to this, it is found that BAs also have influence on causing or preventing the cell death of colorectal epithelial cells with influence on absorption and ingress of substances and bacteria. The epithelial cells interface at the intestinal tract surface and it is, as described, renewed over time^[72].

During this renewal process, some cells are needed to be eliminated and new cells are generated, while BAs can cause the colorectal epithelial cell death and proliferation^[73].

BAs have the capacity to stimulate cell proliferation by activating epidermal growth factor receptor (EGFR) through membrane perturbations in a ligand independent way when at low concentration^[74, 75]. The other way of activating EGFR is that low concentration BAs activate the G protein-coupled receptors (GPCRs) that release some ligands to transactivate the EGFR – for example by causing the release or stimulation of matrix metalloproteinases (MMPs). After the EGFR activation, the extracellular signal-regulated kinase (ERK) and mitogen-activated protein kinases (MAPKs) are activated subsequently that can stimulate cell proliferation^[76] by prostaglandins and cyclooxygenase-2 upregulation. At the same time, the EGFR activation can also stimulate NF- κ B which can prevent cell death. So secondary BAs and the free primary bile acid CDCA are able to act cytoprotectively in some circumstances through stimulation of growth factor pathways (**Figure 4**).

In contrast, when the concentration of BAs is at a high level ^[43], it induces colorectal epithelial cell death that is the intrinsic pathway through reactive oxygen species (ROS)^[77] accumulation first and then mitochondrial membrane permeability (MMP)^[78] and the cytochrome *c* release. Following this, apoptotic protease activating factor 1 (APAF1) is activated by cytochrome *c*, caspases 3,6 and 7 are activated and apoptosis is induced. In other words, the concentration of BAs has an important influence on colorectal epithelial cell proliferation and death. In a further complication, the two effects can co-exist in the same cell type and tissue.

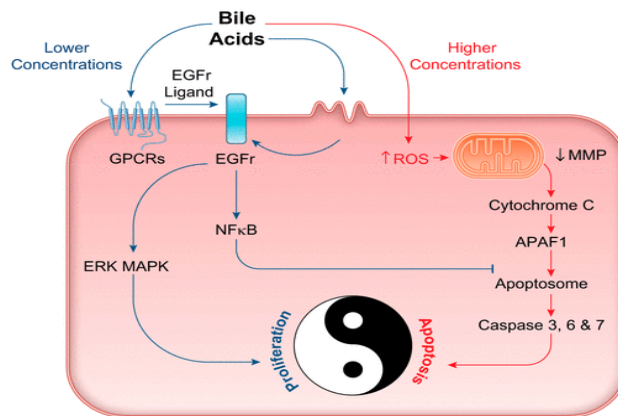


Figure 4. Cell proliferation and cell death regulation by BAs^[79]

2.5 Aims and objectives of the work in this Chapter

It is known that apoptosis plays an important role in the inflammatory diseases of the colon and it is found that some BAs are able to prevent colorectal epithelial cell death. Therefore, the aim of this Chapter is to create a colon apoptosis model and this model was used to screen the cytoprotective actions of BAs compounds in the colon cells.

This chapter describes an attempt to create a colon apoptosis model. It is preferable to trigger colonic cell death by a cocktail of TNF- α (tumor necrosis factor-alpha) and IFN- γ (interferon-gamma) because they are released by the colon epithelial cells to cause cell death under the pathophysiological condition of IBD. However, the cocktails of these two cytokines do not cause obvious apoptosis so alternatively primary BAs was added to create a colon apoptosis model depending on its cytotoxicity. This provides a tool with which to study whether there is a relationship between BAs chemical structure and cytoprotection/cytotoxicity.

2.6 Results for TNF- α , IFN- γ and BAs in causing bile acid induced cell death in colorectal cell lines

2.6.1 Results for TNF- α , IFN- γ effect on proliferation

2.6.1.1 MTT Assay

Caco-2 cells were treated with different concentrations of TNF- α , IFN- γ and cocktail of TNF- α and IFN- γ respectively for 24 h in the 37 °C incubator. 10 μ L of 2.5 mg/mL MTT (3-(4,5-Dimethylthiazol-2-yl)-2,5-diphenyltetrazolium bromide) was added into the supernatant in the last 2 h of treatment. Finally, the medium was removed and formazan was dissolved in 100 μ L DMSO. The 96-well plate was read by absorbance at 570 nm. The vehicle was 1% H₂O in cell medium (DMEM).

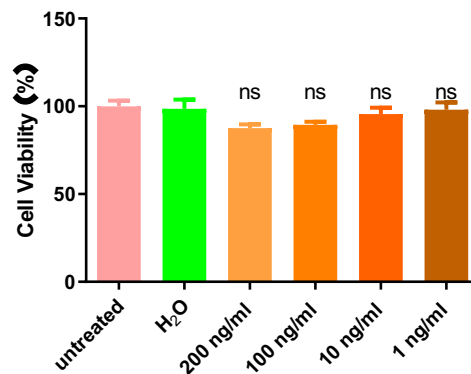


Figure 5. MTT result of TNF- α Caco-2 cells were treated with different concentrations of TNF- α for 24 h in the 37 °C incubator. The vehicle was 1% H₂O. Values of TNF- α were expressed as fold different to the vehicle as mean \pm SEM of triplicate experiments, ns $P > 0.05$ was determined by oneway ANOVA with Dunnett's post-hoc correction.

Figure 5 reveals that there is a modest decrease in the cell viability at 100 ng/ml TNF- α and 200 ng/ml TNF- α . But the difference between 200 ng/ml TNF and

control group is not significant so it means that the 200 ng/mL TNF- α did not have the expected or desired effect on Caco-2 cell proliferation.

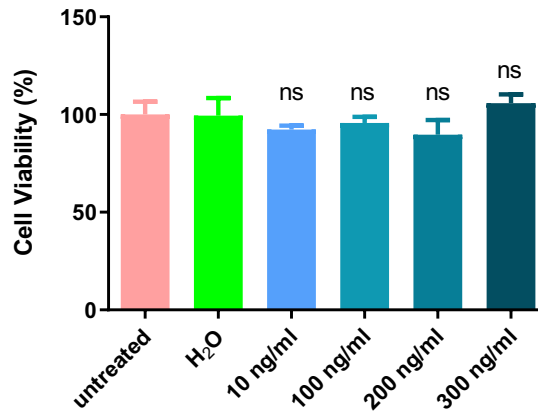


Figure 6. MTT result of IFN- γ *Caco-2 cells treated with different concentrations of IFN- γ for 24 h in the 37°C incubator. The vehicle was 1% H₂O. Values of IFN- γ were expressed as fold different to the vehicle as mean \pm SEM of triplicate experiments, ns $P > 0.05$ was determined by oneway ANOVA with Dunnett's post-hoc correction.*

Similarly, **Figure 6** reveals that there is a slight decrease in the concentration range of IFN- γ from 10 ng/ml to 200 ng/ml while there is mild increase in 300 ng/mL IFN- γ . But the differences between these concentrations and control group are not significant suggesting that at these concentrations of IFN- γ do not affect Caco-2 cell proliferation as measured by MTT.

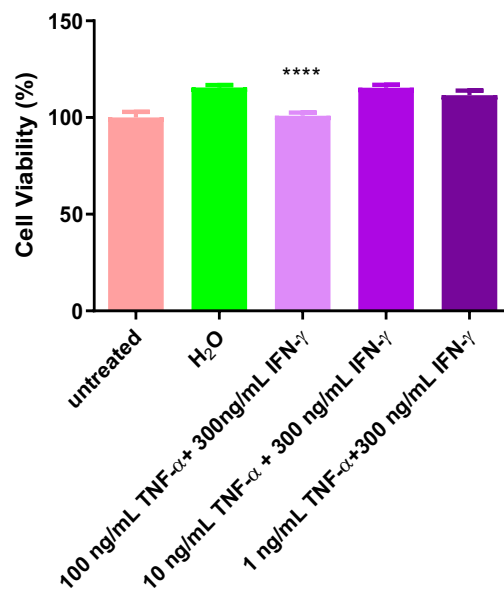


Figure 7. MTT result of mixture of TNF- α and IFN- γ *Caco-2 cells treated with different concentrations of TNF- α and IFN- γ for 24 h in the 37°C incubator. The vehicle was 1 % H₂O. Values of TNF- α & IFN- γ were expressed as fold different to the vehicle as mean \pm SEM of triplicate experiments, **** P <0.0001 was determined by oneway ANOVA with Dunnett's post-hoc correction.*

Figure 7 shows that the mixture of 100 ng/mL TNF- α and 300 ng/mL IFN- γ has an effect on reducing cell proliferation, which was significant statistically. But other concentrations of cocktails of TNF- α and IFN- γ do not cause much cell viability inhibition of Caco-2 cells.

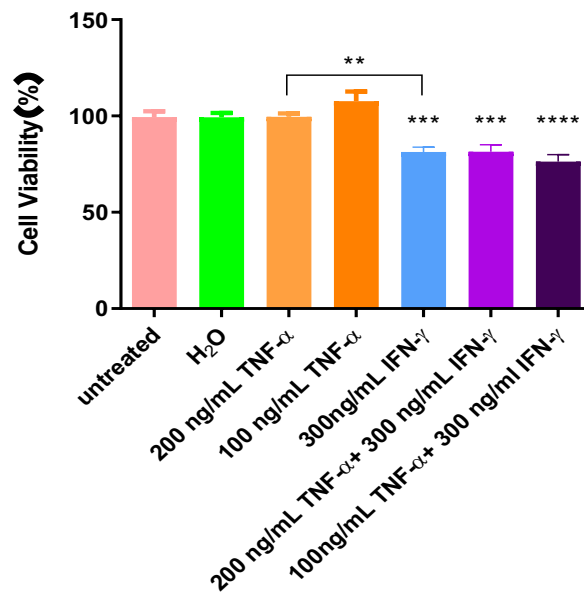


Figure 8. MTT result of TNF- α and IFN- γ *HT-29 cells were treated with different concentrations of TNF- α and IFN- γ for 24 h in the 37°C incubator. The vehicle was 1 % H₂O. Values were expressed as fold difference compared to the vehicle as mean \pm SEM of triplicate experiments, ** p <0.01, *** p <0.001, **** P <0.0001 was determined by oneway ANOVA with Dunnett's post-hoc correction and by t test.*

Figure 8 shows that IFN- γ has stronger effect on cell viability compared with TNF- α on the HT-29 cells but it does not cause much cell death which is less than 20 %). In order to determine if a low level of apoptosis was occurring that was not detectable by MTT, we characterized the treated cells using a flow cytometry PI protocol that could detect the uptake of propidium iodide into late apoptotic cells. As shown in **Table 2** there was a negligible increase in apoptotic cells in HT-29 cells treated with TNF- α and IFN- γ . Nevertheless, this kind of approach appears to be most appropriate for studying the effect of IBD relevant cytokines on cell death in colorectal cell culture.

2.6.1.2 Flow cytometry

Caco-2 cells were treated with different concentrations of TNF- α , IFN- γ and

cocktail of TNF- α and IFN- γ respectively for 24 h in the 37 °C incubator. Cells were trypsinized and neutralized with 10% FBS cell medium (DMEM) after 24 h incubation. Cell pellets were collected after being spun down and resuspended in 200 μ L PBS. 12.5 μ L RNase (10mg/mL) and 37.5 μ L propidium iodide (1 mg/mL) were added and then cells were incubated at room temperature for 30 min avoiding from direct light. Finally, flow cytometry was run in the BD Accuri C6 flow cytometer.

Sample	Apoptosis %	G0G1 %	S %	G2M %	M1 %
PBS vehicle	0.6	53.0	2.6	24.1	16.1
Cell Media	0.7	46.4	4.9	21.6	20.2
IFN 30 ng/mL	0.7	47.1	4.8	22.5	18.6
TNF 100 ng/mL	1.6	60.4	6.1	16.8	11.1
TNF200 ng/mL					
IFN 30 ng/mL	1.7	51.9	7.2	17.6	15.5
TNF100 ng/mL					
IFN 30 ng/mL	1.3	57.0	6.8	18.0	12.4
TNF200 ng/mL	2.0	55.1	8.7	15.6	13.2

Table 2. Flow cytometry result of TNF- α and IFN- γ *HT-29 cells were treated with different concentrations of TNF- α and IFN- γ at around 80% confluency for 24 h in the 37°C incubator before fixing and staining with PI. The vehicle was PBS. Values were expressed as mean \pm SEM of one experiment.*

2.6.2 Results for effect of secondary BA on Caco-2 cell proliferation

Caco-2 cells were treated with different concentrations of BAs respectively for 24 h in the 37 °C incubator. 10 μ L of 2.5 mg/mL MTT was added into the supernatant in the last 2 h of treatment. Finally, the medium was removed and formazan was dissolved in 100 μ L DMSO. The 96-well plate was read by absorbance at 570 nm. The vehicle was 1% DMSO.

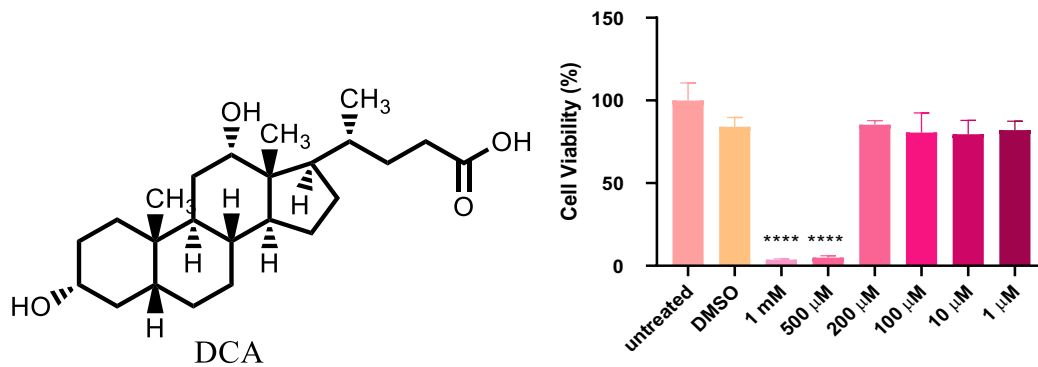


Figure 9. MTT result of DCA *Caco-2* cells were treated with different concentrations of DCA for 24 h in the 37°C incubator. The vehicle was 1 % DMSO. Values of DCA were expressed as fold different to the vehicle as mean \pm SEM of triplicate experiments, **** P <0.0001 was determined by oneway ANOVA with Dunnett's post-hoc correction.

Figure 9 shows that the cell viability effect of DCA depends on the concentration. When the concentration is equal or lower than 200 μ M DCA, there is no significant difference with the control group.

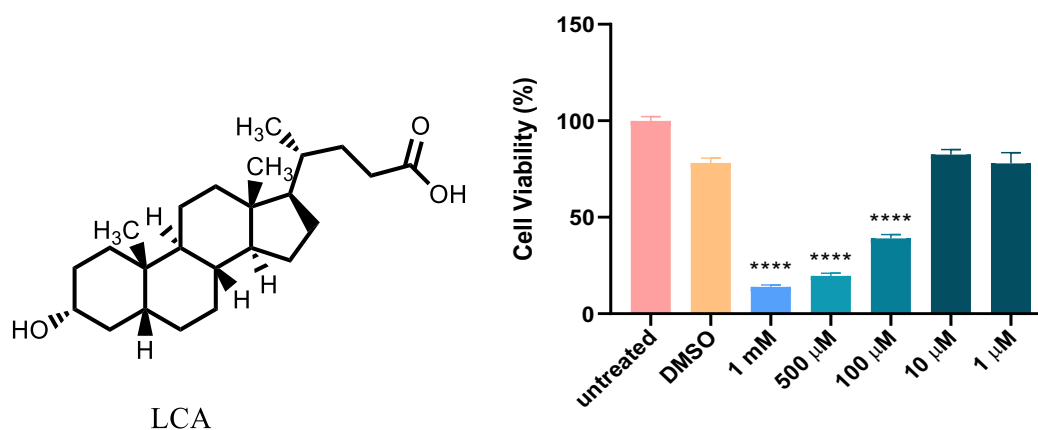


Figure 10. MTT result for LCA *Caco-2* cells were treated with different concentrations of LCA for 24 h in the 37°C incubator. The vehicle was 1% DMSO. Values of DCA were expressed as fold different to the vehicle as mean \pm SEM of triplicate experiments, **** P <0.0001 was determined by oneway ANOVA with Dunnett's post-hoc correction.

The cell viability trend of LCA is similar with the DCA, which depends on the concentration. But the LCA had a larger cytotoxicity effect on Caco-2 cells compared with DCA. It did not cause cell death when the concentration was < 10 μM .

2.6.3 Results for LCA derivatives effects on Caco-2 cell viability in the MTT assay

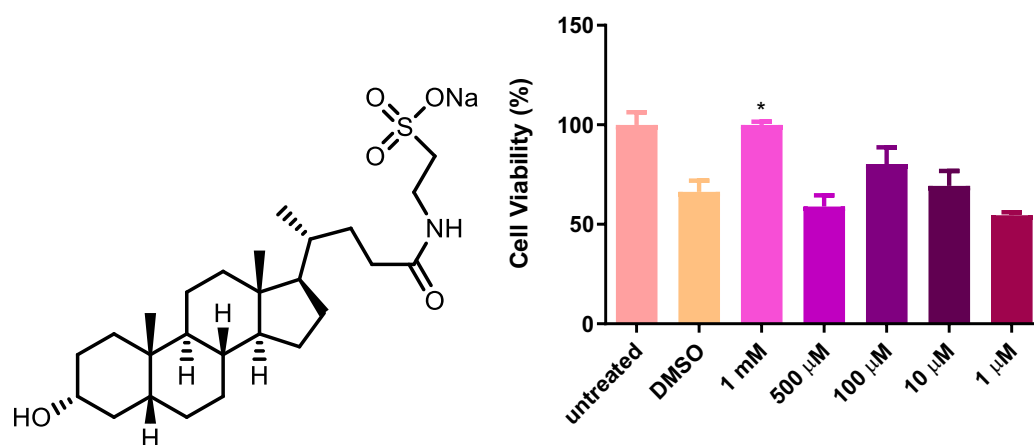


Figure 11. MTT result of sodium TLCA Caco-2 cells were treated with different concentrations of sodium TLCA for 24 h in the 37°C incubator. The vehicle was 1 % DMSO. Values of TLCA were expressed as fold different to the vehicle as mean \pm SEM of triplicate experiments, * $P < 0.05$ was determined by oneway ANOVA with Dunnett's post-hoc correction.

Next, we examined another derivative of LCA, its 3-sulfate metabolite (**Figure 12**) which can be produced in the intestinal wall and is relevant to the physiology of the colon. Surprisingly, treatment with LCA 3-sulfate caused a significant increase in cell proliferation in a concentration dependent manner with greatest effect at 1 mM (**Figure 11**). This may mean that the 3-sulfate can exert a proliferative or even cytoprotective effect in the colon and oppose the

pro-inflammatory effect of other BAs and microflora metabolites. The difference in toxicity between LCA and its 3-sulfate is striking, even if it is more polar.

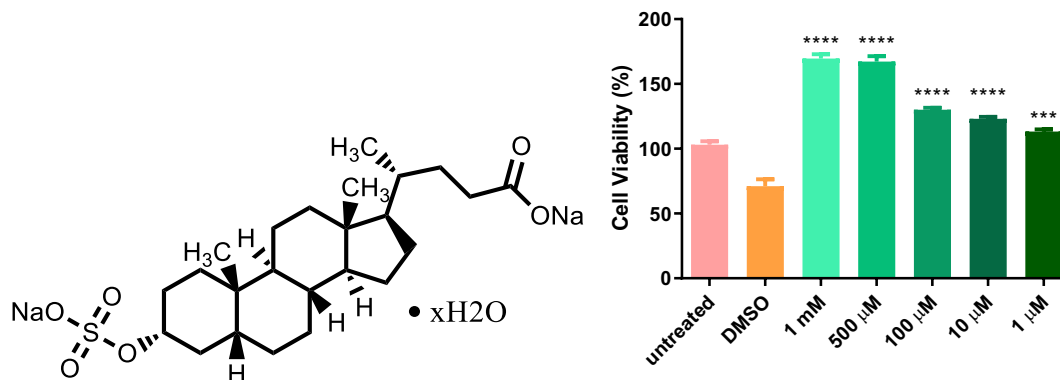


Figure 12. MTT result of LCA 3-sulfate *Caco-2 cells were treated with different concentrations of 3-sulfate LCA for 24 h in the 37 °C incubator. The vehicle was 1 % DMSO. Values of LCA 3-sulfate were expressed as fold different to the vehicle as mean \pm SEM of triplicate experiments, *** $p < 0.001$, **** $P < 0.0001$ was determined by oneway ANOVA with Dunnett's post-hoc correction.*

TLCA 3-sulfate also exerted a significant proliferative/cytoprotective effect on Caco-2 cells that was again unlike its free analogue LCA (**Figure 13**). The effect on cell proliferation depends on the concentration with greatest effects seen at higher concentration. This is contrary to what we expected because in the free BAs that are not 3-conjugated, higher concentrations in the millimolar range cause cell death through multiple mechanisms.

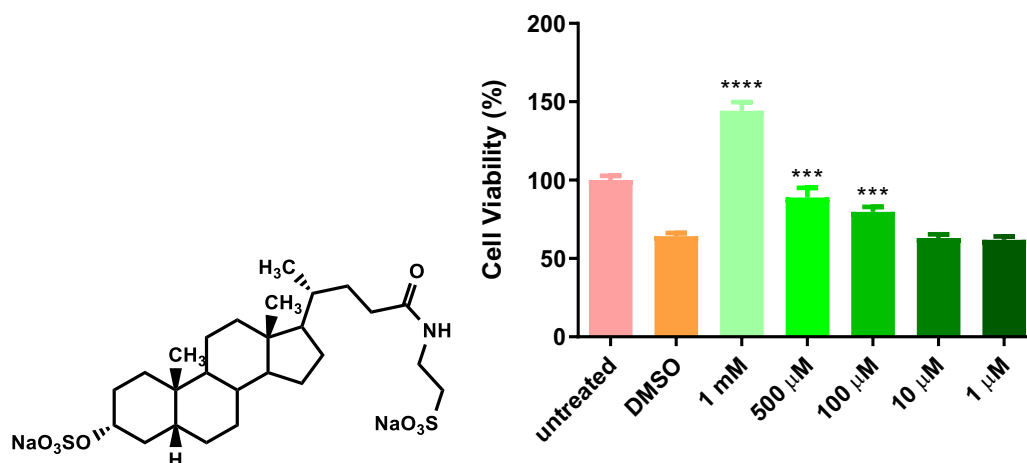


Figure 13. MTT result of TLCA 3-sulfate *Caco-2* cells were treated with different concentrations of TLCA 3-sulfate for 24 h in the 37 °C incubator. The vehicle was 1 % DMSO. Values of TLCA 3-sulfate were expressed as fold different to the vehicle as mean \pm SEM of triplicate experiments, *** $p < 0.001$, **** $P < 0.0001$ was determined by oneway ANOVA with Dunnett's post-hoc correction.

2.6.4 Result for treatment with DCA and combination with TNF- α

Because of the difficulties in obtaining a consistent anti-proliferative effect by the cytokine cocktail by itself we conducted several studies to see the effect of including DCA in order to generate a better model for screening for cytoprotection effect. DCA even at low concentration was able to induce *Caco-2* cell death in combination with TNF- α (**Figure 14**). It was concluded that DCA alone or in cocktail could be a better option for a model of colon cytotoxicity with which to screen for cytoprotection effects of potential UDCA cytoprotection analogues. It is unlikely that the TNF is able to contribute to the effect of DCA under these circumstances because TNF did not exert an effect by itself. Nevertheless, the DCA concentration is low considering the magnitude of the effect.

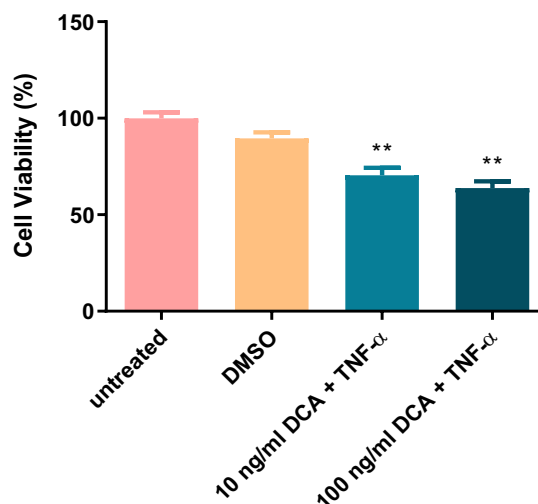


Figure 14. MTT result of cocktail of DCA and TNF- α *Caco-2 cells were treated with different concentrations of DCA with 200 ng/mL TNF- α for 24 h in the 37 °C incubator. The vehicle was 0.5 % DMSO. Values were expressed as fold difference to the vehicle as mean \pm SEM of triplicate experiments, ** $p < 0.01$, was determined by oneway ANOVA with Dunnett's post-hoc correction.*

2.6.5 Studies into the potential cytoprotective effect for 3 α -hydroxy-7 β -(methanesulfonamido)-5 β -cholanoate (**35**) with DCA induced cell death as a model of pathophysiological epithelial apoptosis

Compound **35** is a UDCA analogue that has shown cytoprotective characteristics in the liver cell line Huh 7 (data from the Gilmer group, Gavin PhD). This compound is potentially of interest in the treatment of chronic liver disease conditions involving a cholestasis dimension for example PBC and PSC. Since IBD is an important comorbidity in PSC it was of interest to see if the cytoprotective effects of this compound evident in the liver cell line could be recapitulated in the colon cell line. This might indicate increased potential in PSC treatment but also possible application in IBD where inappropriate apoptosis is a disease driver. The Caco-2 cell line was therefore treated with the compound **35**, first without any apoptosis stimulus – to ensure that the compound itself caused neither proliferation nor inhibition of proliferation.

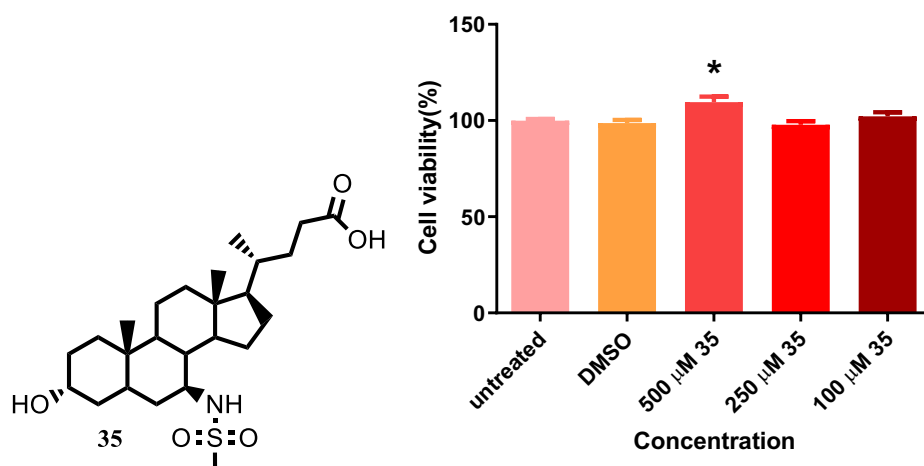


Figure 15. MTT assay result of 3 α -hydroxy- 7 β -(methanesulfonamido)-5 β -cholanoate (35) *Caco-2* cells were treated with different concentrations of compound and 35 for 24 h in the 37 °C incubator. The vehicle was 0.5 %DMSO. Values were expressed as fold difference to the vehicle as mean \pm SEM of triplicate experiments, * p <0.05, was determined by oneway ANOVA with Dunnett's post-hoc correction.

The data in **Figure 15** show that **35** does not reduce cell proliferation in the concentration range 100 to 500 μ M with a suggestion that it may even increase proliferation at highest concentration.

Next, we studied the effect of **35** on cells that were cotreated with DCA to determine its potential to exert a cytoprotective effect, that is to prevent DCA-induced cell death or reduction in cell proliferation. The data for the cotreatment experiment is presented in **Figure 16**. It shows that **35** affects cell proliferation in manner that depends on DCA concentration. When the concentration of DCA is higher than around 350 μ M, **35** has cell protection effect i.e. it reduces the inhibitory effect of DCA. When cells were treated with compound **35** and DCA at lower concentration, the cell viability was reduced compared to treatment with DCA alone.

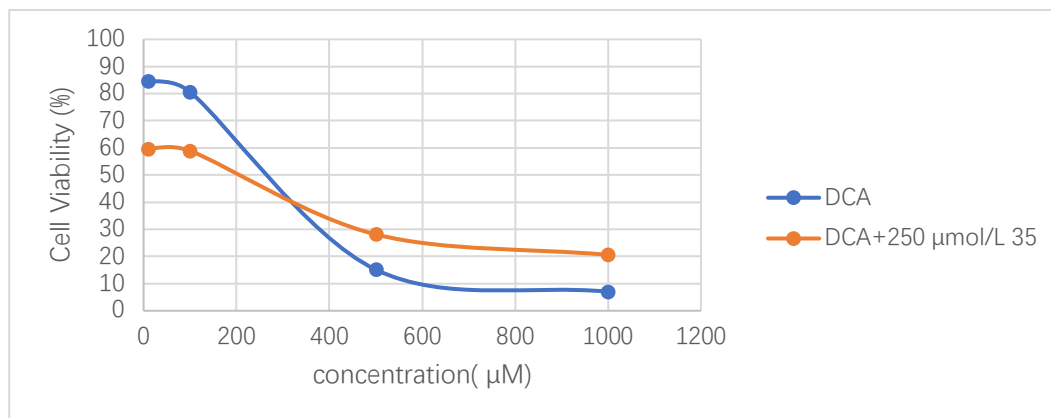


Figure 16. MTT assay result of DCA and 3 α -hydroxy-7 β -(methane sulfonamido)-5 β -cholanoate (35) *Caco-2* cells were treated with 250 μ M 35 for 24 h followed by adding different concentrations of DCA. The vehicle is 1% DMSO.

2.6.6 Discussion

The main objective of this Chapter was to establish a cell culture model of colonic apoptosis that would be relevant to IBD so that compounds could be screened for their potential to elicit a cytoprotective effect. This was achieved to a limited extent using DCA to stimulate apoptosis in *Caco-2* cells and we were able to witness a modest protective effect from compound **35**, a UDCA analogue produced in this lab. Although cell death can be induced by secondary BAs, we chose to look first at models incorporating TNF- α since this is a pathophysiologically relevant cytokine produced in IBD. Furthermore, it is believed that TNF- α causes disease progression in part through triggering apoptosis in the colorectal mucosa. Surprisingly there was little evidence of cell death in response to TNF- α in *Caco-2* or HT-29 cell culture following 24 h treatment. The data are inconsistent with several literature reports including from the Laukens group^[80]. In this work cell death was reportedly detected using a highly sensitive apoptosis protocol. It was further suggested in this work that the apoptotic effect of the cytokine cocktail could be blunted by treatment with TUDCA which made this an attractive approach potentially for screening new

bile acids for cytoprotective effects. It was possible that the level of apoptosis achieved in the present work by TNF- α and TNF- α / IFN- γ cocktails was not reflected in a reduced cell MTT signal since this measure overall metabolic activity in the cell population. A more sensitive assay detecting apoptosis against a negative background may have been more suitable to detect a pro-apoptotic effect and its rescue by potentially cytoprotective BAs. However, when we studied HT-29 treatment with the cytokine cocktail using flow cytometry with PI staining, there was no evidence of increased apoptotic cells. It is possible that the sensitivity of TNF- α receptor was reduced due to the high passage number of the cells used so IFN- γ was added in order to enhance the sensitivity through increase in TNF- α receptor number. However, the effect on cell death was still not obvious. Having failed to generate a useful model of epithelial cell death in response to cytokines we turned our attention to secondary BAs that are known to induce cell death through necrosis and apoptosis. The MTT assay was used to test the cell viability in response to secondary BAs, DCA and LCA. It was possible to detect a cytotoxic effect of these two secondary BAs, although there are experimental difficulties caused by the undesirably high level of DMSO required to introduce the BAs into solution at high concentration. It is a puzzle in the BA field that many observations about these BAs are made in the context of concentrations in water that are unachievable considering their very low aqueous solubility (<30 μ M). LCA and DCA caused around 50% reduction in MTT response at 24 h at around 100 μ M. Surprisingly, TLCA caused a modest stimulatory effect at 1 mM but no cell death compared with DMSO alone. More surprisingly, LCA sulfate and to a lesser extent its tauro-analogue TLCA sulfate both caused a significant increase in proliferation compared with DMSO treatment alone in the treatment range 0.1-1 mM. This was also a concentration dependent effect. This effect may be worth further study because it shows potential for the LCA metabolites to contribute to homeostatic resolution of colorectal inflammation and potential application of

these substances to regulate colorectal inflammation. In the liver, primary BAs are produced from cholesterol and then conjugated with taurine or glycine.^[81] After being released to the intestine, conjugated primary BAs turns into free secondary BAs, DCA and LCA, through complex dehydroxylation reaction lead by colonic bacteria. After that, these secondary BAs are reabsorbed to liver where DCA is also conjugated with taurine or glycine but LCA is conjugated with sulfates.^[82] During the enterohepatic recycling, the LCA-sulfates are released to the small intestine where only small amount of them is absorbed to the liver and the rest of them transports to the large intestine. The LCA-sulfates are desulfated in the large intestine then the released sulfate and some unconjugated LCA are resorbed to the liver while other LCA is excreted in feces. In the systemic blood, LCA-sulfates are extracted in urine because of its higher solubility. It is well-known that UDCA has cytoprotective actions and anti-inflammatory. Compared with UDCA, LCA is capable of reducing cytokine (TNF- α , IL-6, IL-1 β , IFN- γ) release from colon epithelial cells more potently and the ability of suppressing mucosal inflammation in the DSS (dextran sulfate sodium) model of colitis.^[83] In contrast to LCA physiologic functions, LCA is cytotoxic BA and it causes colonic membrane disruption resulted from its detergent properties.^[84] It is found that LCA-sulfates are the most common status of conjugated LCA in the liver and intestine. After LCA is 3-sulfated , its water solubility increases resulting in more elimination and its micellar critical concentration increase lead to eliminate detergent properties against colon membrane.^[85] Besides above side effects, LCA also has hepatobiliary toxicity that induce to cholestasis but this cholestatic activity can be prevented by the taurine-amidation LCA-sulfates.^[86] It is valuable to explore the potency and cellular actions of TLCA and LCA-sulfates.

Finally, the putative cytoprotective compound **35**, a sulfonamide analogue of UDCA was studied first by itself for its effects on cell viability of Caco-2 cell

culture. As already seen in Huh 7 cells from the liver, this compound is without toxic effects even at high concentration in colorectal cell lines. This is a peculiar feature for a free bile acid analogue to not be at all toxic and it is consistent with its putative cytoprotective effects. The potential for these in colon cell culture was then studied in combination with DCA at concentration levels at which this bile acid causes cell death. There was some evidence of cytoprotection in the presence of high concentrations of DCA, but at lower concentrations there was a reduction in cell viability. The next Chapter is partly dedicated to further biochemical evaluation of **35** in the context of its anti-inflammatory effects and investigations into the GR activating effects of BAs.

Chapter 3. UDCA analogues as anti-inflammatory agents in cholestatic disease

3.1 Glucocorticoids (Natural and Synthetic GCs)

The term glucocorticoid (GCs) refers to a collection of endogenous steroid hormones^[87, 88] and their synthetic analogues unified by their ability to activate the glucocorticoid receptor (GR)^[89]. Compounds in this class, whether endogenous or exogenous, exert important influence on metabolism and on immune responses.

The main endogenous glucocorticoid is cortisol (**Figure 17**). The synthetic version of this is known as hydrocortisone ((11 β)-11, 17, 21-trihydroxypregn-4-ene-3, 20-dione). Cortisol is produced in the cortex of adrenal glands. Within the cell it can be metabolised to cortisone by the enzyme 11 beta-hydroxysteroid dehydrogenase 1 (11-beta-HSD1)^[90]. Conversely, cortisone is converted into cortisol by 11 beta-hydroxysteroid dehydrogenase 2 (11-beta-HSD2)^[90] (**Figure 17**). The balance of glucocorticoid activity within a cell can be influenced by whichever is the more abundant enzyme. Cells with high levels of HSD1 will have low levels of cortisol or hydrocortisone activity. Cells with high levels of HSD2 will conversely have high levels of cortisol activity. These enzymes are therefore important modern drug discovery targets because of their influence on overall tissue glucocorticoid ‘tone’.

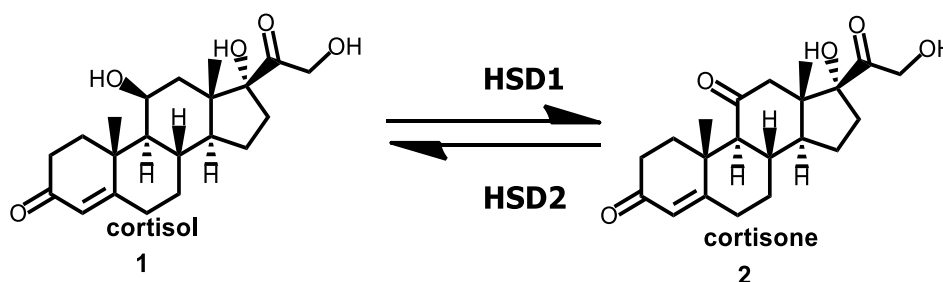


Figure 17. Interconversion between cortisol and cortisone

Cortisol has two basic physiological influences including immune system^[91] suppression and carbohydrate, fat and protein metabolism regulation. Cortisol can suppress the immune system and it also can reduce inflammation^[91]. Its synthetic forms and analogues are therefore described as immunomodulatory^[92]. Cortisol inhibits the production of substances that result in inflammation such as IFN- γ , IFN- α , TNF- α , interleukin-12 (IL-12). However, it increases IL-4, IL-10 and IL-13. For metabolic response, in the fasting state, cortisol stimulates gluconeogenesis or glycogenesis at different stages in order to maintain and increase blood sugar level in the body. Cortisol levels therefore correspond to diurnal variation in energy demand, and are highest in the morning.

Apart from these two essential functions, cortisol also has an effect on sympathetic nervous system activation, blood vessel constriction, bone formation and myriad other physiological systems^[93]. Moreover, cortisol as a naturally-occurring glucocorticoid is able to transmit signals through mineralocorticoid receptors (MR). The MR, which regulates sodium retention at kidney level^[94] and which also plays an important role in the central nervous system (CNS)^[95] is activated by cortisol, but less so by its synthetic analogues such as prednisolone as described below. The endogenous agonist for MR, aldosterone, is produced in much lower quantity than cortisol in the body. MR, which also has a lower prevalence in humans than cortisol, can be protected from undesired activation by endogenous cortisol through local deactivation by HSD enzymes in a form of selectivity sometimes referred to as enzyme gated^[96].

As mentioned, beyond the natural adrenal corticoids there are also many widely used synthetic GCs that have significant clinical utility of anti-inflammation and immunosuppression. They are frequently used anti-inflammatory drugs which

are effective in fighting inflammation caused by numerous immune system disorders ranging from IBD to autoimmune diseases, haematological cancers and neurological disorders. The glucocorticoid drugs have a basic chemical structure of steroid core carbon skeleton the same as endogenous GCs. **(Figure 18)**

In order to decrease the adverse effects and improve the pharmacologic effect and selectivity, many man-made GCs have been produced. Because of the chemical modification such as functional groups changes, these synthetic GCs are more selective for the GR than the mineralocorticoid receptor (MR)^[97], whose activation is responsible for sodium retention. For example, prednisolone (**4**) is more potent by around 5-fold than cortisol with 1/6 of MR activity activation of cortisol. Dexamethasone (**3**) has an over forty-fold increase in GR activity activation and much less MR activity activation than cortisol.

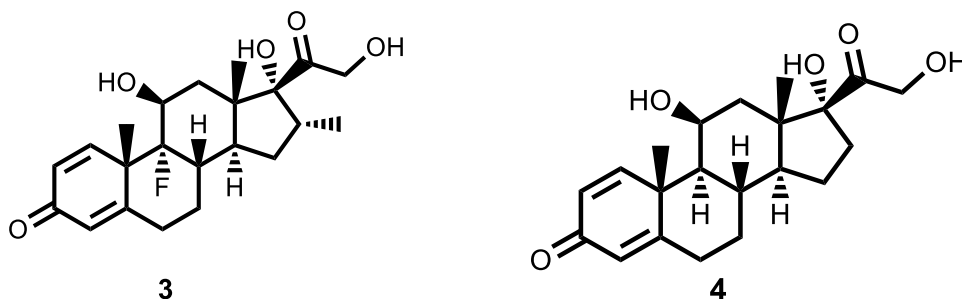


Figure 18. Clinical synthetic GCs Dexamethasone (3) and prednisolone (4)

Aside from the treatment of inflammation^[98, 99], other synthetic GCs and derivatives such as beclomethasone, betamethasone, mometasone, fludrocortisone and so on. are used to treat a wide range of health conditions^[100] including allergies (respiratory reactions, skin responses, anaphylaxis), endocrine issues, adrenal insufficiency, rheumatological diseases, asthma^[101], gastrointestinal problems and so on.

3.2 Side effect of GCs

GCs can exert many beneficial effects and they have widespread use and almost indispensable status in modern medicine. However, GCs cause serious side effects with chronic use^[102]. Some of these include blood sugar level increase that can trigger short-term or permanent diabetes, water retention, weight gain, thinning of skin, immune system suppression, wound healing delay and reduction in bone density^[103]. The collective term for the undesirable human responses to chronic GC use is 'Cushing's Syndrome'. As of yet, and despite many efforts, there are no GCs that only have an anti-inflammatory effect without adverse effects.

3.3 GR Signaling Pathway

In order to understand the reasons for the many effects of the GCs it is necessary to consider their mechanism of action (MOA). Through genomic mechanisms, the GCs activate the GR in the cytoplasm^[104-106]. GR activation followed by translocation and transactivation resulting in a wide range of effects^[107]. Whereas, the other way, transrepression, leads to the decrease in the expression of proinflammatory proteins. Transrepression does not induce the adverse effects of GCs and much effort has been devoted to identifying or designing substances that might cause selective transrepression effects. The GR, a transcription factor activated by a ligand, is localized in the cytosol together with various proteins as heterocomplexes including heat shock protein 90 (hsp90)^[108], heat shock protein 70 (hsp70)^[109] and the immunophilin FKBP52 (FK506-binding protein 52)^[107]. After a glucocorticoid diffuses into the cell, usually through passive transport, it binds to the GR. The receptor dissociates from the heterocomplexes, exposing a nuclear localisation signal. The ligand-bound receptor moves to the nucleus by active transport where it is found as monomers or homodimers (**Figure 19**). The activated GR has two

kinds of direct transcriptional response^[110, 111]. One direct mechanism of action is transactivation. The homodimers bind to glucocorticoid response elements (GREs)^[112] and induces gene transcription that regulates over 100 genes. In this way, some of these genes code for anti-inflammatory proteins and some for proteins involved in inflammation. The homodimeric receptor^[113] may also bind directly to DNA in a manner that suppresses transcription. This is called cisrepression. The other mechanism of action is transrepression. The monomeric form of the receptor can interact with the transcription factors such as NF- κ B or activating protein-1 (AP-1)^[114], which can stop them binding their target genes. This kind of glucocorticoid effect is presumed to exert an anti-inflammatory effect through decreased expression of cytokines such as IL-1 β , IL-8, TNF- α (**Figure 19**).

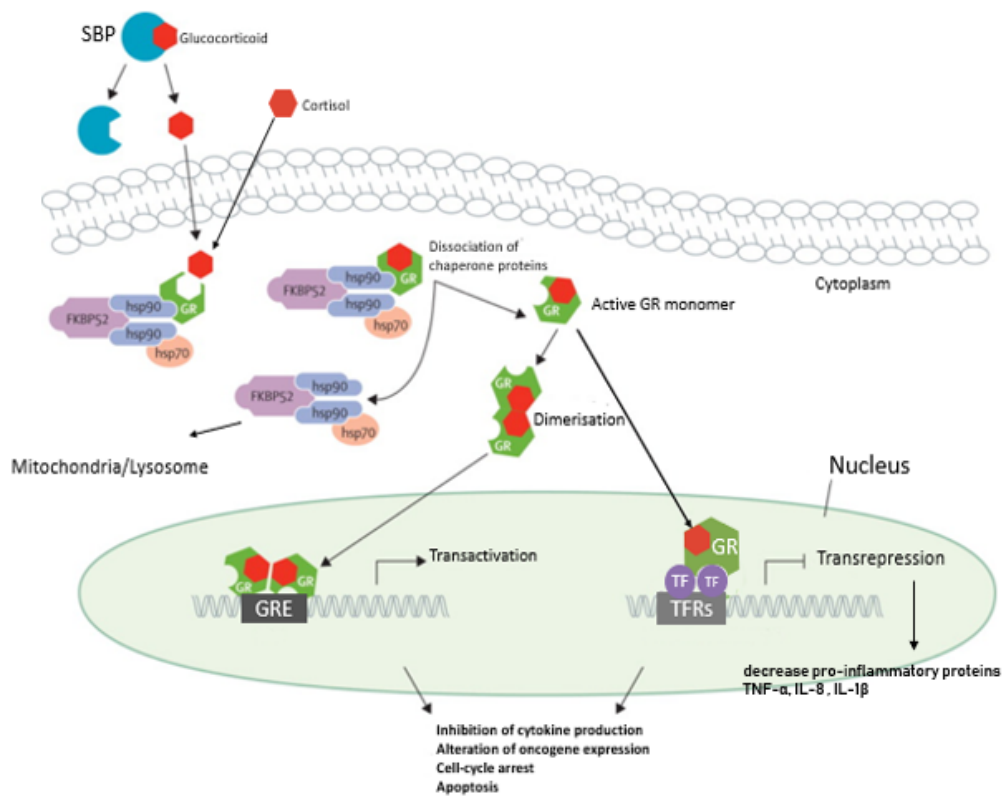


Figure 19. GR Signaling Pathway ^[115, 116]

SBP: steroid binding proteins; GREs: glucocorticoid responsive elements; TFREs: transcription factor responsive elements; HSPs: heat shock proteins; TF: transcription factor.

3.4 NF- κ B Signaling Pathway

NF- κ B (nuclear factor kappa-light-chain-enhancer of activated B cells)^[117], a protein complex, is a family of transcription factors in many mammalian cell types. It plays a key role in DNA transcription, cellular survival, cytokine production and also is involved in regulating inflammatory response.^[118] As we have seen it plays a key role in transmitting signals originating from TNF- α binding at the cell surface. Molecular NF- κ B is a homodimer or heterodimer formed by the NF- κ B family proteins. As of now, it is found that in mammals the NF- κ B family has five members including RelA (p65), RelB, c-Rel, NF- κ B1 (p50/p105) and NF- κ B2 (p52/p100). In the N-termini of dimers, each protein of the NF- κ B family has a Rel homology domain (RHD) consisting of a nuclear localization signal (NLS)^[119], a DNA binding region and a dimer region.^[120] These three regions have corresponding functions of combining with enzyme complexes of I κ B family, binding the κ B sequence on the DNA chain and forming dimers with homologous or heterologous subunits. Beyond that, in their C-termini, p65, RelB and c-Rel share a transactivation domain that can regulate transcription factors in order to active transcription. But p50 and P52 do not have this domain so they are not able to active transcription. Among dimers, p50/p65 dimer^[121] is the most common present in almost all cells^[122]. Under resting state, NF- κ B protein dimers are associated with I κ B proteins which causes them to be retained in the cytoplasm. The I κ B protein family^[123] containing I κ Ba, I κ Bb and I κ Bg are inhibitors that can bind to the RHD and modulate the function of NLS. Therefore, the first step of the activation of NF- κ B molecular is to dissociate the NF- κ B protein from the NF- κ B protein inhibitors allowing the trafficking of NF- κ B dimers to the nucleus.

There are two principal signalling pathways of NF- κ B activation process^[124]. One pathway of NF- κ B activation is the canonical/classical cascade signalling,^[125] beginning from the pro-inflammatory cytokine receptors binding

the ligand. When the extracellular signals are transferred across the cytomembrane through the receptors, the I κ B kinase (IKK)^[126] complex is activated. The complex is composed of a heterodimer of the IKK α , IKK β catalytic subunits and an IKK γ regulatory subunit termed NF- κ B essential modulator (NEMO). The I κ Bs of the IKK complex are activated by phosphorylation and then serines 32 and 36, located in I κ B α , are phosphorylated. After the phosphorylated I κ B α proteins have undergone a ubiquitination process, they are degraded by the 26S proteasome. The released p50/p65 dimers enter the nucleus, bind κ B site of the specific gene and active gene transcription^[127].

The other activation cascade affecting NF- κ B is called non-canonical/alternative pathway cascade^[128]. This pathway is independent of the classical cascade. It activates the NF- κ B dimer of p100/p105. In specific cell types, when activated by the signal transferred by the LT- β or BAFF receptor from outside the cell, the NF- κ B inducing kinase (NIK) induces the IKK α homodimers phosphorylation and then NF- κ B2/p100 sites of the IKK α homodimers is phosphorylated at C-terminal portion. Phosphorylation, polyubiquitination and proteasomal degradation at these sites let the large precursor p100 process to the activated NF- κ B subunits p52-RelB dimers due to the reason that p100 is united with RelB most commonly. The p52-RelB dimers translocate from the cytoplasm into the nucleus, bind to the target gene and active gene transcription^[129].

In conclusion, NF- κ B signalling pathway serves a dual function: it can mediate inflammation and promote apoptosis. The type and number of NF- κ B subunit plays a decisive role in apoptosis. When p65 (RelA) is overexpressed, the NF- κ B pathway can inhibit apoptosis. On the other hand, the NF- κ B pathway can promote apoptosis when the expression of c-Rel is increased^[130]. In pathophysiological process such as immunity, inflammation, cancer formation

and so on, NF- κ B signaling pathway has an effect on suppressing apoptosis [131-133].

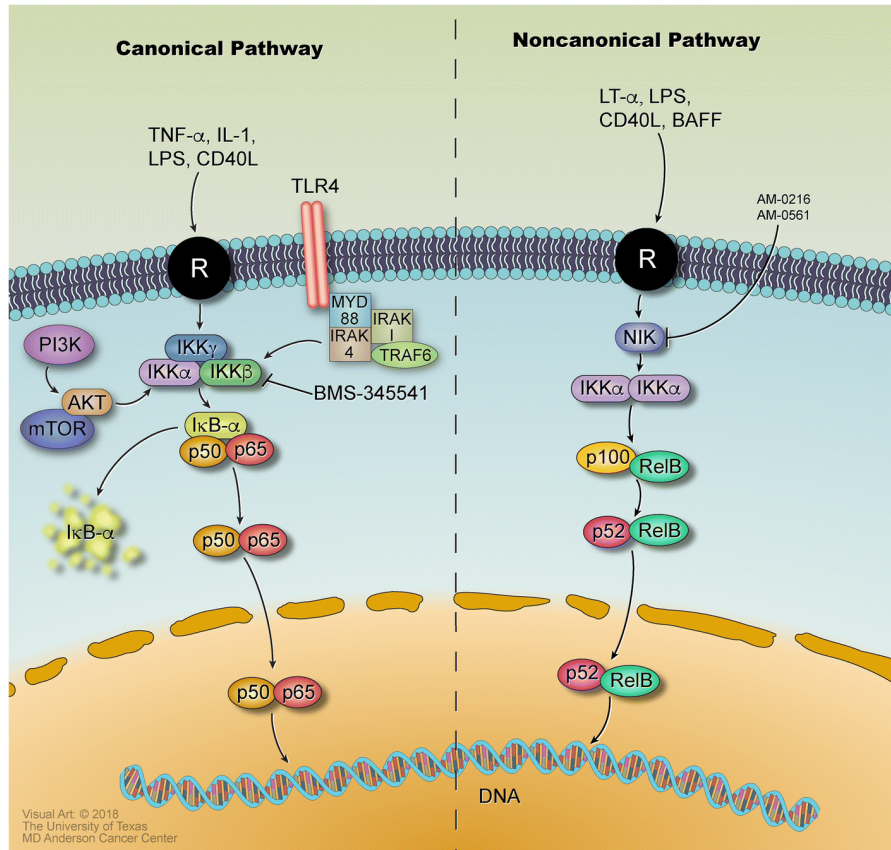


Figure 20. Key NF- κ B Signaling pathways [134] This figure includes the canonical and non-canonical NF- κ B signaling pathway. The enzyme I κ B kinase (IKK) or NF- κ B-inducing kinase (NIK) is activated by various extracellular signals and then triggers a series of reactions.

3.5 Dissociated Steroids

The well-known therapeutic effects of GCs are, as described, limited by the side effects accompanying their chronic use. Due to the important role GCs play in disease treatment, many researchers have attempted to design novel selective nuclear ligands as agonists or antagonists to improve the therapeutic index associated with GC receptor activation.[135] As already mentioned, one approach to improving the GC therapeutic effect and decrease systemic adverse effects,

is the design of GR ligands that can dissociate transactivation and transrepression transcriptional effects. These called dissociated steroids act similarly to classical GCs ligands. These ligand types also bind the GRs causing GR dissociation from the chaperone proteins entering the nucleus. However, the dissociated steroids bias the receptor towards the monomeric form achieving a selective inhibition of proinflammatory factors NF-KB or AP-1 while minimizing direct transcriptional activities that are associated with side effects.

Although there is much promise in this approach, and the idea is interesting, there has been little progress in dissociated steroid discovery and clinical development in the past decade. However, there are some vital clues that the approach could work. For example, RU24858^[136, 137] (**Figure 21**), a GR antagonist, has a similar effect to dexamethasone on repressing the transcriptional activity of AP-1 but compared with dexamethasone, its transactivation activity associated with binding to glucocorticoid responsive elements (GREs) is dramatically lower. This dissociated GC has demonstrated anti-inflammatory properties both in vitro and in vivo but it had a disappointing clinical profile possibly because of poor dissociation in vivo that could be cell type specific.^[138] It was reported that this dissociated GC still has side effects such as osteopenia. This side effect appears because this ligand altered ratio of osteoprotegerin (OPG)/ receptor activator of nuclear factor (NF)-kB-ligand (OPG/RANKL) in the process of OPG production transrepression^[139].

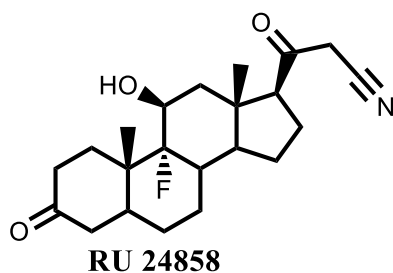


Figure 21. Chemical structure of dissociated steroids RU24858

AL-438^[140, 141] (**Figure 22**), a nonsteroidal GC ligand, interacts with GR only through glutamate receptor interacting protein 1 (GRIP-1), whose mechanism is different to dissociated steroids. Its dissociation of the transactivation and transrepression is achieved by differential recruitment of cofactors. It seems that it acts as a selective nuclear receptor modulator. It showed less presentation of some side effects including osteopenia and hyperglycemia compared with prednisolone^[139, 142]. In vivo, this compound shows potent anti-inflammatory properties comparable to or better than prednisolone.^[143] However in further clinical studies it will be necessary to carefully monitor for other adverse effects before drawing a conclusion on the clinical potential for this compound and the approach.

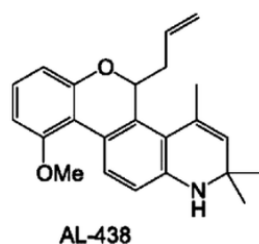


Figure 22. Chemical structure of dissociated steroids AL-438

Although these compounds have obvious anti-inflammatory properties and good dissociation of transactivation and transrepression in cell experiments, a significant increase in therapeutic index did not follow in the *in vivo* experiments. While important medical possibilities and potential for dissociated GCs remains, there is a lot of work to do to achieve something that can have a meaningful clinical impact.

3.6 Structure of UDCA, its chemical and clinical properties and effects

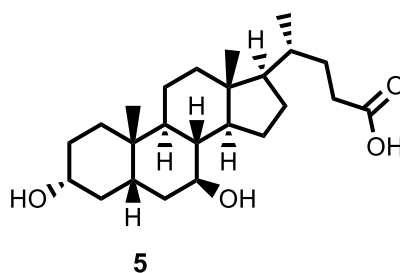


Figure 23. Structure of UDCA

UDCA (**5**), 3 α ,7 β -hydroxyl-5 β -cholanic acid, is hydrophilic bile acid. (**Figure 5**) In clinical practice, it is used to increase bile acid secretion, change composition of bile and reduce the content of cholesterol and cholesteryl ester in bile, which is of benefit to dissolve gallstones. It is reported that UDCA is able to effectively inhibit cholesterol synthesis in the liver, improve cholesterol release from the gallbladder to the intestinal tract and reduce fat stores in the liver tissues. As a traditional medicine, it is used to treat some liver and biliary diseases such as PSC and primary biliary cholangitis (formerly, cirrhosis, PBC) with IBD, CD and UCs, as complications^[144]. UDCA remains the most important drug in the medical management of cholestatic liver disease. Depending on the dosing, up to 60% of patients receiving UDCA in PBC have a satisfactory response. For those refractory to UDCA, obeticholic acid an FXR agonist may be added. The European Crohn's and Colitis Organisation (ECCO) and American College of Gastroenterology (ACG) recommend use of UDCA to treat UC patients whose complication is PSC^[145, 146] although the clinical benefits in this setting are far from clear. This reflects the clinical reality that there are few therapeutic options in this dreadful disease. UDCA has been shown not only to have protective effects on human epithelial cells from the gastrointestinal tract but also immunoregulatory responses regulated through cytokine inhibition in epithelial cells and in immunocytes^[147]. Although UDCA has been investigated extensively, its MOA in clinical use remains obscure and there is no clear target explaining its wide array of mainly immunomodulatory, cytoprotective and even pro-secretory effects.

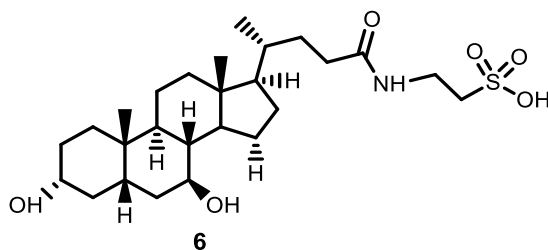


Figure 24. Chemical structure of TUDCA

Tauroursodeoxycholic acid (TUDCA), 3 α ,7 β -hydroxyl cholanic acid-N-taurine, is a conjugated bile acid which is a product from a condensation reaction between the carboxylic acid group of UDCA and the amino group of taurine (**Figure 24**). Compared with UDCA, TUDCA not only has higher ionization, higher hydrophilicity, better bioavailability and faster speed of dissolving gallstones, but also less cell damage and no obvious side effects. The relative efficacy/side effect profiles of UDCA and TUDCA have not been conclusively compared in patients. They are likely to have similar if not interchangeable effects in a range of conditions based on their cellular effects *in vitro*.

3.7 Evidence for UDCA activation of GR

There has been a lot of interest and studies in UDCA, the GR signalling pathway and NF- κ B activity because the immunomodulatory properties of UDCA are similar to glucocorticoid effects^[148]. Some studies have shown that UDCA is able to activate the GR resulting in gene expression regulation without coactivator recruitment. Studies from this lab have shown that UDCA can induce GR translocation from cytoplasm to nucleus with the same efficacy as dexamethasone, the GR agonist, in a SKGT-4 (oesophageal cancer) cell-based assay and other cells models^[149-151]. Moreover, there is evidence that UDCA can, in the absence of glucocorticoid ligand, induce GR translation via the GR-ligand binding domain (LBD). It is reported that the biological action of UDCA, NF- κ B-dependent transcription suppression, is mediated selectively by GR

activation^[152]. This suggests that UDCA may be an interesting chemotype for the generation of new GR ligands potentially with better therapeutic index. It reported that amido derivatives of UDCA were capable of causing GR translocation and NF-kB activity inhibition. These derivatives bind to the LBD rather than interacting with the traditional GC site thereby having the ability to induce coactivator recruitment and induce transactivation. This indicates a mechanism of action of a novel GR modulators.^[153] Among another interesting series of compounds identified in this lab are a series of novel GR modifiers with the general chemical structure correction 7 below. These are amides of UDCA in which the 3-OH groups have been replaced with an amine with retention of configuration (alpha).

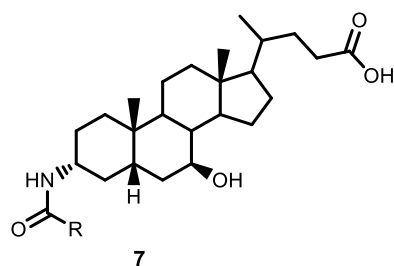


Figure 25. Novel GR chemical structure

The research groups are searching for analogues of UDCA that retain its useful features but reducing its metabolic liabilities. For example, UDCA and its analogues are retained in the enterohepatic circulation^[152]. It is known that in UDCA the 7 β -OH is required for its disease modifying properties, including secretagogue and cytoprotective properties, and probably also its capacity to influence the GR^[154]. On the other hand, the 7-OH is dehydroxylated by the intestinal bacteria, which reduces circulating UDCA, while increasing the concentration of LCA, a toxic metabolite. The Gilmer group has produced analogues of UDCA in which the 7-OH group is replaced with functionality that has reduced tendency to be metabolically removed, but potentially have the same binding properties to UDCA target proteins. Some of these are also

studied in the present work.

TUDCA (**6**) whose chemical structure is almost the same as UDCA can also cause translocation of GR and mineralocorticoid receptor (MR), suggesting that the sidechain is not important for interactions between UDCA/TUDCA and the GR^[154]. It appears that the steroid part of UDCA is largely responsible for the dissociation and nuclear translocation of GR. It suggests that the side chain can be modified to achieve better targeted effect and improve pharmacodynamics as shown in the previous work from the group^[58].

3.8 Aims and objectives

The main aim of the following work was to characterise biochemically a series of UDCA-3 amides in liver and inflammatory cells. The specific objectives were to produce further test quantities and synthesise UDCA derivatives appropriately substituted to learn more about the structure activity requirements for the GR modulating effect. This could inform future work towards more potent or effective UDCA-based GR modulators, and it would also be of scientific interest to understand how the analogues exert the observed effects. A related aim was to see if the effects on triggering GR translocation, which were observed in the SKGT4 oesophageal cancer cell line, would transfer or could also take place in liver cells, since these are a potential target for a bile acid-based GR agonist. Accordingly, we intended to test UDCA derivatives as GR agonists in liver cells, first using the GR translocation assay and then by assessing its anti-inflammatory effects on liver cells and PBMCs associated with NF- κ B inhibition.

3.9 Design and Synthesis of UDCA derivatives.

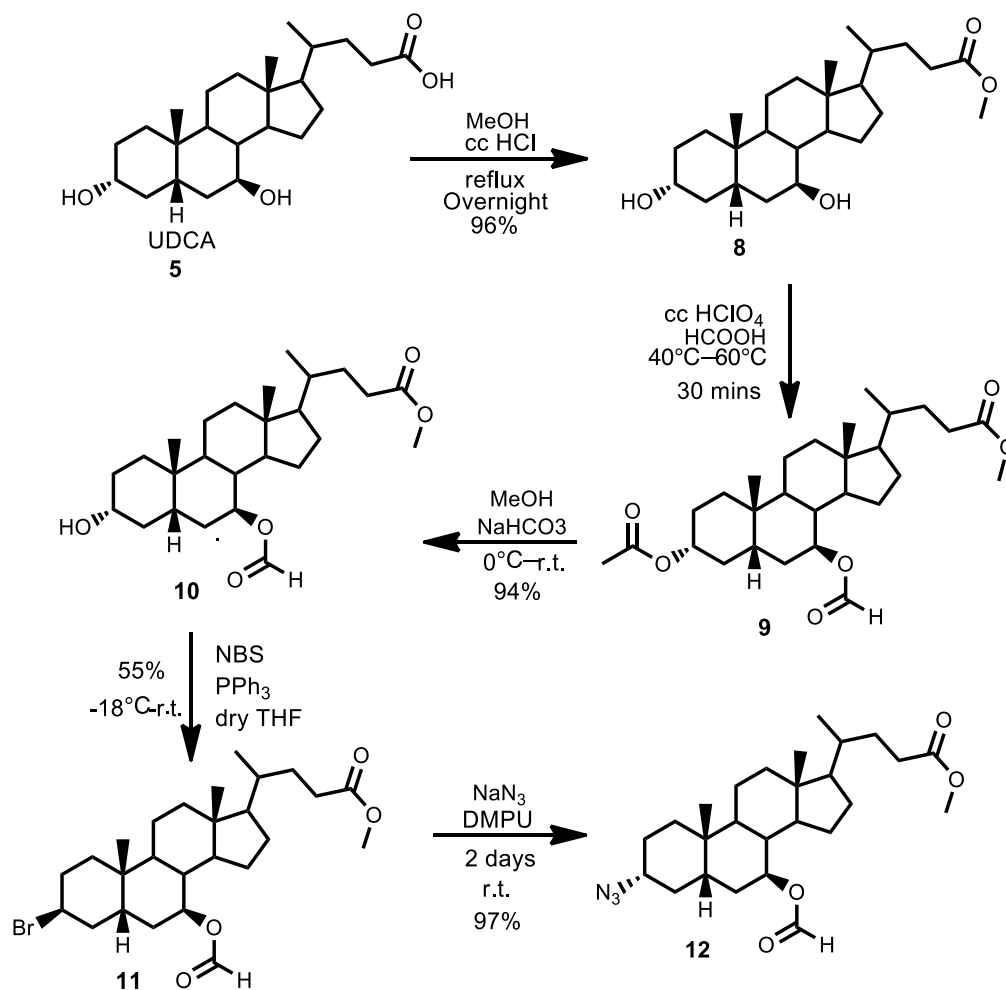
Much research has been done on the relationship between chemical modification and biological activities for several decades, and it is widely accepted that chemical structure modification can improve the potency and cytotoxicity of BAs^[43, 155, 156]. In the chemical synthesis, we started with 3 α -azide, 3 β -azide and 7 β -azide formations of UDCA. Then these compounds were converted into 3 α -amino, 3 β -amino and 7 β -amino compounds, respectively, before producing benzamide, chlorobenzamide, methanesulfonamido. A novel 7-beta triazole derivative was produced via a click reaction. The BAs synthesis methods were conducted according to the previous work of the Gilmer BA group in Trinity College.

We started with the synthesis of two 3 α -benzamides of UDCA, one substituted with chlorine at position 4 and the other unsubstituted (**Scheme 1**). In these compounds the critical UDCA 7-position is left unaffected. In the first step, UDCA was protected by methyl ester formation using a catalytic quantity of HCl in MeOH. The methyl ester (**8**) was isolated in 96% yield (**Scheme 1**). The hydroxyl groups at positions 3- and 7- were then protected as formyl esters using formic acid with a small amount of perchloric acid. Then the 3-formate was selectively removed using weak aqueous base hydrolysis. The deprotected alcohol was converted to beta bromide by treatment with NBS and PPh₃ in dry THF following work described in the Ph.D. thesis of Ferenc Majer and Jason Gavin in the Gilmer group^[157, 158]. The bromine was displaced with inversion of configuration (S_N2) with azide in DMPU producing the 3 α -azide (**12**). This was reduced over Pd/C in an atmosphere of H₂. The resultant amine was amidated using either the benzoyl chloride or the chlorobenzoyl chloride, producing the amide that was most active in the work of Jason Gavin in causing GR translocation (**15,17,23,24**). After that, we synthesized two 3 β -amides (**19**) of UDCA derivatives.

The obvious advantage of this approach is that it can achieve stereospecificity obviating the difficulties of separation of the mixture of α - and β -amides. In previous studies carried out in the Gilmer group, a Boc protecting group was added to the azide, and then displaced to the amine product. However, it is found that it is unnecessary to add this group because the amine product can be made from azide product directly, and the failure rate of turning 24-methyl-3 β -(N-Boc)-7-acetoxy-5 β -cholanoate/24-Methyl-3 α -(N-Boc)-7-acetoxy-5 β -cholanoate to 3 α and 3- β azide products is high. Thus, we chose to eliminate the Boc-protection step. Then, following deprotection, the relevant amines were coupled with benzoyl chloride or 4-chlorobenzoyl chloride to make the target UDCA derivatives.

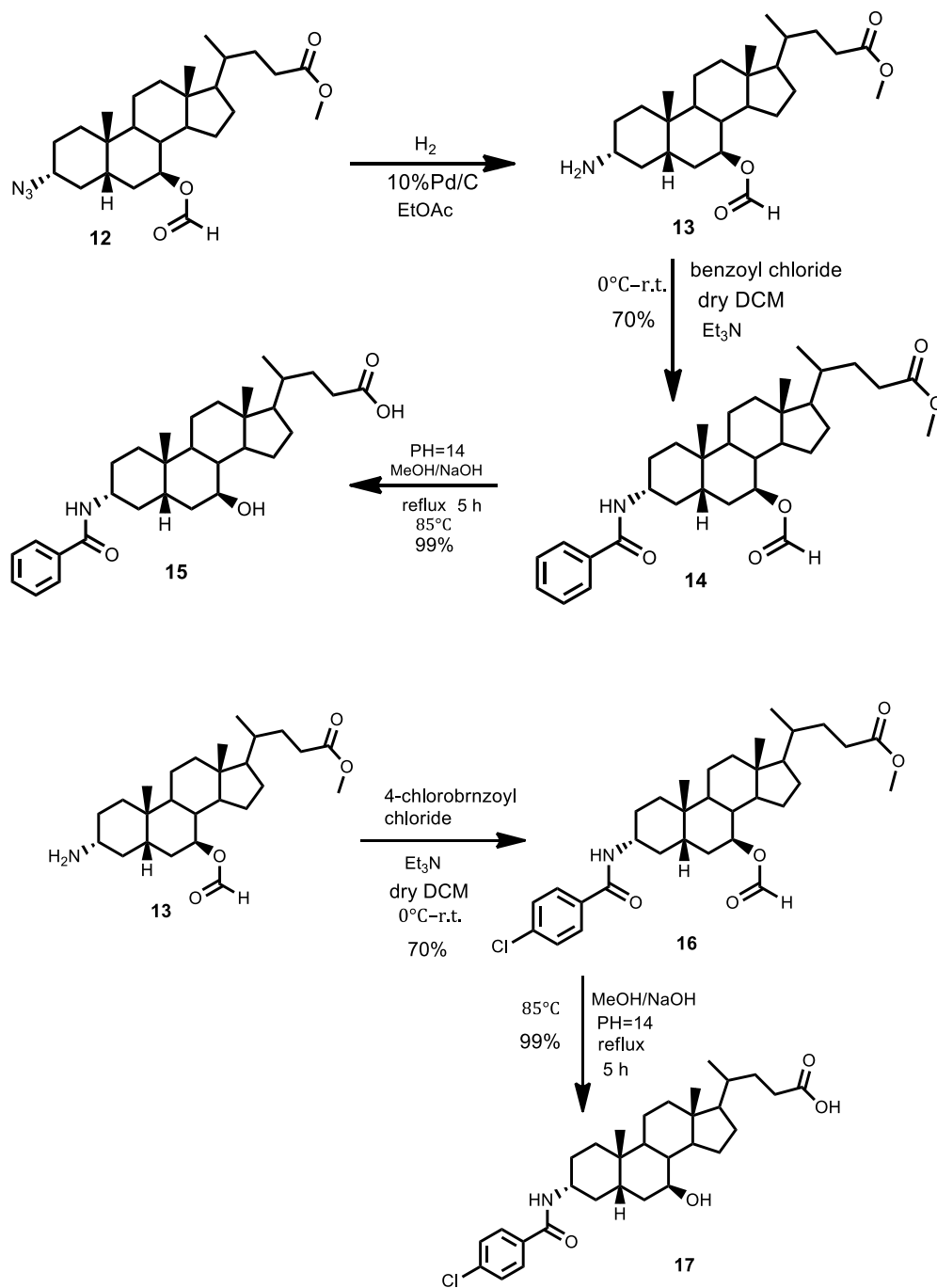
3.9.1 Synthesis of 3 α -(benzamido)-7 β -hydroxy-5 β -cholanoate (15) and 3 α -(4-chlorobenzamido)-7 β -hydroxy-5 β -cholanoate (17)

The alpha amide compounds were produced from UDCA (**Scheme 1**). The first step is to protect the hydroxy at the C-3, C-7 and C-24 position in order to add the chemical function group into targeted position. Then the carboxyl to hydroxy at C-3 position was reduced and the hydroxy was substituted by bromine atom. 3 α -azide (**12**) was synthesized by the nucleophilic substitution.



Scheme 1. Synthesis of 3 α -azide of UDCA

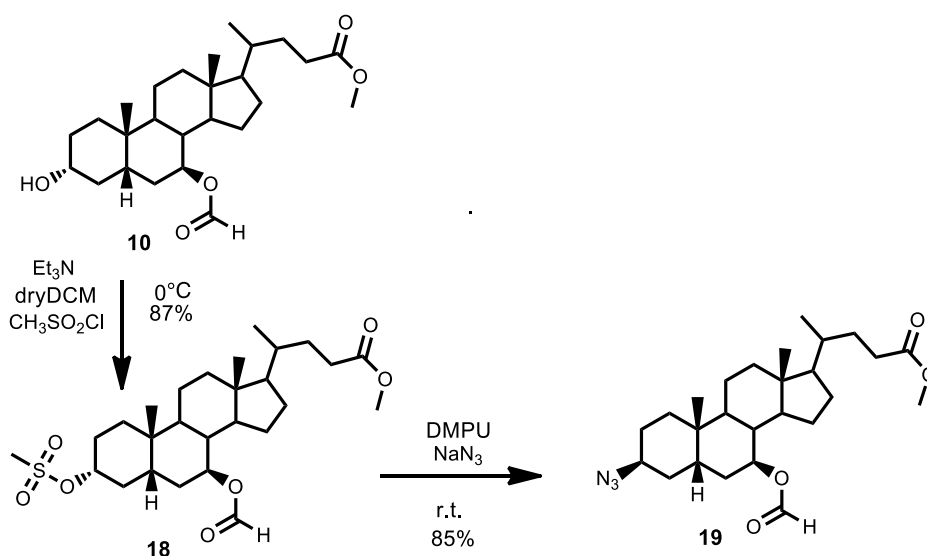
3 α -azide was reduced to primary amines which is unstable so compound **13** is required to react immediately without being purified (**Scheme 2**). Either Benzoyl chloride or chlorobenzoyl chloride was added to synthesize compounds (**14**, **17**) and return the methyl to hydroxy through hydrolytic reaction.



Scheme 2. Formation of 3 α -benzamido and 3 α -chlorobenzamido of UDCA

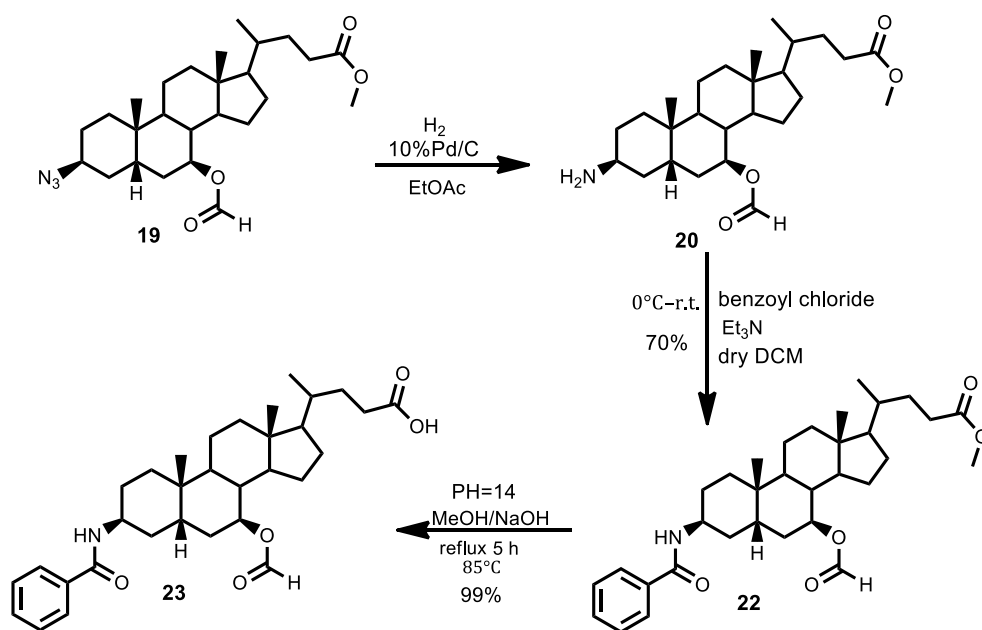
3.9.2 Synthesis of 3 β -(benzamido)-7 β -hydroxy-5 β -cholanoate (**23**) and 3 β -(4-chlorobenzamido)-7 β -hydroxy-5 β -cholanoate (**24**)

The beta amide compounds were produced from the more directly accessible 3 β -azide (**Scheme 3**). These were produced from the selectively protected UDCA derivative **10** from the work described above. The 3-OH was activated towards nucleophilic substitution by sulfonation with methanesulfonyl chloride in the presence of a tertiary base (**10**). This was substituted by treatment with NaN₃ in the polar aprotic solvent DMPU at room temperature for several days. The lower temperature delays the reaction in this case but reduces the competing C 3-elimination.



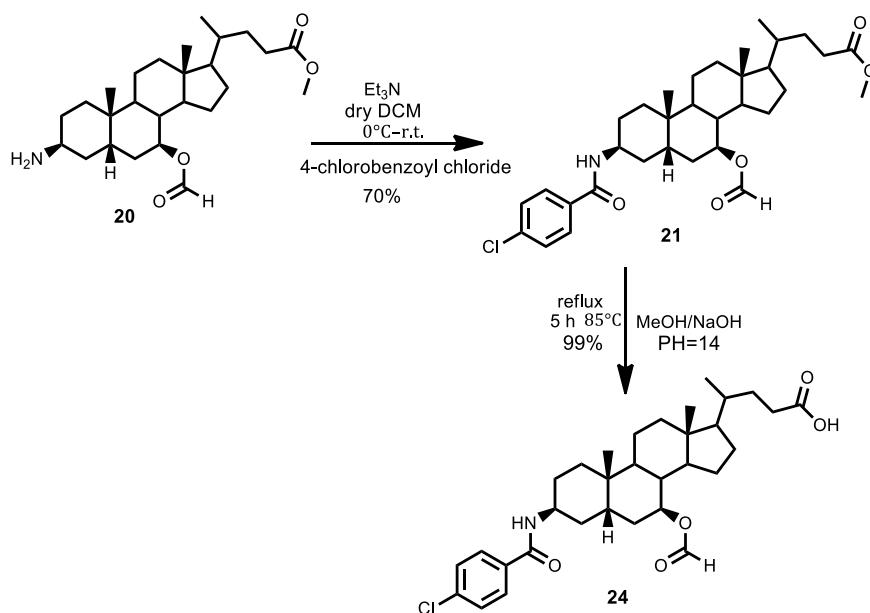
Scheme 3. Synthesis of 3 β -azide of UDCA

The 3 β -azide was reduced in the presence of Pd/C under an atmosphere of hydrogen. The product **20** was not isolated because it is expected to be unstable. Instead the amine was acylated directly as indicated in **Scheme 4** producing the 3 β -benzamide **22**. This was deprotected through aqueous hydrolysis with hydroxide producing target compound **23**.



Scheme 4. Formation of 3 β -benzamido of UDCA

The corresponding chlorobenzamide was produced from **20** by treatment with chlorobenzoyl chloride in the presence of a tertiary base. Deprotection was accomplished as already described for **22**.

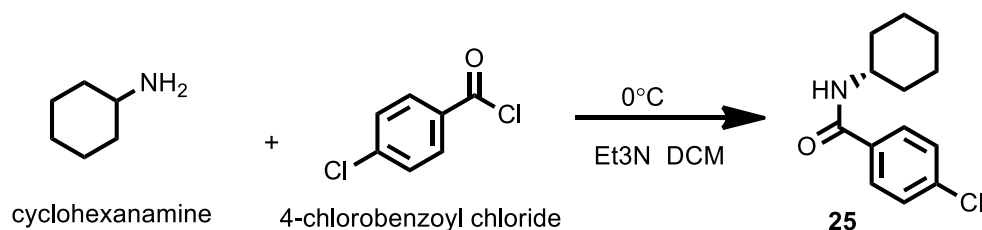


Scheme 5. Formation of 3 β -chlorobenzamido of UDCA

Two further set of compounds were prepared as controls and for further

investigation. Since the earlier work had identified the GR translocating activity of 3 α -chlorobenzoyl amide, it was decided to prepare a control compound retaining this group but without the UDCA scaffold. The intention was to use this to explore or verify the role of the UDCA framework in enabling the chlorine substituted amide in causing GR translocation. Accordingly, cyclohexylamine was acylated directing with chlorobenzoyl chloride and the product purified by flash chromatography.

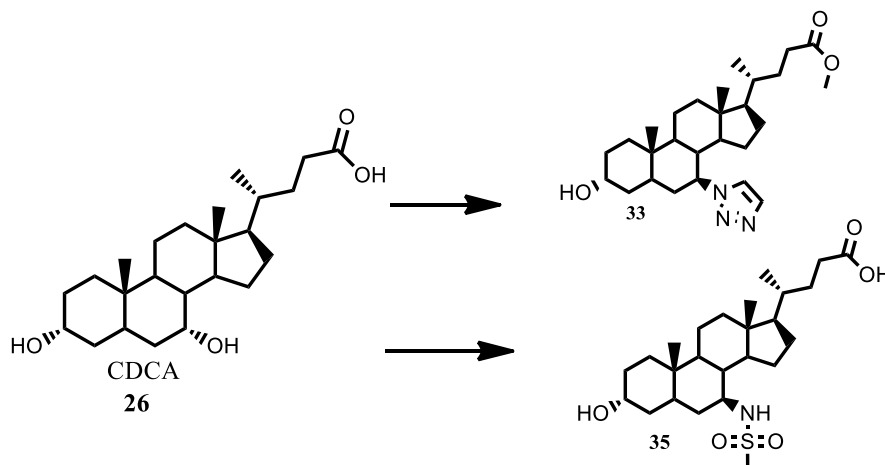
3.9.3 Synthesis of N-cyclohexylbenzamide (25)



Scheme 6. Formation of N-cyclohexylbenzamide (25)

3.9.4 Synthesis of 3 α -hydroxy-7 β -(1H-1,2,3-triazol-1-yl)-5 β - cholanoate (33) and 3 α -hydroxy-7 β -(methanesulfonamido)-5 β - cholanoate (35)

Compound **33**, the UDCA-based triazole and compound **35**, the sulfonamide were prepared with the assistance of the Gilmer group from CDCA. The methods for producing these are described in the PhD thesis of Gavin (Trinity College Dublin, 2017).



Scheme 7. Formation of 3 α -hydroxy-7 β -(1H-1,2,3-triazol-1-yl)-5 β -cholanoate (33**) and 3 α -hydroxy-7 β -(methanesulfonamido)-5 β -cholanoate (**35**)**

These compounds 3 α -hydroxy-7 β -(1H-1,2,3-triazol-1-yl)-5 β -cholanoate (**33**) and 3 α -hydroxy-7 β -(methanesulfonamido)-5 β -cholanoate (**35**) were prepared from CDCA and provided by the members of Gilmer Group.

3.10 Effect of BAs derivatives on cell viability by MTT and

Alamar blue

The first studies conducted were on the effect of the compounds on the proliferation of the study cell types to ensure that anti-inflammatory effects observed were not due to induction of cell death. Bile acids can induce cell death through a variety of pathways and the amide derivatives were expected to be toxic or partly toxic in the concentration range they were to be studied as anti-inflammatory agents.

3.10.1 MTT Assay

MTT assay can not only be used to measure cell viability, but also to assess cytotoxicity and cytostatic activity. Cell respiration generates NAD(P)H-dependent cellular oxidoreductase enzymes which can reduce the

tetrazolium dye MTT (3-(4,5-dimethylthiazol-2-yl)-2,5-diphenyltetrazolium bromide) to a purple insoluble formazan which accumulates in cells. And then the formazan is solubilized by dimethyl sulfoxide (DMSO) before optical density is determined by absorbance at 570 nm.

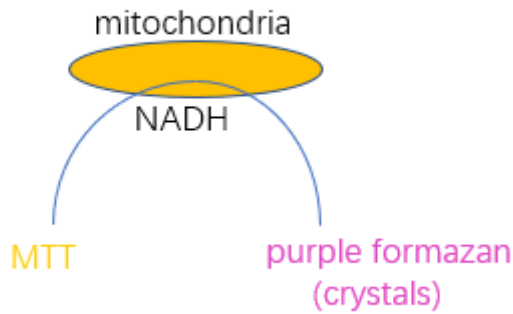


Figure 26. MTT Assay ^[159] *MTT Assay is an enzyme-based method that is used widely in cell toxicity and cell viability through coloring reagent and dehydrogenase. In the figure, nicotinamide adenine dinucleotide (NADH) consists of nicotinamide adenine dinucleotide (NAD) + hydrogen (H). It is essential in the energy generation reaction in all living cells.*

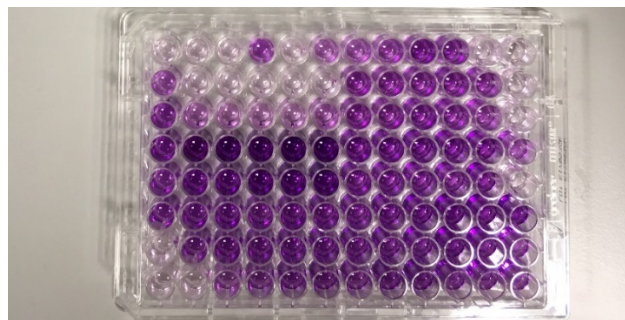


Figure 27. MTT assay

3.10.2 Alamar Blue Assay

Alamar Blue Assay is used to quantify metabolic activity of cells related to cell proliferation. The reagent of alamar blue is a ready-to-use blue resazurin solution that can measure the cell viability through the reducing power of viable cells turning the non-fluorescent blue ingredient in the reagent into fluorescent red resorufin. In this way, the cell viability is easily detected by a fluorescence-

(more accurate) at 530–560 nm or an absorbance-based plate reader at 570 nm.

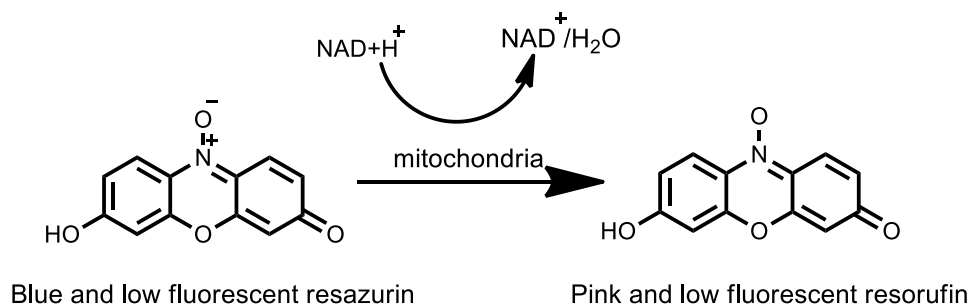


Figure 28. Alamar Blue Assay ^[160] *The assay relies on the metabolic activity in the mitochondria of cells. It is a fluorometric method that is based on the reduction reaction transforming blue resazurin to resorufin.*

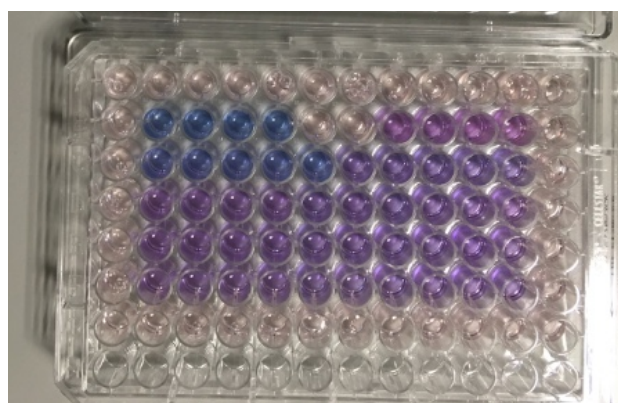


Figure 29. Alamar blue assay

3.10.3 Cytotoxicity studies on the Caco-2 cell line

Caco-2 cells were treated with different concentrations of BAs derivatives respectively for 24 h in the 37 °C incubator. 10 μ L of 2.5 mg/mL MTT was added into the supernatant in the last 2 h of treatment. Finally, the medium was removed and formazan was dissolved in 100 μ L DMSO. The 96-well plate was read by absorbance at 570 nm. The vehicle was 0.5 % DMSO.

Effect of 3 α -(4-chlorobenzamido)-7 β -hydroxy-5 β -cholanoate (17) on cell viability

Figure 30 shows Alamar Blue data for treatment of THP-1 Blue cells with the active chlorobenzamide compound 17. The compound causes cell death or reduces cell proliferation in a concentration dependent manner in the range 100-500 μ M.

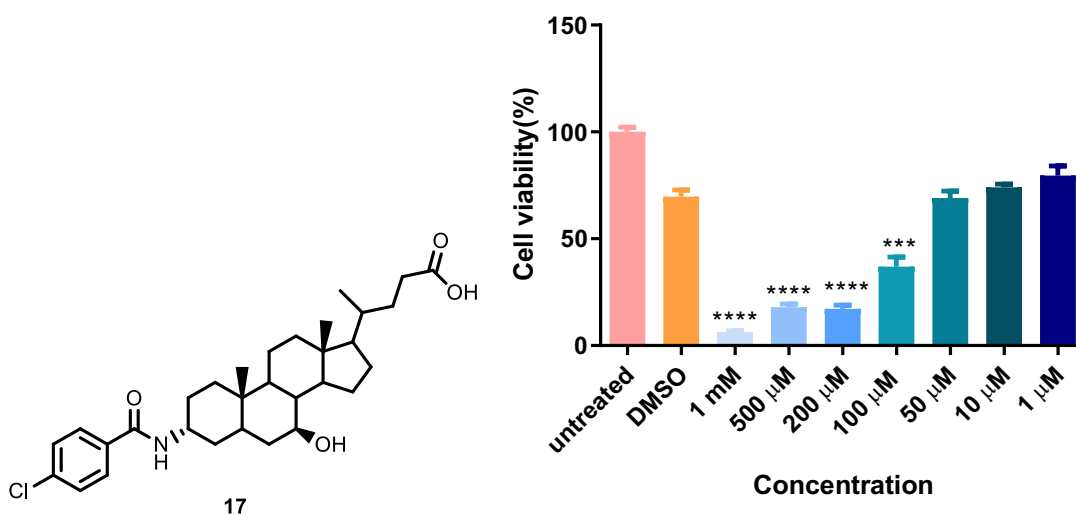


Figure 30. Alamar Blue assay result of 3 α -(4-chlorobenzamido)-7 β -hydroxy-5 β -cholanoate (17) Caco-2 cells were treated with different concentrations of 3 α -(4-chlorobenzamido)-7 β -hydroxy-5 β -cholanoate (17) for 24 h in the 37 °C incubator. The vehicle was 0.5 % DMSO. Values were expressed as fold difference compared to the vehicle as mean \pm SEM of triplicate experiments, *** $p < 0.001$, **** $P < 0.0001$ was determined by oneway ANOVA with Dunnett's post-hoc correction.

Effect of 3 α -(benzamido)-7 β -hydroxy-5 β -cholanoate (15) and 3 β -(benzamido)-7 β -hydroxy-5 β -cholanoate (23) on cell viability

Next, we studied the effect of the epimeric 3-benzamides 15 and 23 on cell

viability of the Caco-2 cell line using the MTT assay (**Figure 31**). In the MTT assay graph, the cell viability of 3 α -(benzamido)-7 β -hydroxy-5 β -cholanoate (**15**) is higher than 3 β -(benzamido)-7 β -hydroxy-5 β -cholanoate (**23**) except at concentration of 50 μ M. Even though the molecular formula of these two compounds is the same, different configurations have different cytotoxicity. Moreover, compared with 3 α -(4-chlorobenzamido)-7 β -hydroxy-5 β -cholanoate (**17**), the cell viability of 3 α -(benzamido)-7 β -hydroxy-5 β -cholanoate (**15**) is also higher. It seems that in the alpha configuration, the addition of the chloride group in 3 α -benzamido increases the toxic effects.

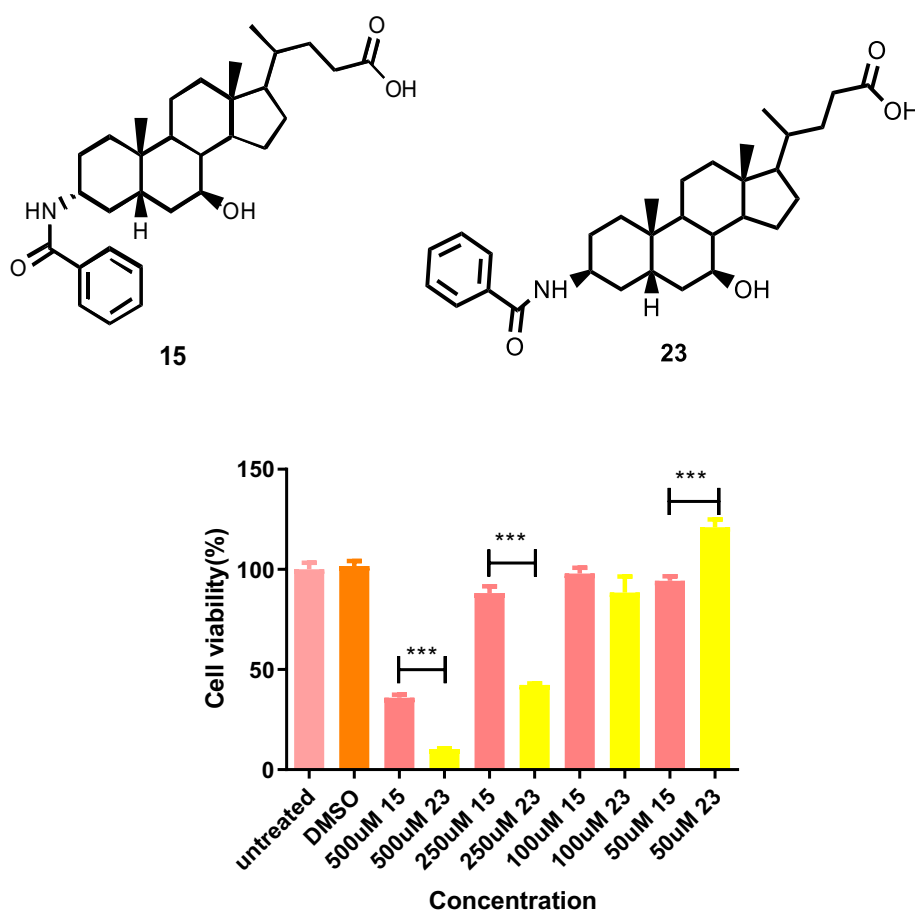


Figure 31. A comparison of the effect of 3 α -(benzamido)- 7 β -hydroxy-5 β -cholanoate (**15**) and 3 β -(benzamido)-7 β -hydroxy-5 β -cholanoate (**23**) Caco-2 cells were treated with different concentrations of 3 α -(benzamido)-7 β -hydroxy-5 β -cholanoate (**15**) and 3 β -(benzamido)-7 β -hydroxy-5 β -cholanoate (**23**) for 24 h. The vehicle was 0.5 % DMSO. Values were expressed as fold difference compared to the vehicle as mean \pm SEM of triplicate experiments, *** $P < 0.001$, was determined by oneway ANOVA with

Dunnett's post-hoc correction.

Effect of 3 β -(4-chlorobenzamido)-7 β -hydroxy-5 β -cholanoate (24) on cell viability

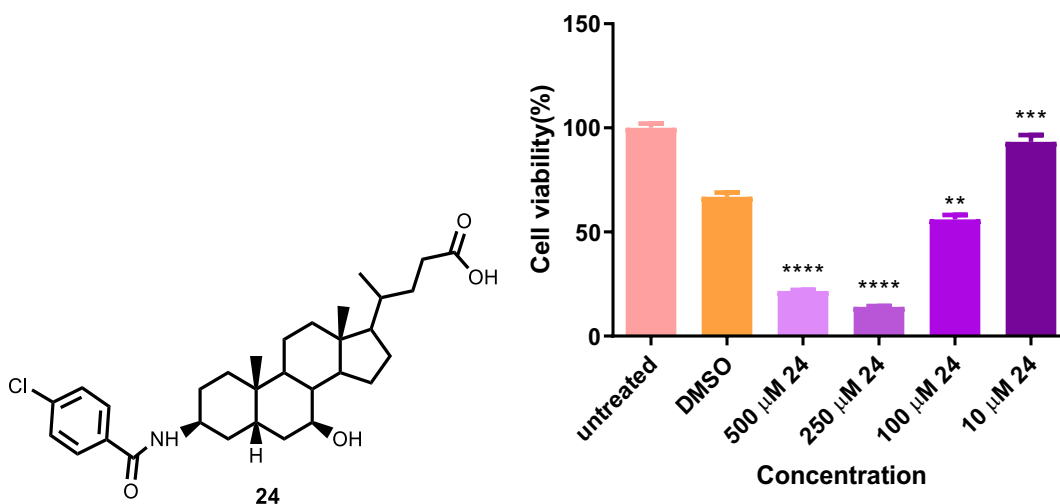


Figure 32. MTT assay result of 3 β -(4-chlorobenzamido)-7 β -hydroxy-5 β -cholanoate (24) Caco-2 cells were treated with different concentrations of compound 24 for 24 h. The vehicle is 0.5 %DMSO. Values were expressed as fold difference compared to the vehicle as mean \pm SEM of triplicate experiments, ** p <0.01, *** p <0.001, **** P <0.0001 was determined by oneway ANOVA with Dunnett's post-hoc correction.

Effect of 3 α -(4-chlorobenzamido)-7 β -hydroxy-5 β -cholanoate (17) and 3 β -(4-chlorobenzamido)-7 β -hydroxy-5 β -cholanoate (24) on cell viability

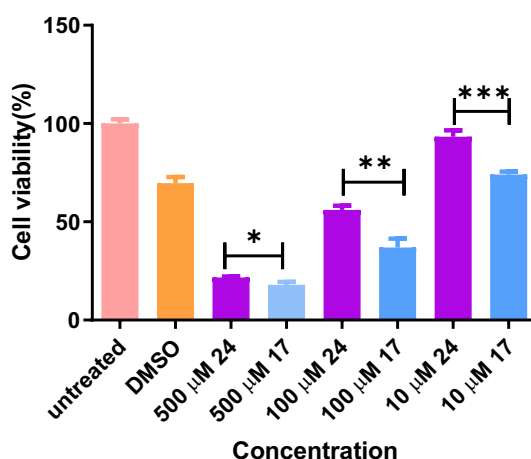


Figure 33. A comparison of the effect of 3 α -(4-chlorobenzamido)-7 β -hydroxy-5 β -cholanoate (**17**) and 3 β -(4-chlorobenzamido)-7 β -hydroxy-5 β -cholanoate (**24**) Caco-2 cells were treated with different concentrations of 3 α -(4-chlorobenzamido)-7 β -hydroxy-5 β -cholanoate (**17**) and 3 β -(4-chlorobenzamido)-7 β -hydroxy-5 β -cholanoate (**24**) for 24 h. The vehicle was 0.5 % DMSO. Values were expressed as fold difference compared to the vehicle as mean \pm SEM of triplicate experiments, *** $P < 0.001$, was determined by oneway ANOVA with Dunnett's post-hoc correction.

Compared with 3 β -(benzamido)-7 β -hydroxy-5 β -cholanoate (**23**), the cytotoxicity of 3 β -(4-chlorobenzamido)-7 β -hydroxy-5 β -cholanoate (**24**) is similar to **23**. It indicates that adding chloride does not decline dramatically the cell viability in alpha and beta configuration.

In conclusion, the cell viability following treatment with these four compounds, 4-chloro-N-cyclohexylbenzamide(**24**),3 α -(benzamido)-7 β -hydroxy-5 β -cholanoate(**15**),3 α -(4-chlorobenzamido)-7 β -hydroxy-5 β -cholanoate(**17**),3 β -(benzamido)-7 β -hydroxy-5 β -cholanoate(**23**),3 β -(4-chlorobenzamido)-7 β -hydroxy-5 β -cholanoate (**24**) depends on treatment concentration. At a given concentration, the compound **24** causes the least cell toxicity among these four above compounds.

Effect of 3 α -hydroxy-7 β -(1H-1, 2, 3-triazol-1-yl)-5 β -cholanoate (33) and 3 α -hydroxy-7 β -(methanesulfonamido)-5 β -cholanoate (35) on cell viability

In **Figure 34**, compound **33** and **35** do not cause cell death of Caco-2 cells and even have cytoprotection at 500 μ M. Compared with 3 β -amido, 7 β -amido has much less cytotoxicity.

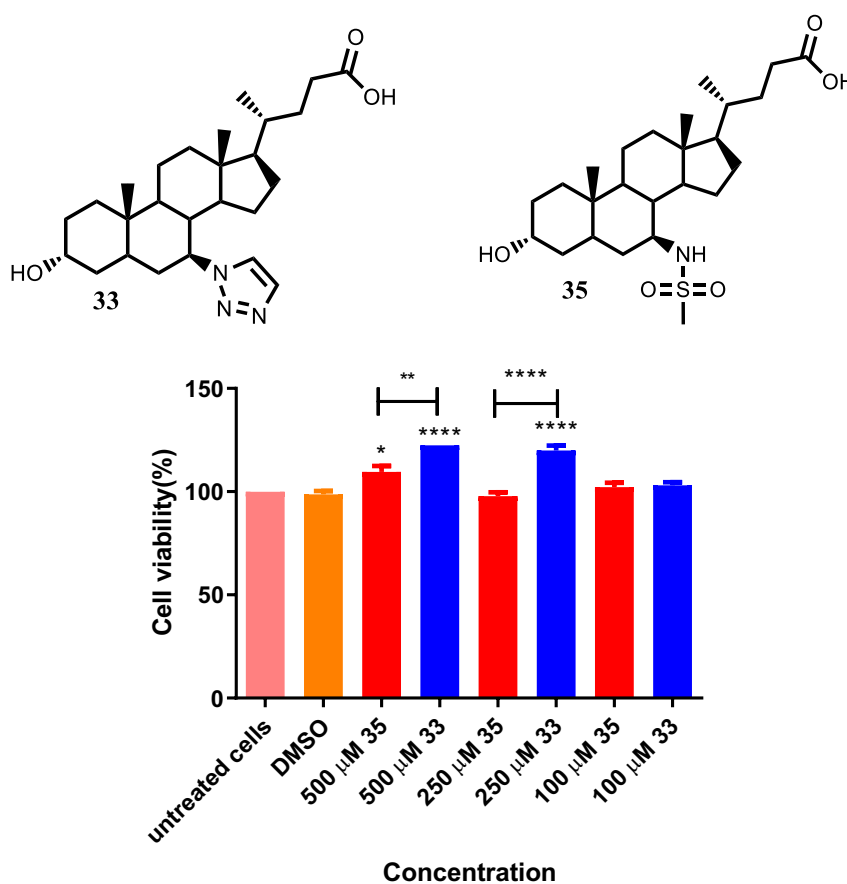


Figure 34. MTT assay result of 3 α -hydroxy-7 β -(1H-1,2,3-triazol-1-yl)-5 β -cholanoate(33) and 3 α -hydroxy-7 β -(methanesulfonamido)-5 β -cholanoate (35) Caco-2 cells were treated with different concentrations of compound **33** and **35** for 24 h in the 37 $^{\circ}$ C incubator. The vehicle is 0.5 %DMSO. Values were expressed as fold difference compared to the vehicle as mean \pm SEM of triplicate experiments, * p <0.05, ** p <0.01, *** p <0.001, **** P <0.0001 was determined by oneway ANOVA with Dunnett's post-hoc correction and by t test.

3.10.4 Cytotoxicity studies on the Huh 7 cell line

Having studied the effect of the BA derivatives on the Caco-2 cell line we next turned our attention to their effects on the hepatoma cell line Huh 7. The data presented in **Figure 35** show that the Huh 7 cell line is more resistant to cell death induction in the presence of the test compounds than the Caco-2 cell line. Modest but statistically significant reduction in cell number could be observed on treatment with **35**, **15**, **24**, but the levels were not sufficiently high to predict an interference on subsequent cell signaling or anti-inflammatory assays.

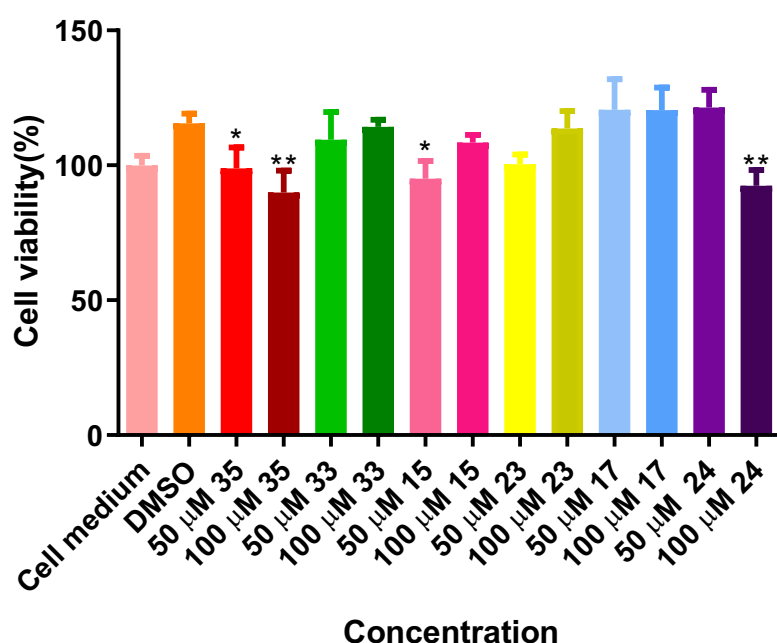


Figure 35. MTT Assay result of bile acid derivatives *Huh 7*, a hepatocarcinoma cell line, was treated with different concentrations (50, 100 µM respectively) of six BAs analogues for 24 h. The vehicle control is 0.5 %DMSO. Values were expressed as fold difference compared to the vehicle as mean ± SEM of triplicate experiments, * $p < 0.05$, ** $p < 0.01$, was determined by oneway ANOVA with Dunnett's post-hoc correction.

3.10.5 Cytotoxicity studies on the THP 1-Blue cell line using the MTT assay

Next, we studied the anti-proliferative effect of the compounds on the THP

1-Blue cell line since, as described below, we intended to use this cell line to measure effects of the test compounds on the activity of the major pro-inflammatory transcription factor NF- κ B. One reason for studying NF- κ B is that its activity is under the influence of the GR.

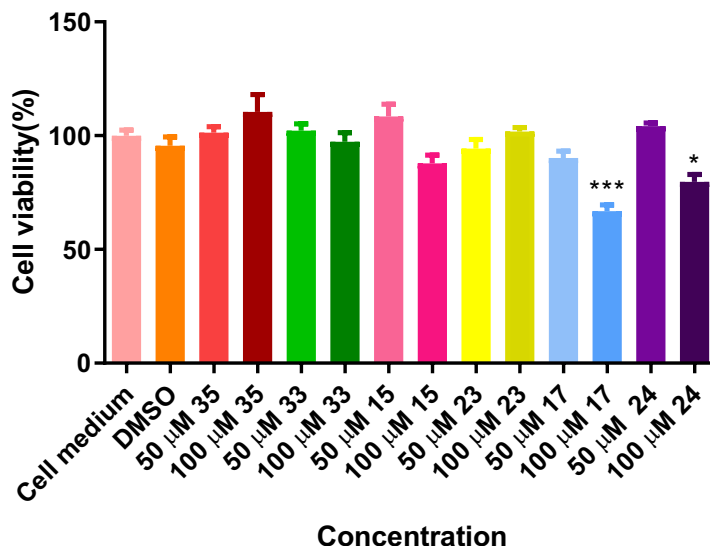


Figure 36. MTT Assay result of bile acid derivatives on THP 1-Blue Peripheral blood mononuclear cells (PBMCs) were treated with different concentrations of BA analogues for 24 h. The following procedures are the same. The vehicle control is 0.5 % DMSO. Values were expressed as fold difference compared to the vehicle as mean \pm SEM of triplicate experiments, * p <0.05, *** p <0.001, was determined by oneway ANOVA with Dunnett's post-hoc correction.

Statistically in the case of **17** and **24** at higher (100 μ M) concentration, the compounds were markedly inhibitory towards PBMC proliferation. It was decided to assess the effect of the compounds on TNF- α induced NF- κ B signaling preferably at 50 μ M since the level of inhibition of proliferation at this concentration was relatively low across the compound set.

3.11 Effect of BAs on THP1-Blue stimulated with TNF- α

3.11.1 QUANTI-Blue Assay (The THP1-Blue reporter assay for NF- κ B)

QUANTI-Blue assay is a commercial colorimetric assay for quantifying alkaline phosphatase (AP) activity in the supernatant of human monocyte cell line THP 1-Blue. The AP activity is related to secreted embryonic alkaline phosphatase (SEAP), a truncated form of placental AP, that is secreted out of the cells in response to NF- κ B activation. Following stimulation by endotoxin such as lipopolysaccharides (LPS) and activation of NF- κ B induced by TNF α , the NF- κ B activation leads to the SEAP expression. In the presence of SEAP, the medium changes from pink to purple, thus indicating whether or not the NF- κ B pathway is activated.

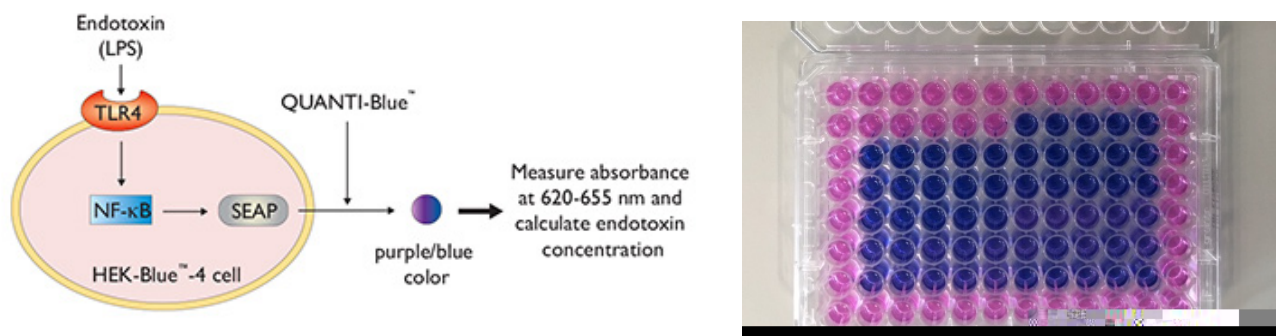


Figure 37. QUANTI-Blue Assay *The SEAP is secreted into cell supernatant different with intracellular reporters. QUANTI-Blue Assay, colorimetric assay, determines the SEAP activity in cell supernatant.*

3.11.2 Result of BAs effect on THP 1-Blue stimulated with TNF- α

THP 1-Blue cells were treated with 10 ng/ml TNF- α and together with different concentrations of compounds. Then cells were incubated for 24 h. 20 μ L cell supernatant was added into 200 μ L QUANTI-Blue reagent for 20 minutes in dark environment after 24 h incubation. Absorbance was read at 620–655 nm

was normalised to 0.5 % DMSO. The vehicle is 0.5 % DMSO.

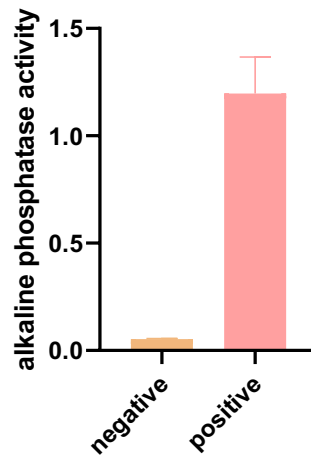


Figure 38. QUANTI-Blue assay result of TNF- α *In the negative group THP 1-Blue cells were treated with 0.5 % DMSO cell medium (RPMI-1640 Medium) alone for 24h. THP 1-Blue cells were treated with 10 ng/ml TNF- α in 0.5 % DMSO cell medium for 24h in the positive group.*

Figure 38 shows that after being treated with TNF- α , in the positive group the AP activity was stimulated dramatically compared with the negative group. In the following experiments, the negative group and the positive group were added. The project then moved to the evaluation of the potential anti-inflammatory effect of the bile acid derivatives. First it was decided to assess the activity of two important control substances in this context; the GR agonist dexamethasone, and TUDCA, the tauro derivative of UDCA which has putative anti-inflammatory effect.

Effect of Dexamethasone on TNF- α induced AP activity

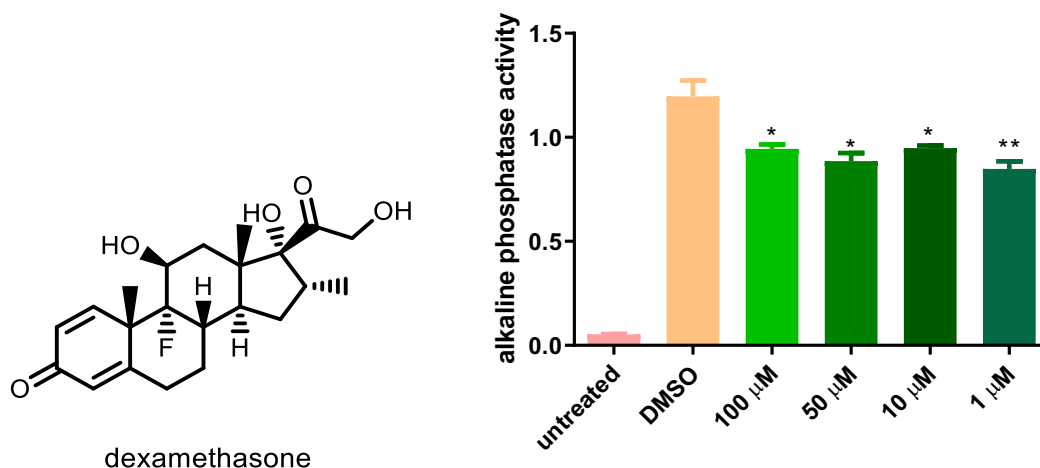


Figure 39. QUANTI-Blue assay result of dexamethasone THP1-Blue cells were treated with 10 ng/ml TNF- α and different concentrations of dexamethasone for 24 h. Values were expressed as fold difference compared to the vehicle as mean \pm SEM of triplicate experiments, * $p < 0.05$, ** $p < 0.01$, was determined by oneway ANOVA with Dunnett's post-hoc correction.

The inhibitory effect of dexamethasone on AP reached a maximum of around 25% inhibition relative to control at a concentration of 1 μ M. This demonstrates that in this assay system, NF- κ B activity is only partly under the influence of the GR because dexamethasone is a high efficacy GR agonist. For the purposes of the following studies 1 μ M dexamethasone was used as positive control.

Effect of TUDCA on TNF- α induced THP-1 Blue activity

Figure 40 shows the data for the treatment with TUDCA. TUDCA did not cause an inhibition of SEAP activity in response to TNF- α , indeed it caused a small but statistically significant increase in SEAP activity in a concentration dependent effect. This was surprising because TUDCA is regularly referred to as anti-inflammatory, indeed it may be the active substance during the clinical use of UDCA.^[161-164]

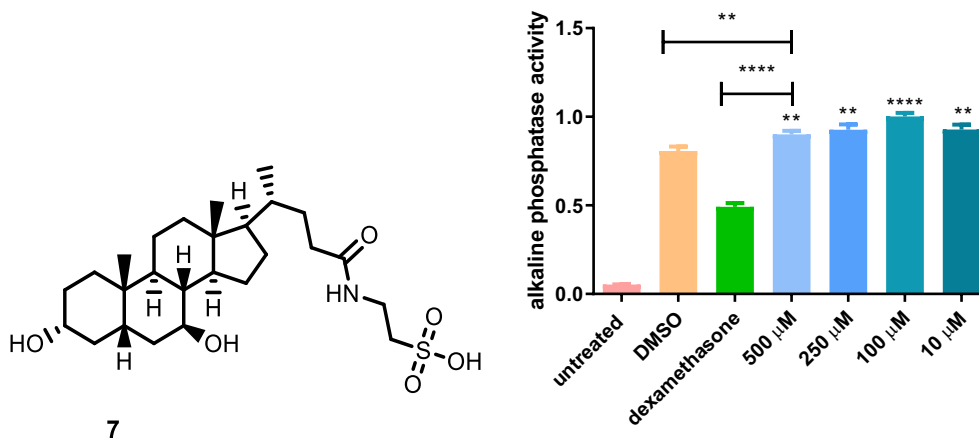


Figure 40. QUANTI-Blue assay result of TUDCA (7) THP-1 Blue cells were treated with 10 ng/ml TNF- α and different concentrations of TUDCA for 24 h. The vehicle is 0.5 %DMSO. The dexamethasone concentration is 1 μ M. Values were expressed as fold difference compared to the vehicle as mean \pm SEM of triplicate experiments, ** $p < 0.01$, **** $P < 0.0001$ was determined by oneway ANOVA with Dunnett's post-hoc correction and by *t* test.

Effect of compound 17 on TNF- α induced SEAP activity

The most active compounds in the GR translocation assays in the Ph.D. thesis of Jason Gavin, the 3 α -(4-chlorobenzamido)-7 β -hydroxy-5 β -cholanoate (**17**) was studied next. Here, It caused a concentration dependent inhibition of THP 1-Blue production of SEAP activity in response to TNF- α (**Figure 41**). However, previous studies had shown that it also caused reduction in THP-1 proliferation, most likely through a cytotoxic effect in the concentration range above 100 μ M. However, here a modest inhibitory effect was observed at 50 μ M where previously it was shown to not affect cell viability at this concentration. This indicates a potential inhibitory effect on TNF- α stimulated SEAP secretion/activity.

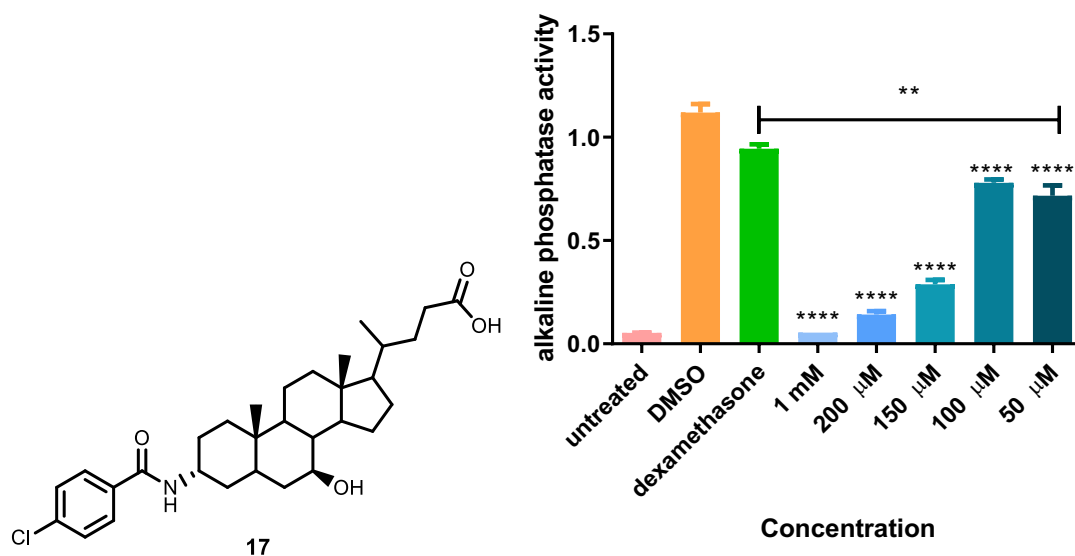


Figure 41. QUANTI-Blue assay result of 3 α -(4-chlorobenzamido)-7 β -hydroxy-5 β -cholanoate (17) THP1-Blue cells were treated with different concentrations of 3 α -(4-chlorobenzamido)-7 β -hydroxy-5 β -cholanoate (17) and 10ng/ml TNF- α for 24 h. The vehicle is 0.5 %DMSO. The dexamethasone concentration is 1 μ M. Values were expressed as fold difference compared to the vehicle as mean \pm SEM of triplicate experiments, ** p <0.01, **** P <0.0001 was determined by oneway ANOVA with Dunnett's post-hoc correction and by *t* test.

Effect of compound 15 on TNF- α induced SEAP activity

Next, we studied the effect of 3 α -(benzamido)-7 β -hydroxy-5 β -cholanoate (15) on SEAP activity in response to TNF- α . Compared with 17, 15 was a little less effective at inhibiting TNF- α induced SEAP activity (**Figure 42**).

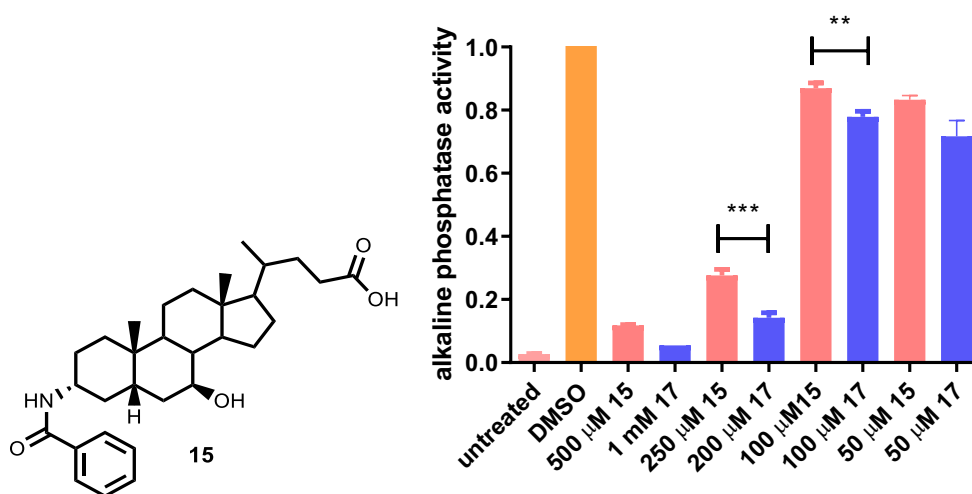


Figure 42. Comparison of the QUANTI-Blue assay result of 3 α -(benzamido)-7 β -hydroxy-5 β -cholanoate(**15**) and 3 α -(4-chlorobenzamido)-7 β -hydroxy-5 β -cholanoate (**17**) THP1-Blue cells were treated with 10 ng/ml TNF- α and different concentrations of either 3 α -(benzamido)-7 β -hydroxy-5 β -cholanoate (**15**) or 3 α -(4-chlorobenzamido)-7 β -hydroxy-5 β -cholanoate (**17**) for 24 h. The vehicle is 0.5 %DMSO. Values were expressed as fold difference as mean \pm SEM of triplicate experiments, ** p <0.01, *** p <0.001, was determined by *t* test.

Effect of compound 23 on TNF- α induced SEAP activity

Data for the unsubstituted beta amide, 3 β -(benzamido)-7 β -hydroxy-5 β -cholanoate (**23**), are presented in **Figure 43** in comparison with compound **15**. Interestingly, compound **23** was significantly less active than its alpha analogue, with no evidence of inhibition at concentration levels that did not induce cell death in this cell line in the earlier studies.

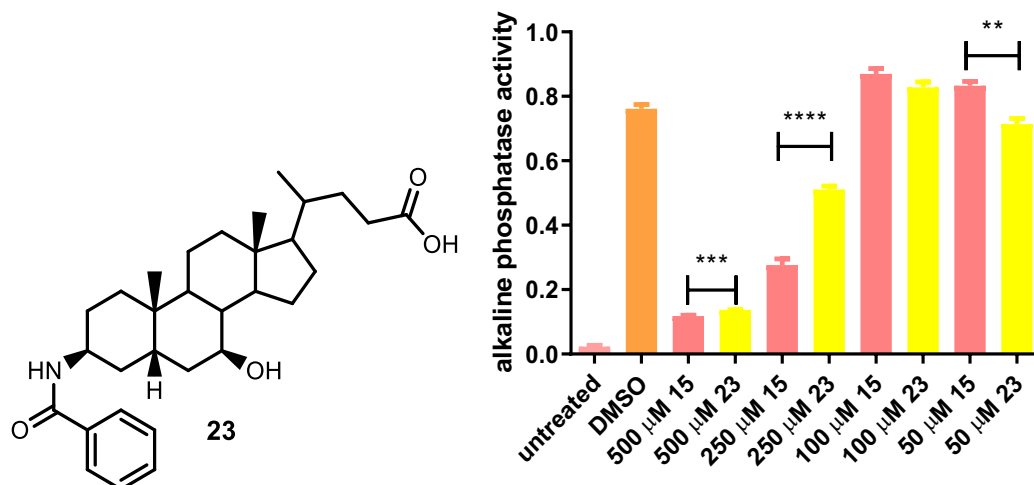


Figure 43. Comparison of the QUANTI-Blue assay result of 3β-(benzamido)-7β-hydroxy-5β-cholanoate (23) and 3α-(benzamido)-7β-hydroxy-5β-cholanoate (15) THP1-Blue cells were treated with 10 ng/ml TNF-α and different concentrations of either 3β-(benzamido)-7β-hydroxy-5β-cholanoate (23) or 3α-(benzamido)-7β-hydroxy-5β-cholanoate (15) for 24 h. The vehicle is 0.5 %DMSO. Values were expressed as fold difference compared to the vehicle as mean ± SEM of triplicate experiments, ** $p < 0.01$, *** $p < 0.001$, **** $P < 0.0001$ was determined by *t* test.

Effect of compound 24 on TNF-α induced SEAP activity

Finally, in this series we studied compound **24**, the chlorobenzamide with beta configuration. As with **23**, this compound caused inhibition of SEAP activity in response to TNF-α, but only at concentration levels where it also caused inhibition of cell proliferation. This compound was not as active as its alpha isomer, just as the unsubstituted beta compounds **23**, **24** was not as active as its alpha isomer.

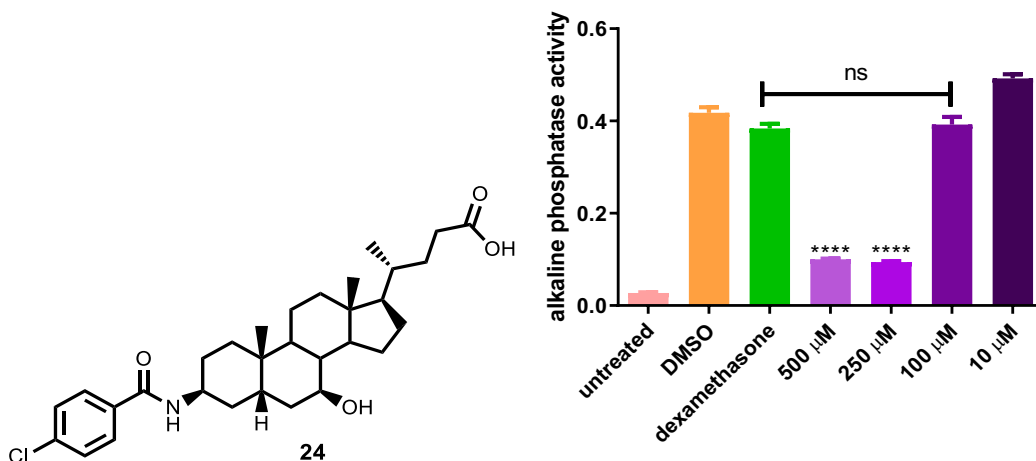


Figure 44. QUANTI-Blue assay result of 3β-(4-chlorobenzamido)-7β-hydroxy-5β-cholanoate (24) THP1-Blue cells were treated with 10ng/ml TNF-α and different concentrations of 3β-(4-chlorobenzamido)-7β-hydroxy-5β-cholanoate (24) for 24 h. The vehicle is 0.5 %DMSO. The dexamethasone concentration is 1 μM. Values were expressed as fold difference compared to the vehicle as mean ± SEM of triplicate experiments, ns P>0.05, ****P <0.0001 was determined by oneway ANOVA with Dunnett's post-hoc correction and by t test.

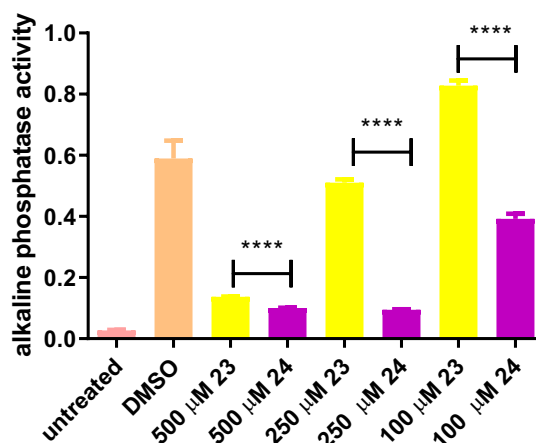


Figure 45. Comparison of the QUANTI-Blue assay result of 3β-(benzamido)-7β-hydroxy-5β-cholanoate (23) and 3β-(4-chlorobenzamido)-7β-hydroxy-5β-cholanoate (24) THP1-blue cells were treated with 10 ng/ml TNF-α and different concentrations of these compounds for 24 h. The vehicle is 0.5 %DMSO. Values were expressed as fold difference as mean ± SEM of triplicate experiments, ****P <0.0001 was determined by t test.

3 β -(4-chlorobenzamido)-7 β -hydroxy-5 β -cholanoate (**24**) has an influence on reducing AP activity depending on its concentration. Compared with 3 β -(benzamido)-7 β -hydroxy-5 β -cholanoate (**23**), compound **24** caused a more significant decrease of AP activity. This would suggest that introducing the chloride side chain increases NF- κ B inhibitory activity in both 3-alpha and 3-beta configuration.

Effect of the 7-substituted compounds **33** and **35** on TNF- α induced SEAP activity

Finally, we studied the two 7-substituted UDCA analogues (**33**, **35**) for their effect on TNF- α induced SEAP activity (**Figure 46**, **Figure 47**). These compounds were active at the concentration (>250 μ M) showing similar or greater activity than dexamethasone under conditions where no cell death or reduction in proliferation had been observed in the earlier studies while dexamethasone has serious side effects with chronic use^[102]. Given their overall profile and lack of inhibitory activity on proliferation in multiple cell lines, these may be promising analogues for pharmacological development.

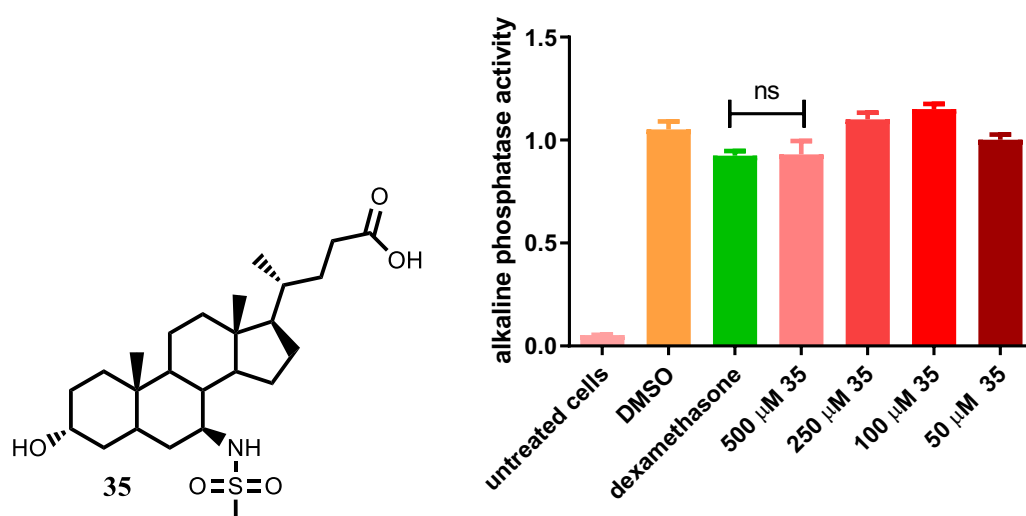


Figure 46. QUANTI-Blue assay result of 3 α -hydroxy-7 β -(methanesulfonamido)-5 β -cholanoate (**35**) *THP1-Blue cells were treated with*

different concentrations of **compound 35** with 10 ng/ml TNF- α for 24 h. The vehicle is 0.5 %DMSO. The concentration of dexamethasone is 1 μ M. Values were expressed as mean \pm SEM of triplicate experiments, ns $p > 0.05$, was determined by *t* test.

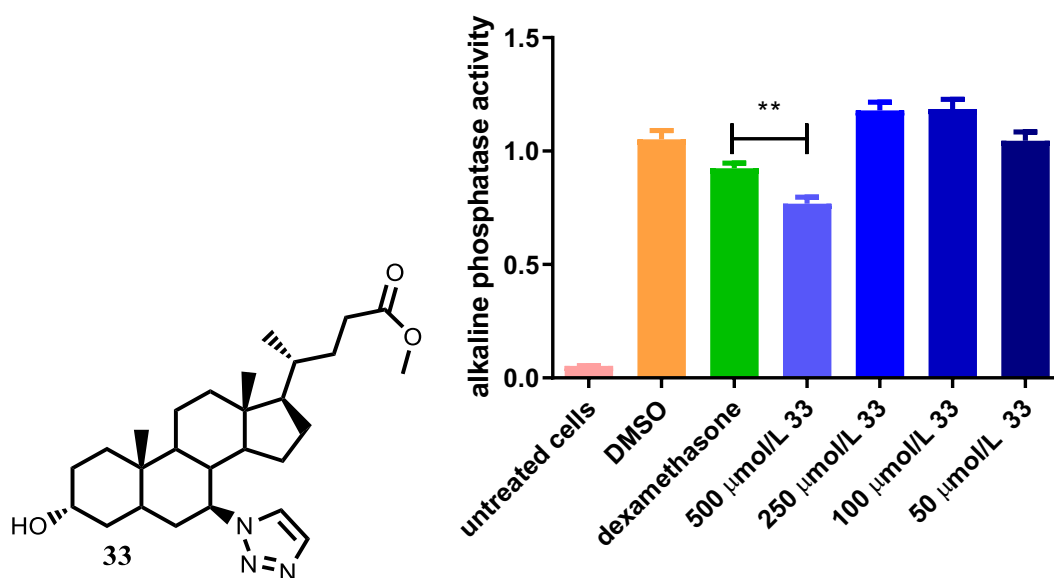


Figure 47. QUNATI-Blue assay results for UDCA-based triazole 33. THP1-Blue cells were treated with different concentrations of 3 α -hydroxy-7 β -(1H-1,2,3-triazol-1-yl)-5 β -cholanoate (**33**) with 10 ng/ml TNF- α for 24 h. The vehicle is 0.5 %DMSO. The concentration of dexamethasone is 1 μ M. Values were expressed as mean \pm SEM of triplicate experiments, ** $p < 0.01$, was determined by *t* test.

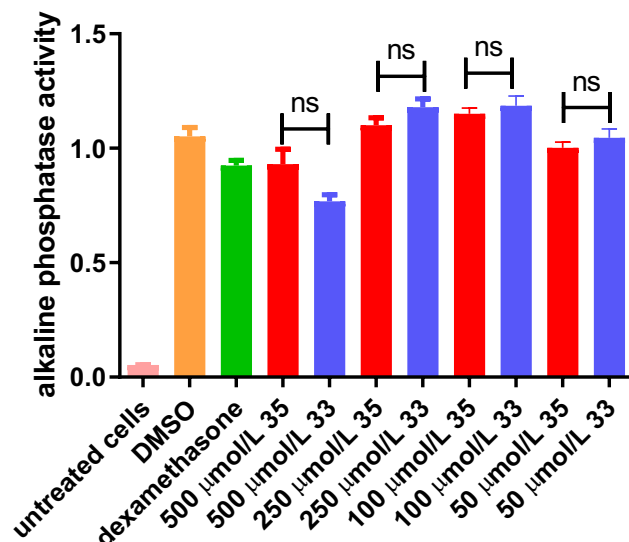


Figure 48. Comparison of the QUANTI-Blue assay result of UDCA-based triazole (33) and UDCA-based sulfonamide (35) *THP1-Blue cells were treated with 10 ng/ml TNF- α and different concentrations of compound 33 and 35 for 24 h. The vehicle is 0.5 % DMSO. The dexamethasone concentration is 1 μ M. Values were expressed as mean \pm SEM of triplicate experiments, ns $p > 0.05$, was determined by t test.*

Effect of the compound 25 on TNF- α induced SEAP activity

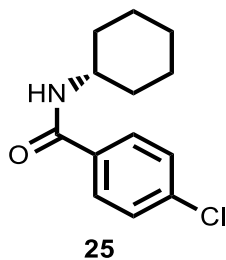
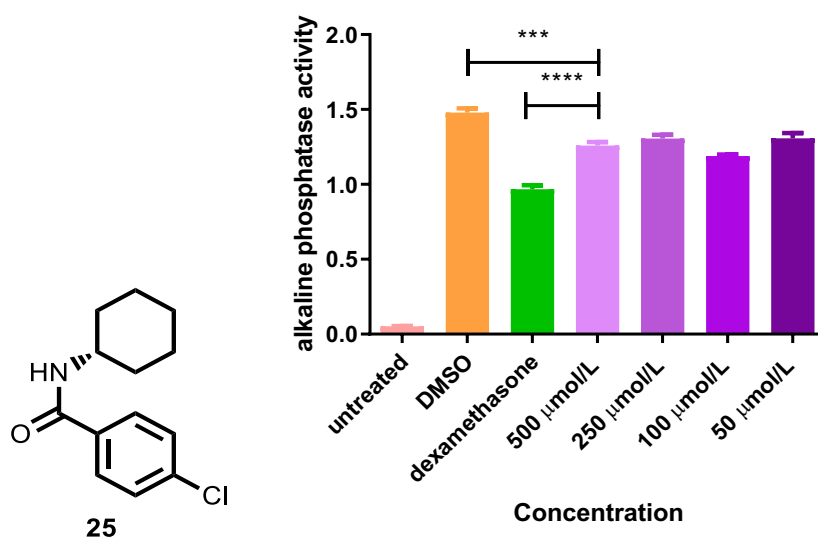


Figure 49. QUANTI-Blue assay results for 4-chloro-N-cyclohexyl benzamide (25) *THP1-Blue cells were treated with different concentrations of 4-chloro-N-cyclohexylbenzamide (25) and 10 ng/ml TNF- α for 24 h. The vehicle*

is 0.5 %DMSO. The dexamethasone concentration is 1 μ M. Values were expressed as fold difference compared to the vehicle as mean \pm SEM of triplicate experiments, *** $p < 0.001$, **** $P < 0.0001$ was determined by *t* test.

The chloro-substituted benzamide of cyclohexylamine (**25**) was tested as a control for the effect of the UDCA scaffold on the activity of the compound set. This compound induced an apparent reduction in SEAP activity in response to TNF- α but it did not reduce apparent NF- κ B activity in a concentration dependent way. This study is overall inconclusive because of this inhibition relative to DMSO control, but failure to observe a concentration dependence suggests it was artifactual.

3.12 Effect of the compounds on IL-8 stimulated by inflammatory promoters in Caco-2, PBMC and Huh7 cell lines.

Having shown that the BA derivatives above possess anti-inflammatory effects in a genetically engineered NF- κ B reporter cell line we now turned our attention to primary monocytes using IL-8 measurement as an indicator of NF- κ B activity. We decided to use a range of inflammatory stimuli to screen for inhibitory effect. The stimuli we used were 1 μ g/mL LPS, 10 μ g/mL TNF- α as a pro-inflammatory cytokine, 50 μ g/mL phorbol 12-myristate 13-acetate (PMA) and 200 μ M DCA. The UDCA derivatives were tested at a concentration of 50 μ M because they were shown to not possess cytotoxicity effect on PBMCs at this concentration. Therefore, an inhibition of IL-8 production could be attributed to an anti-inflammatory effect rather than a cytotoxic effect. After 24 h incubation, the supernatant was collected and IL-8 concentration was determined by ELISA. UDCA was used as a control because we were seeking evidence of an increased anti-inflammatory effect in UDCA analogues. The experiments were performed in liver cells and PBMCs.

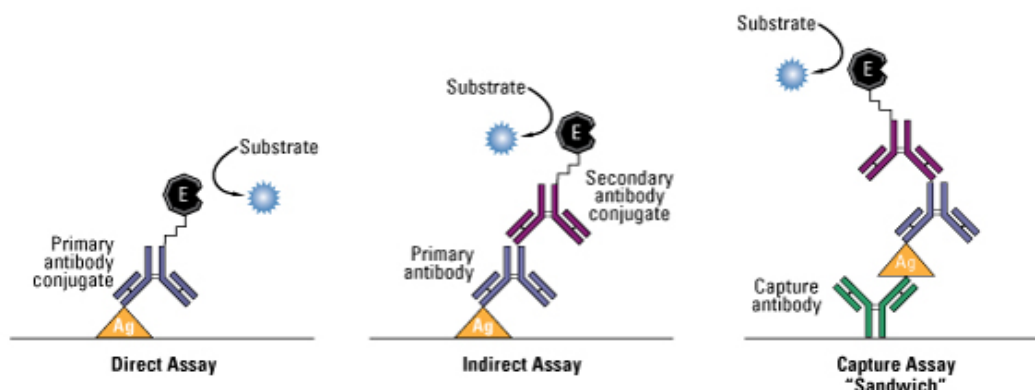


Figure 50. ELISA ^[165, 166] *In the assay, the antigen immobilization has direct and indirect way including absorption to the plate and attaching to an antibody. Also, the antigen is detected by the primary antibody conjugated with enzyme or by the unlabeled primary antibody and secondary antibody.*

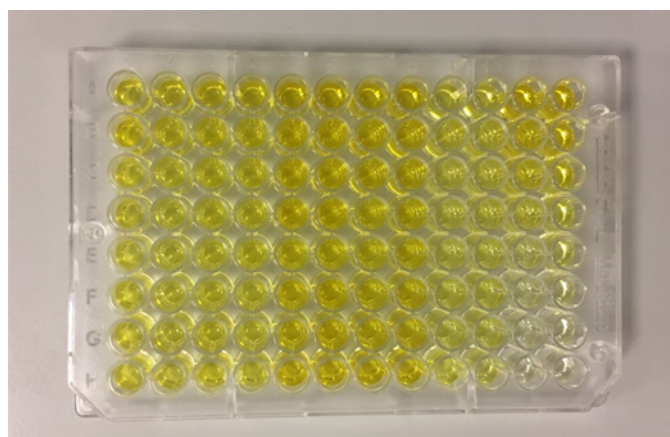


Figure 51. ELISA from one of the IL-8 assay

3.12.1 IL-8 estimation for BA derivatives effect on Caco-2 cells

Before assessing the activity in PBMCs, we decided to investigate the effect of the compounds in Caco-2 cells in the context of inflammatory stimulus. Caco-2 cells were therefore treated with a TNF- α /IFN- γ cocktail to induce NF- κ B activity in order to screen for an inhibitory effect of the BA panel. Unfortunately, we were not able to produce a significant induction of IL-8 under these

circumstances in the presence of the stimulus alone, although a small statistically insignificant inhibitory effect was observed in the compound **15** (Figure 52).

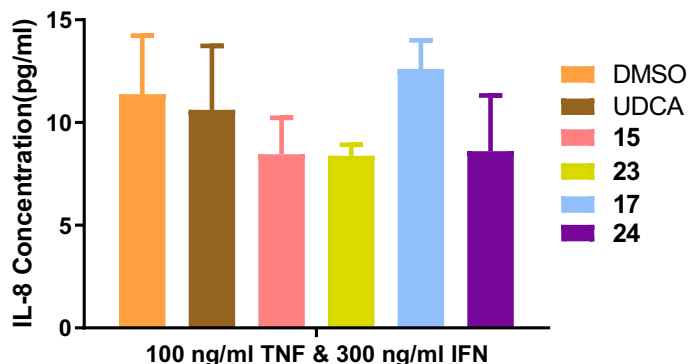


Figure 52. IL-8 result of BAs TNF- α and IFN- γ stimulation *Caco-2* were treated with 100 ng/mL TNF- α and 300 ng/mL IFN- γ for 30 minutes and then bile acid analogue solution (final concentration is 100 μ M) was added into each well before 24 h incubation. 50 μ L cell supernatant was used to do the ELISA. The vehicle control is 0.5 % DMSO. Values were expressed as fold difference as mean \pm SEM of triplicate experiments.

3.12.2 IL-8 estimation for BA derivatives on PBMCs

Primary PBMCs were treated for 24 h with compounds in the presence of four different inflammatory agonists, LPS, TNF- α , PMA, DCA. Supernatant was collected and analysed by ELISA for secreted IL-8.

In all, PBMC preparations from three different patients were subjected to treatment in triplicate. There was large intersubject variability evident and also large variation within a single subject in the magnitude of response to the stimuli and variation in inhibitory effect. Therefore, sample data presented here show the results of several experiments rather than the average which obscures effects observable in single patient samples.

In the experiment, PBMCs were treated with different agonist for 30 min and then bile acid analogues solution (final concentration is 50 μ M) was added into each well before 24 h incubation. 50 μ L cell supernatant was used to do the ELISA. The positive control is 0.5 % DMSO.

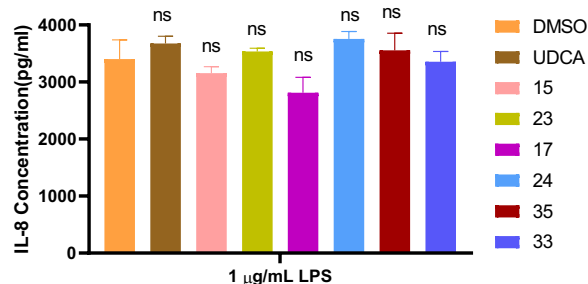


Figure 53. LPS stimulation on experiment 1 PBMCs were treated with 1 μ g/mL LPS for 30 min and then bile acid analogues solution (final concentration is 50 μ M) for 24 h incubation. Values were expressed as mean \pm SEM of one experiment compared to PBMCs treated with LPS, ns $p > 0.05$, was determined by *t* test.

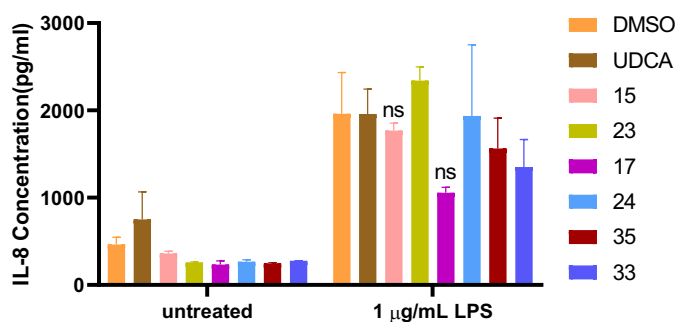


Figure 54. LPS stimulation on experiment 2 PBMCs were treated with 1 μ g/mL LPS for 30 min and then bile acid analogues solution (final concentration is 50 μ M) for 24 h incubation. Values were expressed as mean \pm SEM of one experiment compared to PBMCs treated with LPS, ns $p > 0.05$, was determined by *t* test.

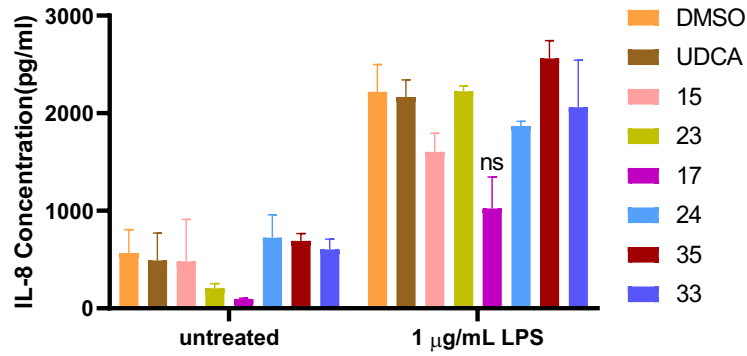


Figure 55. LPS stimulation on experiment 3 PBMCs were treated with 1 µg/mL LPS for 30 min and then bile acid analogues solution (final concentration is 50 µM) for 24 h incubation. Values were expressed as mean ± SEM of one experiment compared to PBMCs treated with LPS, ns $p > 0.05$, was determined by *t* test.

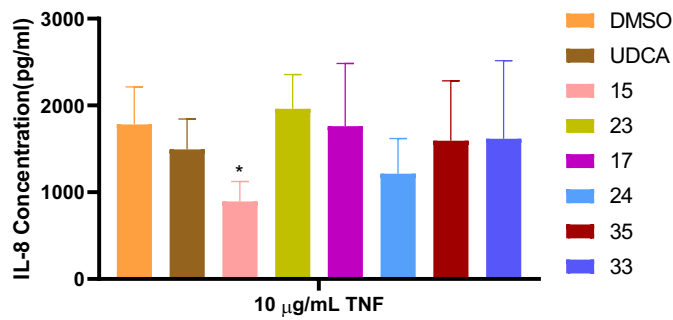


Figure 56. TNF-α stimulation on experiment 1 PBMCs were treated with 10 µg/mL TNF-α for 30 min and then bile acid analogues solution (final concentration is 50 µM) for 24 h incubation. Values were expressed as mean ± SEM of one experiment compared to PBMCs treated with TNF-α, * $p < 0.05$, was determined by *t* test.

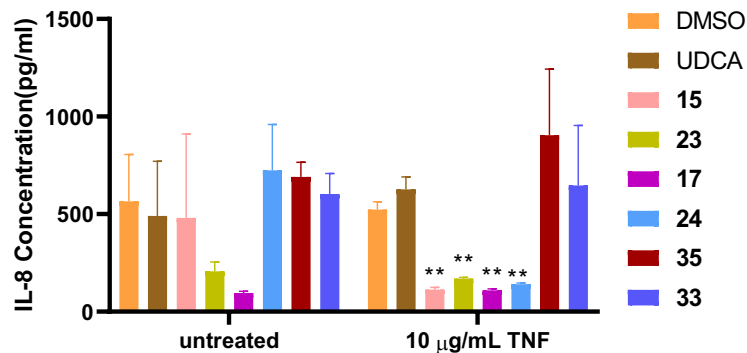


Figure 57. TNF-α stimulation experiment 2 PBMCs were treated with 10

$\mu\text{g/mL TNF-}\alpha$ for 30 min and then bile acid analogues solution (final concentration is $50 \mu\text{M}$) for 24 h incubation. Values were expressed as mean \pm SEM of one experiment compared to PBMCs treated with TNF- α , $**p < 0.01$, was determined by t test.

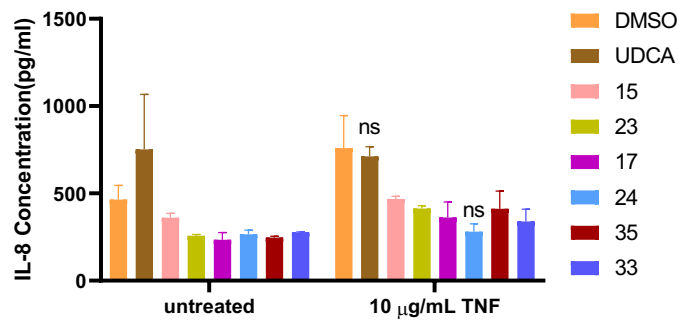


Figure 58. TNF- α stimulation on experiment 3 PBMCs were treated with $10 \mu\text{g/mL TNF-}\alpha$ for 30 min and then bile acid analogues solution (final concentration is $50 \mu\text{M}$) for 24 h incubation. Values were expressed as mean \pm SEM of one experiment compared to PBMCs treated with TNF- α , ns $p > 0.05$, was determined by t test.

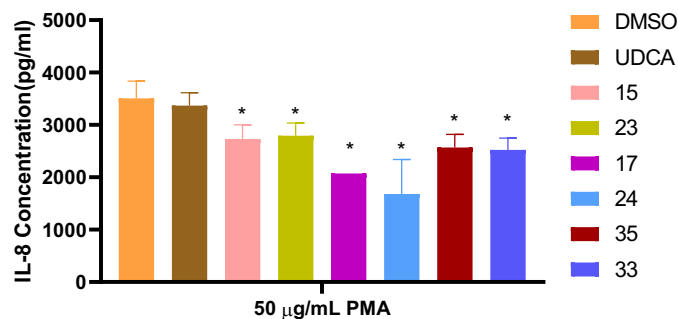


Figure 59. PMA stimulation on experiment 1 PBMCs were treated with $50 \mu\text{g/mL PMA}$ for 30 min and then bile acid analogues solution (final concentration is $50 \mu\text{M}$) for 24 h incubation. Values were expressed as mean \pm SEM of one experiment compared to PBMCs treated with PMA, * $p < 0.05$, was determined by t test.

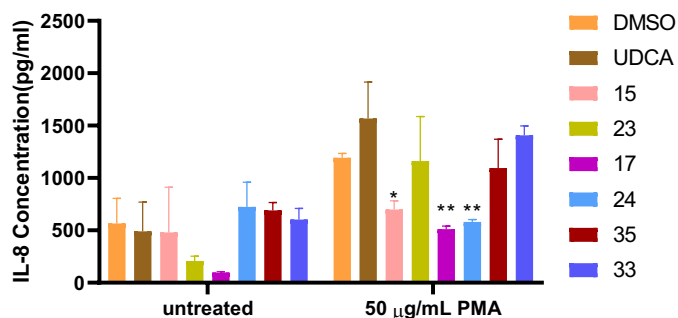


Figure 60. PMA stimulation experiment 2 PBMCs were treated with 50 µg/mL PMA for 30 min and then bile acid analogues solution (final concentration is 50 µM) for 24 h incubation. Compound 5 is UDCA. Values are expressed as mean ± SEM of one experiment compared to PBMCs treated with PMA, * $p < 0.05$, ** $p < 0.01$, was determined by *t* test.

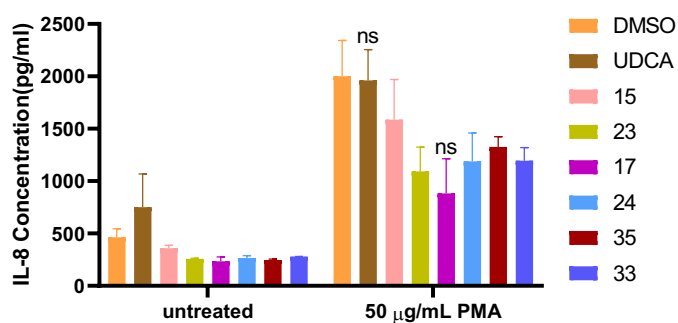


Figure 61. PMA stimulation on experiment 3 PBMCs were treated with 50 µg/mL PMA for 30 min and then bile acid analogues solution (final concentration is 50 µM) was added into each well before 24 h incubation. 50 µL cell supernatant was used to do the ELISA. The positive control is 0.5 % DMSO. Values were expressed as mean ± SEM of one experiment compared to PBMCs treated with PMA, ns $p > 0.05$, was determined by *t* test.

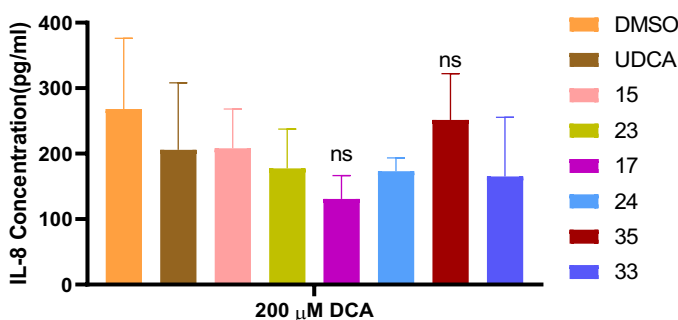


Figure 62. DCA stimulation on experiment 1 PBMCs were treated with 200 µM DCA for 30 min and then bile acid analogues solution (final concentration is

50 μM) was added into each well before 24 h incubation. Values were expressed as mean \pm SEM of one experiment compared to PBMCs treated with DCA, ns $p > 0.05$, was determined by *t* test.

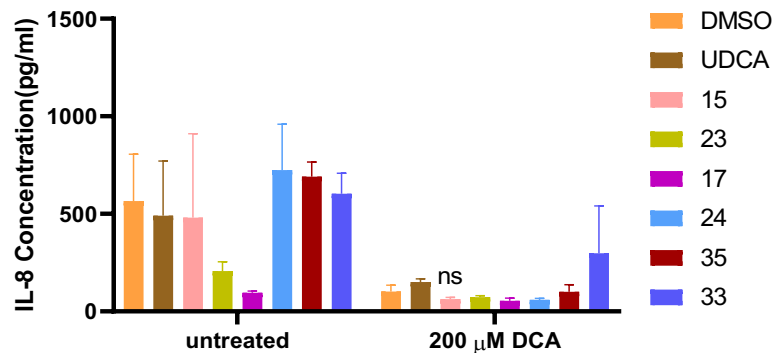


Figure 63. DCA stimulation experiment 2 PBMCs were treated with 200 μM DCA for 30 min and then bile acid analogues solution (final concentration is 50 μM) was added into each well before 24 h incubation. Values were expressed as mean \pm SEM of one experiment compared to PBMCs treated with DCA, ns $p > 0.05$, was determined by *t* test.

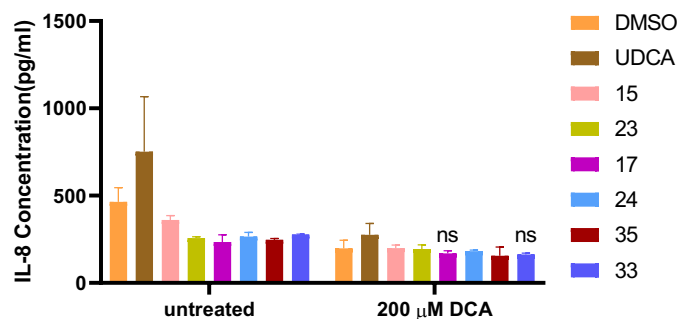


Figure 64. DCA stimulation on experiment 3 PBMCs were treated with 200 μM DCA for 30 min and then bile acid analogues solution (final concentration is 50 μM) was added into each well before 24 h incubation. Values were expressed as mean \pm SEM of one experiment compared to PBMCs treated with DCA, ns $p > 0.05$, was determined by *t* test.

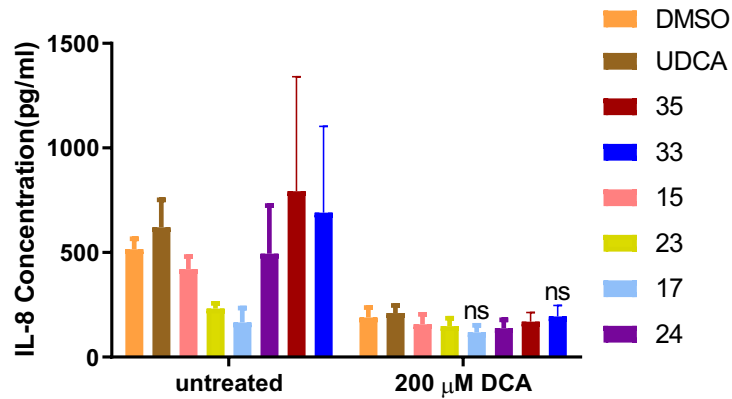


Figure 65. DCA stimulation, mean of three experiments PBMCs were treated with 200 μM DCA for 30 min and then bile acid analogues solution (final concentration is 50 μM) was added into each well before 24 h incubation. Values were expressed as mean ± SEM of one experiment compared to PBMCs treated with DCA, ns $p > 0.05$, was determined by *t* test.

3.12.3 IL-8 estimation for BA derivatives on Huh7

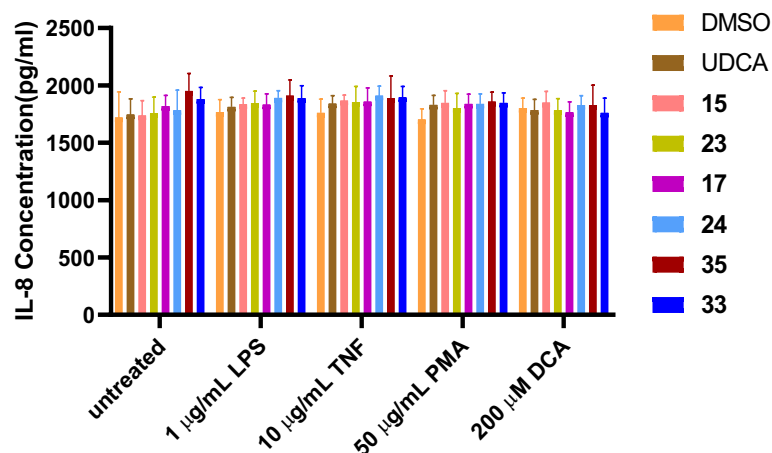


Figure 66. IL-8 estimation of bile acid derivatives Huh7 cells were treated with different agonists for 30 min and then bile acid analogues solution (final concentration is 50 μM) was added into each well before 24 h incubation. Values were expressed as fold difference as mean ± SEM of triplicate experiments.

IL-8 levels were measured in Huh7 cells treated with the panel of inflammatory mediators. Unfortunately, there was no evidence of induction of IL-8 in response

to the agonists apparently because the constitutive level of IL-8 in these cells was already very high. There were no inhibitory effects evident. Huh7 is a hepatoma cell line and it is not a good choice for this kind of assay. The experiment should be repeated in another more suitable immortalized cell line or in primary human or rodent hepatocytes. This might allow more accurate evaluation of the inhibitor potential of the bile acid analogues than Huh7 cells.

3.12.4 IL-6 estimation for BA derivatives on Huh7

Since the Huh7 cells produced already very high IL-8 levels under basal conditions that were not increased in the presence of the inflammatory stimuli, our attention was turned to IL-6, which was suggested to be under inflammatory mediator control (**Figure 67**). The IL-6 levels in the unstimulated cells were very low in comparison to the IL-8 data. There was also significant variability which prevents any conclusion to be reached about the effect of the compounds on the basal or unstimulated IL-6 levels. No significant change could be observed in IL-6 levels following stimulation with DCA, TNF- α or LPS. However, there was a significant increase in the presence of PMA (**Figure 68**).

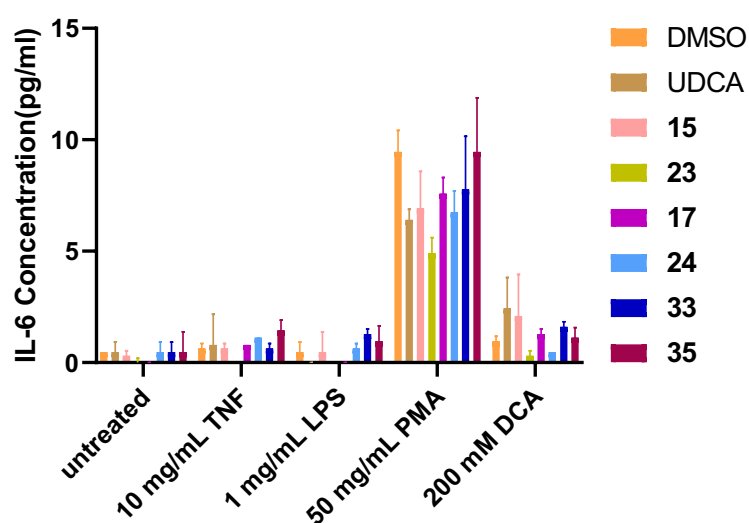


Figure 67. IL-6 secretion in response to stimuli and bile acid derivatives Huh7 cells, were treated with different agonists for 30 min and then bile acid

analogues solution (final concentration is 50 μ M) was added into each well before 24 h incubation. 100 μ L cell supernatant was used to do the ELISA. The vehicle control is 0.5 % DMSO. Values were expressed as fold difference as mean \pm SEM of triplicate experiments.

PMA caused a significant induction of IL-6 secretion. UDCA caused a significant decrease in the IL-6 response to PMA, perhaps the only evidence of an anti-inflammatory effect in these studies. The amide derivatives were not different in effect to UDCA in this study, whereas the two 7-substituted derivatives, **33** and **35** were without any observable effect.

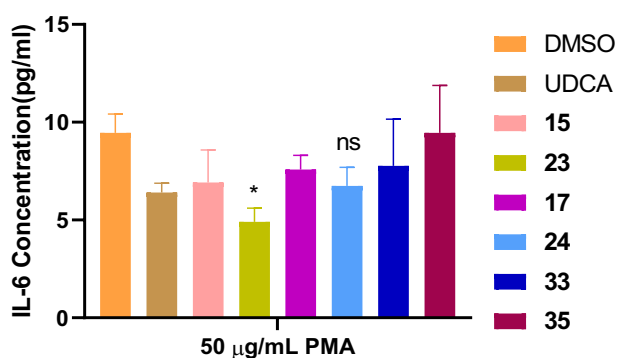


Figure 68. IL-6 following PMA stimulation *Huh7* cells were treated with 50 μ g/mL PMA for 30 min and then bile acid analogues solution was added into each well before 24 h incubation. Aliquots of 100 μ L cell supernatant was obtained for ELISA. The vehicle was 0.5 % DMSO. Values were expressed as mean \pm SEM of triplicate experiments compared to PBMCs treated with DCA, ns $p > 0.05$, was determined by *t* test.

3.13 Discussion

UDCA is used to treat a range of cholestatic liver disease conditions, a clinical effect that is underpinned and consistent with a range of immune-modulatory and anti-inflammatory effects in cell culture. Some of these effects may be attributed to activation of the GR but the precise binding mode of UDCA is not clear under these circumstances and it has low potency. UDCA is also subject to poor bioavailability connected to its low water solubility, and it is metabolized

extensively in the colon, producing LCA. There is conflicting evidence regarding the effects of LCA in the colon with some studies showing that it is cytotoxic, pro-inflammatory, and others showing that it is anti-inflammatory.^[147] In general, the production of LCA by UDCA administration is regarded as a restraint on its clinical efficacy rather than a bonus. Under these circumstances the Gilmer group has targeted several chemocentric modifications to UDCA and LCA with the aim of improving potency and specificity towards anti-inflammatory targets while reducing its potential to undergo hepatic or colorectal metabolism. One of the challenges in the field, is that many possible synthetic modifications to UDCA, especially those that increase hydrophobicity, can also increase toxicity, an important limitation to potential therapeutic effect. The present work concerned the characterization of a group of compounds that were developed for potential activity at the GR. This was based on preliminary data from earlier work that some phenyl amide substituted 3α -amines, especially those substituted at phenyl C-4 with chloride atom, can cause GR translocation. The compounds were characterized first for their cytotoxicity considering their greater lipophilicity than UDCA. In general, the benzamide compounds were toxic at concentration levels greater than 100 μ M in a range of cell types including Caco-2, Huh-7, THP 1-Blue and primary PBMCs from human volunteers; perhaps greatest toxicity was observed in the colorectal cell line. Conversely, the triazole and sulfonamide compounds **33** and **35** which are highly polar were non-toxic. This is consistent with expectations from the BA literature, that chemical manipulations resulting in more or less hydrophobicity are associated with more or less toxicity, respectively. Having surveyed the cytotoxicity/antiproliferative effects, we then assessed the inhibitory properties of the compounds on TNF- α driven NF- κ B stimulation in a THP 1-Blue reporter assay which causes secretion of SEAP in response to stimulation of receptors upstream of NF- κ B, including TLRs and TNF receptors. The polar analogues **33** and **35** were non-toxic in several cell lines and they inhibited NF- κ B activity in

the SEAP assay in THPs at high and probably suprapharmacological concentration (>250 μM). In the panel of 3-benzamides, the chlorobenzamide compound, which had earlier been shown to be capable of causing GR translocation in the range 50-100 μM , was most active in causing inhibition of TNF- α stimulated NF-kB activity. In general, the two α -benzamide compounds (**15**, **17**) were most active, with the chloride compound **17** being the more active of the two. The data are consistent with the idea that **17**, the chlorobenzamide substituted UDCA compound, can inhibit NF-kB activity through a GR mediated effect. Interestingly, N-cyclohexylbenzamide (**25**), a compound without a BA scaffold did not exert a concentration dependent effect on NF-kB activity in the THP reporter assay. It did appear to have reduced activity overall but the data are not conclusive because of a lack of concentration dependence. In the GR assay, the cyclohexamide compound was not active (data not shown). In the primary PBMCs drawn from healthy human volunteers, there was great variability in IL-8 production as a surrogate for NF-kB activation in response to a range of stimuli. Some subjects showed already very high IL-8 levels even without stimulation. In one subject whose PBMCs responded appropriately to a range of pro-inflammatory stimuli, it was possible to measure inhibitory effects that were consistent with the previous data. In general, UDCA did not exert an inhibitory effect in PBMCs stimulated with TNF- α , LPS, PMA or DCA. This was unexpected because of the published literature showing that UDCA at 50 μM can affect inflammatory signaling in monocytes^[167]. In this assay system **17** exerted a consistent inhibitory effect at 50 μM when PBMCs were stimulated with TNF α , LPS and PMA. Inhibitory effects against DCA induced inflammatory signaling were not observed but in this case, there is likely to have been cell death through the cumulative effects of hydrophobic BAs. There were modest but not consistent effects with the triazole compound **33** and compound **35**, the UDCA sulfonamide, suggesting that these may have promise as UDCA analogues with enhanced activity and pharmaceutical properties such as

solubility, polarity and cytotoxicity. Overall the data suggest that compound **17**, and perhaps its unsubstituted analogue **15**, possess interesting anti-inflammatory potential. Compound **17** strongly mediates GR translocation in SKGT4 cells. It was active in the THP 1-Blue/NF-kB reporter assay and it inhibits secretion of IL-8 in a range of cell types, especially PBMCs, and to a range of stimuli. Although it is toxic in higher concentrations, it may be possible to define a pharmacological window where it exerts selective anti-inflammatory actions. Future work could assess the functional activity of the compound in appropriate inflammatory *in vivo* models and potentially in models of cholestatic disease where GR activation may be beneficial in some circumstances.

Chapter 4. Methodology

4.1 Chemistry

4.1.1 General synthetic method

All chemicals we used were produced by Sigma-Aldrich. Thin-Layer Chromatography (TLC) was used to monitor progress of reactions. All products were characterised by Nuclear Magnetic Resonance spectroscopy (NMR) including ^1H NMR and ^{13}C NMR on Agilent 400MR DD2 spectrometer (400.13MHz, ^1H ; 100.61MHz, ^{13}C) using trichloromethane as internal standard. Chemical shifts were recorded parts per million (ppm) and coupling constants were recorded in Hertz (Hz). For ^1H -NMR, chemical shifts are reported, shift value, peak integration reflected the number of proton and description of absorption (s) singlet, (d) doublet, (t) triplet, (q) quartet, (m) multiple.

4.1.2 Procedure for the 3α -, 3β -amides formation

24-methyl- 3α -azido-7-acetoxy- 5β -cholanoate (0.25 g, 0.54 mmol/L) (**12**) or 24-methyl- 3β -azido-7-acetoxy- 5β -cholanoate (0.25 g, 0.54 mmol/L) (**19**) was dissolved in EtOAc (10 mL) and 10 % Pd/C (0.12 g, 1.13 mmol/L) was also dissolved in EtOAc (20 mL). These two solutions were combined and stirred under hydrogen environment at room temperature for 36 h until TLC analysis (Hexane:EtOAc 4:1) showed starting material disappearance. The solvent was purified by celite pad in order to get rid of 10 % Pd/C. The solvent was removed *in vacuo* and the crude was reacted without further washing up due to its instability. The crude was dissolved in dry DCM (10 mL) and stirred on ice. Before the temperature of the reaction rose to room temperature, triethylamine was added and hydrochloric acid was added drop by drop. The reaction was stirred overnight, until TLC showed disappearance of starting material. The solvent was removed *in vacuo* and then the residue was purified through flash

column chromatography (Hexane:EtOAc=4:1). 2M NaOH(5mL) was added into a solution of the protected amide in MeOH (16 mL) and stirred under reflux at 85°C for around 5 h until the starting material disappeared in the TLC. The solvent was removed *in vacuo* and 1M HCl was added into the reaction mixture in order to neutralize the PH value. The solution was extracted with EtOAc (3*50 mL). The organic layer was collected and washed with water (2*50 mL) and brine (50mL). Before removing the solvent, the solution was dried over MgSO₄ and filtered in order to get rid of solid impurities. Finally, the solvent was removed, giving the amide product.

4.1.3 Procedure for the 7β-amides formation

24-Methyl 3α-acetoxy- 7β-azido-5β-cholanoate (**31**) and hydrochloric acid were dissolved in the 5 mL EtOAc and then this solution was added to a solution of 10% Pd/C in 5 mL EtOAc. The reaction was stirred under hydrogen at room temperature overnight. After the reaction complete (TLC, Hexane: EtOAc=3:1), the solution was filtered through celite pad and washed with EtOAc. The solvent was removed by the vacuum and the resulting compound was brought on to the next step immediately due to its chemical instability. 5 mL dry DCM was used to dissolve the amine and then triethylamine and HCl were added drop by drop at 0 °C. The solution was allowed to come to room temperature and the reaction was left stirring overnight. The solvent was removed by vacuum, and the compound was redissolved in 10 mL EtOAc and washed twice with 10 mL HCl, 10 mL water and 10 mL brine. The organic layer was collected, dried over MgSO₄ and then filtered. The compound dried by vacuum and the resulting solid was purified by flash column chromatography (Hexane: EtOAc). The resultant compound was dissolved in 5 mL MeOH and the pH adjusted to 14 using 2 M NaOH This was stirred at reflux 2 h. Upon completion of the reaction, the mixture was added into 20 mL 1 M HCl and washed with 20 mL EtOAc for three

times. The organic layer was collected and then washed with water and brine.

4.1.4 Synthesis of UDCA derivatives

3 α -(benzamido)-7 β -hydroxy-5 β -cholanoate (15)

Compound **13** (140 mg, 0.3229 mmol) was reacted with triethylamine (0.05 mL, 0.5979 mmol) and benzoyl chloride (0.083 mL, 0.7145 mmol) to yield a white solid (130.1 mg, 0.2624 mmol, 91 %). This was hydrolysed and purified by flash column chromatography (EtOAc: hexane 3:1) to afford a white solid (114.1 mg, 0.2301 mmol, 88 %).

¹H NMR (400 MHz, CHLOROFORM-d) δ ppm 1.56(1H, m, 1-CH₂), 1.66(1H, d, 2-CH₃), 3.64(1H, m, 3 α -H), 1.78(2H, d, 4-CH₂), 1.41(1H, d, 5-CH), 1.76(2H, d, 6-CH₂), 4.34(1H, m, 7 α -H), 2.02(1H, m, 8-CH), 1.40(1H, m, 9-CH), 1.04(3H, m, 19-CH₃), 1.52(2H, m, 11-CH₂), 1.56(2H, m, 12-CH₂), 1.04(3H, m, 18-CH₃), 1.40(1H, m, 14-CH), 1.60(2H, m, 15-CH₂), 1.60(2H, m, 16-CH₂), 1.47(1H, m, 17-CH), 0.65(3H, s, 18-CH₃), 1.01(3H, s, 19-CH₃), 0.89(3H, d, 21-CH₃), 1.64(1H, m, 22-CH), 1.89(2H, m, 23-CH₂), 3.64(3H, s, 25-CH₃), 6.38(1H, d, -NH), 7.40(2H, m, aromatic-H), 7.42(1H, m, aromatic-H), 7.74(2H, d, aromatic-H).

¹³C NMR (101 MHz, CHLOROFORM-d) δ ppm 37.5(1-C, CH₂), 28.6(2-C, CH₃), 76.7(3-C, 3 α -C), 35.2(4-C, CH₂), 38.6(5-C, CH), 33.5(6-C, CH₂), 49.0(7-C, α -C), 37.5(8-C, CH), 46.6(9-C, CH), 35.2(10-C, CH₃), 20.7(11-C, CH₂), 40.2(12-C, CH₂), 42.7(13-C), 50.6(14-C, CH), 24.2(15-C, CH₂), 28.3(16-C, CH₂), 56.01(17-C, CH), 13.5(18-C, 18-CH₃), 13.6(19-C, CH₃), 35.2(20-C, CH), 19.1(21-C, CH₃), 31.2(22-C, CH), 31.4(23-C, CH₂), 173.1(24-C, C=O), 51.9(25-C, CH₃), 126.8(aromatic-C, CH), 128.3(aromatic-C, CH), 136.0(aromatic-C, CH), 134.2(aromatic-C, CH), 185.0(24-C, COOH).

3 α -(4-chlorobenzamido)-7 β -hydroxy-5 β -cholanoate (17)

Compound **13** (140 mg, 0.3229 mmol) was reacted with triethylamine (0.05 mL, 0.5979 mmol) and 4-chlorobenzoyl chloride (0.083 mL, 6.474 mmol) to yield an off-white solid (346.5 mg, 0.6368 mmol, 94%). The solid (300 mg, 0.5513 mmol) was hydrolysed and purified by flash column chromatography (EtOAc : Hexane 1:1 containing 0.1 % AcOH) to afford a white solid (251 mg, 0.4735 mmol, 86%).

¹H NMR (400 MHz, CHLOROFORM-d) δ ppm 1.56(1H, m, 1-CH₂), 1.66(1H, d, 2-CH₃), 3.95(1H, m, 3 α -H), 1.78(2H, d, 4-CH₂), 1.41(1H, d, 5-CH), 1.76(2H, d, 6-CH₂), 4.34(1H, m, 7 α -H), 2.02(1H, m, 8-CH), 1.40(1H, m, 9-CH), 1.04(3H, m, 19-CH₃), 1.52(2H, m, 11-CH₂), 1.56(2H, m, 12-CH₂), 1.04(3H, m, 18-CH₃), 1.40(1H, m, 14-CH), 1.60(2H, m, 15-CH₂), 1.60(2H, m, 16-CH₂), 1.47(1H, m, 17-CH), 0.70(3H, s, 18-CH₃), 1.03(3H, s, 19-CH₃), 0.95(3H, d, 21-CH₃), 1.64(1H, m, 22-CH), 1.89(2H, m, 23-CH₂), 3.64(3H, s, 25-CH₃), 6.27(1H, d, -NH), 7.40(2H, d, aromatic-H), 7.42(1H, m, aromatic-H), 7.69(2H, d, aromatic-H).

¹³C NMR (101 MHz, CHLOROFORM-d) δ ppm 37.5(1-C, CH₂), 28.6(2-C, CH₃), 76.7(3-C, 3 α -C), 35.2(4-C, CH₂), 38.6(5-C, CH), 33.5(6-C, CH₂), 49.0(7-C, α -C), 37.5(8-C, CH), 46.6(9-C, CH), 35.2(10-C, CH₃), 20.7(11-C, CH₂), 40.2(12-C, CH₂), 42.7(13-C), 50.6(14-C, CH), 24.2(15-C, CH₂), 28.3(16-C, CH₂), 56.01(17-C, CH), 13.5(18-C, 18-CH₃), 13.6(19-C, CH₃), 35.2(20-C, CH), 19.1(21-C, CH₃), 31.2(22-C, CH), 31.4(23-C, CH₂), 173.1(24-C, C=O), 51.9(25-C, CH₃), 126.8(aromatic-C, CH), 128.3(aromatic-C, CH), 136.0(aromatic-C, CH), 134.2(aromatic-C, CH), 185.0(24-C, COOH).

3 β -(benzamido)-7 β -hydroxy-5 β -cholanoate (23)

Compound **20** (140 mg, 0.3229 mmol) was reacted with triethylamine (0.05 mL,

0.5979 mmol) and benzoyl chloride (0.083mL, 0.7145 mmol) to yield a white solid (130.1 mg, 0.2624 mmol, 91 %). This was hydrolysed and purified by flash column chromatography (EtOAc:Hexane 3:1) to afford a white solid (114.1 mg, 0.2301 mmol, 88 %).

¹H NMR (400 MHz, CHLOROFORM-d) δ ppm 1.56(1H, m, 1-CH₂), 1.66(1H, d, 2-CH₃), 3.64(1H, m, 3 β -H), 1.78(2H, d, 4-CH₂), 1.41(1H, d, 5-CH), 1.76(2H, d, 6-CH₂), 4.34(1H, m, 7 α -H), 2.02(1H, m, 8-CH), 1.40(1H, m, 9-CH), 1.04(3H, m, 19-CH₃), 1.52(2H, m, 11-CH₂), 1.56(2H, m, 12-CH₂), 1.04(3H, m, 18-CH₃), 1.40(1H, m, 14-CH), 1.60(2H, m, 15-CH₂), 1.60(2H, m, 16-CH₂), 1.47(1H, m, 17-CH), 0.65(3H, s, 18-CH₃), 1.01(3H, s, 19-CH₃), 0.89(3H, d, 21-CH₃), 1.64(1H, m, 22-CH), 1.89(2H, m, 23-CH₂), 3.64(3H, s, 25-CH₃), 6.38(1H, d, -NH), 7.40(2H, m, aromatic-H), 7.42(1H, m, aromatic-H), 7.74(2H, d, aromatic-H).

¹³C NMR (101 MHz, CHLOROFORM-d) δ ppm 37.5(1-C, CH₂), 28.6(2-C, CH₃), 76.7(3-C, 3 α -C), 35.2(4-C, CH₂), 38.6(5-C, CH), 33.5(6-C, CH₂), 49.0(7-C, α -C), 37.5(8-C, CH), 46.6(9-C, CH), 35.2(10-C, CH₃), 20.7(11-C, CH₂), 40.2(12-C, CH₂), 42.7(13-C), 50.6(14-C, CH), 24.2(15-C, CH₂), 28.3(16-C, CH₂), 56.01(17-C, CH), 13.5(18-C, 18-CH₃), 13.6(19-C, CH₃), 35.2(20-C, CH), 19.1(21-C, CH₃), 31.2(22-C, CH), 31.4(23-C, CH₂), 173.1(24-C, C=O), 51.9(25-C, CH₃), 126.8(aromatic-C, CH), 128.3(aromatic-C, CH), 136.0(aromatic-C, CH), 134.2(aromatic-C, CH), 185.0(24-C, COOH).

3 β -(4-chlorobenzamido)-7 β -hydroxy-5 β -cholanoate (24)

Compound **20** (140 mg, 0.3229 mmol) was reacted with triethylamine (0.05 mL, 0.5979 mmol) and 4-chlorobenzoyl chloride (0.083mL, 6.474 mmol) to yield an offwhite solid (346.5 mg, 0.6368 mmol, 94 %). The solid (300 mg, 0.5513 mmol) was hydrolysed and purified by flash column chromatography

(EtOAc:Hexane=1:3) to afford a white solid (251 mg, 0.4735 mmol, 86 %).

¹H NMR (400 MHz, CHLOROFORM-d) δ ppm 1.56(1H, m, 1-CH₂), 1.66(1H, d, 2-CH₃), 3.95(1H, m, 3β-H), 1.78(2H, d, 4-CH₂), 1.41(1H, d, 5-CH), 1.76(2H, d, 6-CH₂), 4.34(1H, m, 7α-H), 2.02(1H, m, 8-CH), 1.40(1H, m, 9-CH), 1.04(3H, m, 19-CH₃), 1.52(2H, m, 11-CH₂), 1.56(2H, m, 12-CH₂), 1.04(3H, m, 18-CH₃), 1.40(1H, m, 14-CH), 1.60(2H, m, 15-CH₂), 1.60(2H, m, 16-CH₂), 1.47(1H, m, 17-CH), 0.70(3H, s, 18-CH₃), 1.03(3H, s, 19-CH₃), 0.95(3H, d, 21-CH₃), 1.64(1H, m, 22-CH), 1.89(2H, m, 23-CH₂), 3.64(3H, s, 25-CH₃), 6.27(1H, d, -NH), 7.40(2H, d, aromatic-H), 7.42(1H, m, aromatic-H), 7.69(2H, d, aromatic-H).

¹³C NMR (101 MHz, CHLOROFORM-d) δ ppm 37.5(1-C, CH₂), 28.6(2-C, CH₃), 76.7(3-C, 3α-C), 35.2(4-C, CH₂), 38.6(5-C, CH), 33.5(6-C, CH₂), 49.0(7-C, α-C), 37.5(8-C, CH), 46.6(9-C, CH), 35.2(10-C, CH₃), 20.7(11-C, CH₂), 40.2(12-C, CH₂), 42.7(13-C), 50.6(14-C, CH), 24.2(15-C, CH₂), 28.3(16-C, CH₂), 56.01(17-C, CH), 13.5(18-C, 18-CH₃), 13.6(19-C, CH₃), 35.2(20-C, CH), 19.1(21-C, CH₃), 31.2(22-C, CH), 31.4(23-C, CH₂), 173.1(24-C, C=O), 51.9(25-C, CH₃), 126.8(aromatic-C, CH), 128.3(aromatic-C, CH), 136.0(aromatic-C, CH), 134.2(aromatic-C, CH), 185.0(24-C, COOH).

N-cyclohexylbenzamide (25)

cyclohexylamine (1.15 mL, 10.158 mmol) was dissolved in DCM (30 mL) and triethylamine (6.00 mL, 29.735 mmol) was added on ice, and then 4-chlorobenzoyl Chloride (1.377 mL, 10.740 mmol) was added dropwise. The reaction was allowed to come to room temperature while it was stirring for 1 h. The solvent was removed *in vacuo* and the residue was dissolved in EtOAc (10 mL) and then was washed with HCl (1 mol/L, 3x10 mL), NaHCO₃ (2x10 mL) and brine (2x10 mL). The organic layer was collected and then dried over MgSO₄.

^1H NMR (400 MHz, CHLOROFORM- d) δ ppm 7.97(2H,d,aromatic-H), 7.67(2H,d,aromatic-H),8.03(1H,d,-NH),3.54(1H,m, β -H),1.77(2H,m, cyclohexane-C),1.55(2H,m,cyclohexane-C),1.21(2H,m,cyclohexane-C), 1.10(2H,m, cyclohexane-C), 1.47(2H,m, cyclohexane-C).

^{13}C NMR (101 MHz, CHLOROFORM- d) δ ppm 130.1(aromatic-C,2CH), 128.9(aromatic-C,2CH),132.3(aromatic-C,CH),137.7(aromatic-C,CH), 51.6(β -C,CH),32.3(cyclohexane-C,2CH $_2$),24.8(cyclohexane-C,2CH $_2$), 51.6(cyclohexane-C,CH $_2$), 25.7(cyclohexane-C,CH).

4.2 Cell Culture

4.2.1 Counting

Cell counting is used to quantify the cell number in research through a bright-line haemocytometer (Hausser Scientific, Horsham, P.A., USA) and the dye 0.4% trypan blue (Sigma, St. Louis, MO, USA) which colours dead cells selectively. 20 μL of cell medium was added into 180 μL trypan blue which is 1 in 10 dilution and then mixed well. 10 μL mixture was injected into the haemocytometer and it was covered with a glass slide. Cells were counted per counting chamber and the average was calculated. The counting chamber was 0.1 mm^3 so the cell density was calculated as average \times 10 (trypan blue dilution) \times 10 4 (counting chamber factor: \times 10 5) per mL.

4.2.2 Cryopreserve and revival cells

Normally, cells were cultured in T-75 flask and then split using trypsin-EDTA. After centrifugation, the supernatant was removed and then the cell pelleted was gently resuspended in 3 mL of cell medium with 5 % DMSO. 1 mL of this

cell solution was added into a sterile cryovial and all these cryovials were placed in -20 °C for 30 min. Before transferring them to a liquid nitrogen tank for long-term storage, they were placed in a -80 °C freezer overnight.

To revive cell stock, the cryovial was taken from the liquid nitrogen tank and put in a 37°C water bath for several seconds. Once the cell solution had thawed, 9 mL cell medium was added gently to the cell solution. The cells were centrifuged at 900 rpm for 4 min and the supernatant removed from the cell pellet. Cells were resuspended in 5 mL of relevant media and transferred to a T-25 flask. Cells were split to a T-75 flask once they had reached 90% confluency. Media was changed every 2-3 days and cells were split as required using trypsin-EDTA.

4.2.3 Caco-2

Caco-2 cells were provided by ATCC (American Type Culture Collection). In the T-75 flask Caco-2s were cultured in minimum Essential Media (MEM) with 20% FBS, 2.2 g/L sodium bicarbonate, 1% sodium pyruvate, 6 mg/L penicillin G, 10 mg/L streptomycin, 5 mg/L gentamicin and the PH value is around 7.3. All these ingredients above should be sterile filtered through 0.22 µM filter before adding into the MEM. Cells were incubated in a humidified incubator under the condition of 37 °C, 5% CO₂. When the cell confluence reached around 80 %, they were split using trypsin-EDTA and then cultured in new flasks. Normally, media was changed every 2-3 days. Caco-2 cells were used until the passage number is over 40.

4.2.4 HT-29

HT-29 cells were provided by ATCC. In the T-75 flask (75cm³ flask), HT-29s

were cultured in McCoy's 5a Medium Modified with L-glutamine, sodium bicarbonate, 10% FBS, 10 mg/L streptomycin and 5 mg/L gentamicin. All these ingredients above should be sterile filtered through 0.22 µm filter before adding into the McCoy's 5a Medium. Cells were incubated in a humidified incubator under the condition of 37 °C, 5% CO₂. When the cell confluence reached around 80 %, they were split using trypsin-EDTA and then subcultured into new flasks. Media was changed every 2-3 days

4.2.5 THP1-Blue

THP1-Blue cells were obtained from ATCC. Cells were maintained in RPMI-1640 with 1.5 g/L sodium bicarbonate, 2 mM L-glutamine, 1.0 mM sodium pyruvate, 4.5 g/L glucose, 10 mM HEPES and 10% FBS (fetal bovine serum) and placed at 37°C in 5% CO₂ incubation. THP1-Blue were cultured in T-75 in a volume of 15 mL medium and passaged twice a week or as required (1 in 5 dilution).

4.2.6 Huh-7

Huh 7 were obtained from ATCC. Cells were cultured in DMEM medium with 10% heat-inactivated FBS at 37 °C, 5% CO₂ humidified environment in T-75 flask in a volume of 15 mL medium. Routinely, cells were passaged twice a week (1 in 4 dilution). Cells were washed with 1 mL trypsin and then removed from the flask surface by 3 mL trypsin for 10 min. 9 mL cell medium was added to the flask to stop the digestion and then cell pellet was obtained by centrifuged at 1200 rpm for 4 min. The cell pellet was resuspended in cell medium and transferred to new flask in a volume of 15 mL cell medium.

4.2.7 PBMCs

PBMCs were isolated from heparinised human venous blood. 50 mL blood and 50 mL PBS were taken to a centrifuge tube and then mixed well. 25 mL mixture was gently layered on top of 20 mL lymphoprep (Proteogenix,1114544), being careful not to mix the two. The tube was centrifuged at 1800 rpm, 20 °C for 22 min. The whitish buffy coat (PBMC) was aspirated and then washed twice with 30 mL PBS and 30 mL cell medium and centrifuged at 1300 rpm, 21 °C for 5 min. The supernatant was removed and then resuspended in cell medium. If PBMCs are not used immediately, they are stored in a -80°C freezer.

4.3 Biology

4.3.1 QUANTI-Blue Assay

The NF-κB signaling pathway is detected by the QUANTI-Blue Assay through determining AP activity. 100 μL cell solution was added into 96-well plates at a concentration of 1×10^6 cells/mL (THP 1-Blue). THP 1-Blue was treated with bile acid analogues after 1 h incubation. Before 24 -h incubation, 50 μL TNF-α was added whose final concentration is 10 ng/mL. After that, 20 μL sample supernatant was collected and then added into 200 μL QUANTI-Blue reagent in a 96-well plate. The plate was covered with tin-foil and incubated for 30 min. After the colour turned from pink to purple or blue, the absorbance was read by plate reader in the range of 620-655nm. All these UDCA derivatives were all dissolved in DMSO as a stock solution of 200 mmol/L. In order to reduce the possible effect caused by DMSO, the final concentration of DMSO was 0.5% in the treatment depending on the solubility of compounds. The two control groups, cells were treated with 10 ng/ml TNF-α in the negative group and the cells were treated with 0.5% DMSO cell medium (RPMI-1640) in the positive group.

4.3.2 MTT Assay

Cell viability was tested by the MTT assay. 100 μ L cell solution was added into 96-well plates at a concentration of 1.2×10^5 cells/mL (Caco-2), 5×10^5 cells/mL (HT-29), 1×10^5 cells/mL (Huh7) and 1×10^6 cells/mL (PBMC). The PBMC cells could be used immediately, however the other cells lines were incubated for 24 h to allow the cells to recover and adhere. The vehicles are cell treated with 1% or 0.5% DMSO and dexamethasone. The next day, cell medium was removed and then cells were treated with 100 μ L TNF- α , IFN- γ or BAs solution (in cell medium without serum) for 24 h. For cells treated with cocktail, after cell medium was removed, cells were treated with 50 μ L BAs solution for 1 h and then 50 μ L TNF- α with or without IFN- γ was added into wells finally. After 22 h, 10 μ L of 2.5 mg/mL MTT was added into each well., the plate was placed back to the incubator for last 2 h incubation, and then shaken for 10 min. Then the absorbance was read by Microplate Reader at 570nm. During this process, the bile acid derivatives were all dissolved in DMSO as a stock solution of 200 mmol/L. In order to reduce the possible effect caused by DMSO, the final concentration of DMSO was 1 % or 0.5 % in the treatment. The cells in the untreated group are all incubated in the medium without adding anything.

4.3.3 Flow Cytometry

In the T-25 flask (25cm³ flask), HT-29 cells were cultured in McCoy's 5a Medium Modified with L-glutamine, sodium bicarbonate, 10% FBS, 10 mg/L streptomycin and 5 mg/L gentamicin. After HT-29 cells were adherent to the flask at around 80% confluency, cells were treated with different concentrations of TNF- α , IFN- γ and cocktail of TNF- α , IFN- γ for 24 hours in 37 °C incubator. After 24 h, cells were rinsed by 1 mL PBS and trypsinized by trypsin. Before being spun down by centrifuge, trypsin was neutralized with 10 % PBS cell medium. Cell pellet was

collected and resuspended in 100 μ L iced-cold PBS. If cells were not run immediately, 1 mL 70 % ethonal was added and cells were stored in -20°C freezer. Cells were taken out of freezer and defrosted at room temperature. 2 mL extra PBS were added in order to reduce ethonal concentration and aid pelleting. Before removing all the solution and invert tubes on tissue paper to remove the last drop, samples were centrifuged at 2000 rpm for 5 min. Cell pellets were resuspended in 200 μ L PBS and transferred to FACS tubes. 12.5 μ L, 10 mg/mL RNase A (Sigma, R4875) and 37.5 μ L, 1 mg/mL propidium iodide(Sigma, R4170) were added into each sample and incubated samples for 30 min avoiding direct light. After that, flow cytometry was run on BD Accuri C6 flow cytometer.

4.3.4 Alamar Blue Assay

Cell viability was tested though adding the ready-to-use Alamar Blue solution. 100 μ L cell solution was added into 96-well plates at a concentration of 1.2×10^5 cells/mL (Caco-2). Cells need to incubate for 24 h before treatment in order to let these cells adhere to the surface of plate. The control group was treated with 0.5% DMSO. After 22 h incubation with treatments, the supernatant of each sample was collected and transferred to other 96-well plate and 20 μ L Alamar Blue solution was added, followed by 2 h incubation at 37°C . Then the fluorescence was read at 570 nm. During this process, all these bile acid derivatives were dissolved in DMSO as a stock solution of 200 mmol/L. In order to reduce the possible effect caused by DMSO, the final concentration of DMSO was 0.5 % in the treatment. The cells in the untreated group are all incubated in the medium without adding anything.

4.3.5 ELISA

Enzyme-linked immunosorbent assay (ELISA) was used to determine the

release of cytokines (IL-8, IL-6, MMP-9). Cell solution was added into 96-well plate at the concentration of 1.2×10^5 cells/mL (Caco-2) and 1×10^6 cells/mL (PBMC). The PBMC cells could be used immediately, however the other cells lines were incubated for 24 h to allow the cells to recover and adhere. The control group was treated with 0.5% DMSO. Cells were divided into four groups and each group was treated with 20 μ L of a different agonist including 1 μ g/mL LPS (Lipopolysaccharides), 10 μ g/mL TNF- α , 50 μ g/mL PMA (Phorbol 12-myristate 13-acetate) and 200 μ mol DCA for 30 min. Before incubation, cells were treated with 80 μ L 50 μ g/mL of these compounds. After treatment with the compounds for 24 h, cell supernatant was collected and 50 μ L of it was used to carry out the ELISA. 50 μ L samples and prepared standards were added into each well. Plat was put in a dark environment and incubated for 2 h at room temperature. After each well was washed 4 times using washing buffer, 100 μ L antibody buffer was added and then the plate was incubated for 30 min at room temperature. The washings were then repeated before adding 100 μ L substrate solution. After 30 min, the stop solution was added, making sure the solution was mixed thoroughly. The optical density of each well was determined after 30 min. All these bile acid analogues were dissolved in the DMSO as a stock solution of 200 mmol/L. In order to reduce the possible effect caused by DMSO, the final concentration of DMSO was either 0.5 % in the assay. PBMCs were treated with 50 μ M of different compounds under the same agonist.

4.3.6 GR translocation

100 μ L, 1×10^5 cells/mL huh7 cells in cell medium was placed into each well of 96-well plate. After 24-h incubation in order to let cells adhere to the bottom of the well, cells were treated with dexamethasone and the relevant compounds at 50 μ M and 100 μ M for 4 h. Then the medium was removed and 200 μ L of 4 % paraformaldehyde (PFA) in sterile PBS was added to each well After 20 minutes, the PFA was removed and each well was washed three time with PBS and then

200 μ L PBS was left in each well. If these cells will not be stained immediately, the plate was covered with tin-foil and kept in the 4 °C fridge until use.

After that, the PBS was removed 50 μ L of 0.3 % (v/v) Triton X in PBS was added for 15 minutes. Then the 0.3 % Triton X was removed and 50 μ L 5 % (v/v) BSA in PBS was added and left for 30 minutes. During this 30 minutes, primary antibody was diluted 1 in 100 with 5 % BSA in PBS. After removing the 5 % BSA, 50 μ L primary antibody (purified monoclonal mouse anti-GR antibody, BD Biosciences) was added to the plate and left at room temperature for 1 h. Then the secondary antibody (AlexaFluor-488-conjugated secondary antibody, Invitrogen) was diluted 1 in 500 in 5 % BSA in PBS and Hoechst 33342 (Invitrogen) was diluted 1 in 1000 in that. The primary antibody was removed and the cells were washed three time with PBS, before being treated with 50 μ L mixture solution for 30 minutes in dark environment at room temperature. Finally, cells were washed three times with PBS and 200 μ L PBS was left in each well. The 96-well plate was covered with tin-foil and ready for image.

There are two images composed of nuclei and GR of each compound were taken by GE Healthcare In Cell 1000. Image Acquisition Parameters were listed in the following. Objective we choose is Nikon 10X/0.45, Plan Apo, CFI/60. The selected wavelength is DAPI and FITC and their exposure time is 372 and 1352 respectively. These pictures and data can be analyzed by the software package of the machine through measuring the ratio of GR in nuclei and in cytoplasmic. The vehicles are untreated cells as negative control and cells treated with dexamethasone as positive control. The ratio calculation is (GR in the nuclei - Background) / (GR in cytoplasmic - Background Intensity).

Chapter 5. References

1. de Aguiar Vallim TQ, Tarling EJ, Edwards PA: **Pleiotropic roles of bile acids in metabolism.** *Cell metabolism* 2013, **17**(5):657-669.
2. Monte MJ, Marin JJG, Antelo A, Vazquez-Tato J: **Bile acids: chemistry, physiology, and pathophysiology.** *World journal of gastroenterology* 2009, **15**(7):804-816.
3. Hofmann AF, Hagey LR, Krasowski MD: **Bile salts of vertebrates: structural variation and possible evolutionary significance.** *Journal of lipid research* 2010, **51**(2):226-246.
4. Russell DW: **The Enzymes, Regulation, and Genetics of Bile Acid Synthesis.** 2003, **72**(1):137-174.
5. Chiang JYL: **Bile acids: regulation of synthesis.** 2009, **50**(10):1955-1966.
6. Hofmann AF: **The Continuing Importance of Bile Acids in Liver and Intestinal Disease.** *Archives of Internal Medicine* 1999, **159**(22):2647-2658.
7. Houten SM, Watanabe M, Auwerx J: **Endocrine functions of bile acids.** *The EMBO journal* 2006, **25**(7):1419-1425.
8. Cohen BI, Matoba N, Mosbach EH, Ayyad N, Hakam K, Suh SO, McSherry CK: **Bile acids substituted in the 6 position prevent cholesterol gallstone formation in the hamster.** *Gastroenterology* 1990, **98**(2):397-405.
9. Gérard P: **Metabolism of Cholesterol and Bile Acids by the Gut Microbiota.** *Pathogens* 2014, **3**(1):14-24.
10. Smith LP, Nierstenhoefer M, Yoo SW, Penzias AS, Tobiasch E, Usheva A: **The bile acid synthesis pathway is present and functional in the human ovary.** *PLoS one* 2009, **4**(10):e7333-e7333.
11. Zhang M, Chiang JY: **Transcriptional regulation of the human sterol 12alpha-hydroxylase gene (CYP8B1): roles of hepatocyte nuclear factor 4alpha in mediating bile acid repression.** *The Journal of biological chemistry* 2001, **276**(45):41690-41699.
12. Bjorkhem I, Araya Z, Rudling M, Angelin B, Einarsson C, Wikvall K: **Differences in the regulation of the classical and the alternative pathway for bile acid synthesis in human liver. No coordinate regulation of CYP7A1 and CYP27A1.** *The Journal of biological chemistry* 2002, **277**(30):26804-26807.
13. Bjorkhem I: **Mechanism of degradation of the steroid side chain in the formation of bile acids.** *J Lipid Res* 1992, **33**(4):455-471.
14. Schwarz M, Lund EG, Setchell KD, Kayden HJ, Zerwekh JE, Bjorkhem I, Herz J, Russell DW: **Disruption of cholesterol 7alpha-hydroxylase gene in mice. II. Bile acid deficiency is overcome by induction of oxysterol 7alpha-hydroxylase.** *The Journal of biological chemistry* 1996, **271**(30):18024-18031.
15. Marrink SJ, Mark AE: **Molecular Dynamics Simulations of Mixed Micelles Modeling Human Bile.** *Biochemistry* 2002, **41**(17):5375-5382.
16. Mertens KL, Kalsbeek A, Soeters MR, Eggink HM: **Bile Acid Signaling Pathways from the Enterohepatic Circulation to the Central Nervous System.** *Frontiers in neuroscience* 2017, **11**:617-617.

17. Russell DW: **The enzymes, regulation, and genetics of bile acid synthesis.** *Annual review of biochemistry* 2003, **72**(1):137-174.
18. Chiang JYL: **Bile acids: regulation of synthesis.** *Journal of lipid research* 2009, **50**(10):1955-1966.
19. Small DM, Dowling RH, Redinger RN: **The Enterohepatic Circulation of Bile Salts.** *Archives of Internal Medicine* 1972, **130**(4):552-573.
20. Wang TY, Liu M, Portincasa P, Wang DQH: **New insights into the molecular mechanism of intestinal fatty acid absorption.** *European journal of clinical investigation* 2013, **43**(11):1203-1223.
21. Li T, Chiang JYL: **Regulation of bile acid and cholesterol metabolism by PPARs.** *PPAR research* 2009, **2009**.
22. Tu H, Okamoto AY, Shan B: **FXR, a bile acid receptor and biological sensor.** *Trends in cardiovascular medicine* 2000, **10**(1):30-35.
23. Kawamata Y, Fujii R, Hosoya M, Harada M, Yoshida H, Miwa M, Fukusumi S, Habata Y, Itoh T, Shintani Y *et al*: **A G protein-coupled receptor responsive to bile acids.** *The Journal of biological chemistry* 2003, **278**(11):9435-9440.
24. Ding L, Yang L, Wang Z, Huang W: **Bile acid nuclear receptor FXR and digestive system diseases.** *Acta pharmaceutica Sinica B* 2015, **5**(2):135-144.
25. Alvarez-Sola G, Uriarte I, Latasa MU, Fernandez-Barrena MG, Urtasun R, Elizalde M, Barcena-Varela M, Jiménez M, Chang HC, Barbero R *et al*: **Fibroblast growth factor 15/19 (FGF15/19) protects from diet-induced hepatic steatosis: development of an FGF19-based chimeric molecule to promote fatty liver regeneration.** 2017, **66**(10):1818-1828.
26. Lundasen T, Galman C, Angelin B, Rudling M: **Circulating intestinal fibroblast growth factor 19 has a pronounced diurnal variation and modulates hepatic bile acid synthesis in man.** *Journal of internal medicine* 2006, **260**(6):530-536.
27. Kusters A, Karpen SJ: **Bile acid transporters in health and disease.** *Xenobiotica; the fate of foreign compounds in biological systems* 2008, **38**(7-8):1043-1071.
28. Zhu C, Fuchs CD, Halilbasic E, Trauner M: **Bile acids in regulation of inflammation and immunity: friend or foe?** *Clin Exp Rheumatol* 2016, **34**(4 Suppl 98):25-31.
29. Pols TW, Nomura M, Harach T, Lo Sasso G, Oosterveer MH, Thomas C, Rizzo G, Gioiello A, Adorini L, Pellicciari R *et al*: **TGR5 activation inhibits atherosclerosis by reducing macrophage inflammation and lipid loading.** *Cell Metab* 2011, **14**(6):747-757.
30. Wang YD, Chen WD, Yu D, Forman BM, Huang W: **The G-protein-coupled bile acid receptor, Gpbar1 (TGR5), negatively regulates hepatic inflammatory response through antagonizing nuclear factor kappa light-chain enhancer of activated B cells (NF-kappaB) in mice.** *Hepatology (Baltimore, Md)* 2011, **54**(4):1421-1432.
31. Guo C, Xie S, Chi Z, Zhang J, Liu Y, Zhang L, Zheng M, Zhang X, Xia D, Ke Y *et al*: **Bile Acids Control Inflammation and Metabolic Disorder through Inhibition of NLRP3 Inflammasome.** *Immunity* 2016, **45**(4):802-816.
32. Pavlidis P, Powell N, Vincent RP, Ehrlich D, Bjarnason I, Hayee B: **Systematic review: bile acids and intestinal inflammation-luminal aggressors or regulators of mucosal defence?** *Alimentary pharmacology & therapeutics* 2015, **42**(7):802-817.
33. Li T, Apte U: **Bile Acid Metabolism and Signaling in Cholestasis, Inflammation, and**

- Cancer. *Advances in pharmacology (San Diego, Calif)* 2015, **74**:263-302.**
34. Duboc H, Rajca S, Rainteau D, Benarous D, Maubert MA, Quervain E, Thomas G, Barbu V, Humbert L, Despras G *et al*: **Connecting dysbiosis, bile-acid dysmetabolism and gut inflammation in inflammatory bowel diseases.** *Gut* 2013, **62**(4):531-539.
 35. Pavlidis P, Powell N, Vincent R, Ehrlich D, Bjarnason I, Hayee Bh: **Systematic review: Bile acids and intestinal inflammation-luminal aggressors or regulators of mucosal defence?**, vol. 42; 2015.
 36. Irving MH, Catchpole B: **ABC of colorectal diseases. Anatomy and physiology of the colon, rectum, and anus.** 1992, **304**(6834):1106-1108.
 37. Betts JG: **Anatomy & Physiology.** 2017, **Chapter3**:1118-1119.
 38. Phillips M, Patel A, Meredith P, Will O, Brassett C: **Segmental colonic length and mobility.** *Annals of the Royal College of Surgeons of England* 2015, **97**(6):439-444.
 39. Slack WW: **The anatomy, pathology, and some clinical features of diverticulitis of the colon.** 1962, **50**(220):185-190.
 40. Hussein MR, Musalam AO, Assiry MH, Eid RA, El Motawa AM, Gamel AM: **Histological and ultrastructural features of gastrointestinal basidiobolomycosis.** *Mycological research* 2007, **111**(Pt 8):926-930.
 41. Clevers H: **The intestinal crypt, a prototype stem cell compartment.** *Cell* 2013, **154**(2):274-284.
 42. Blachier F, de Sá Resende A, da Silva Fogaça Leite G, Vasques da Costa A, Lancha Junior AHJN: **Colon epithelial cells luminal environment and physiopathological consequences: impact of nutrition and exercise.** 2018, **43**(1):2.
 43. Barrasa JI, Olmo N, Lizarbe MA, Turnay J: **Bile acids in the colon, from healthy to cytotoxic molecules.** *Toxicology in vitro : an international journal published in association with BIBRA* 2013, **27**(2):964-977.
 44. Gerbe F, Legraverend C, Jay P: **The intestinal epithelium tuft cells: specification and function.** *Cellular and molecular life sciences : CMLS* 2012, **69**(17):2907-2917.
 45. Mosenthin R: **Physiology of Small and Large Intestine of Swine - Review.** *Asian-Australas J Anim Sci* 1998, **11**(5):608-619.
 46. Abraham C, Cho JH: **Inflammatory bowel disease.** *The New England journal of medicine* 2009, **361**(21):2066-2078.
 47. Conrad K, Roggenbuck D, Laass MW: **Diagnosis and classification of ulcerative colitis.** *Autoimmunity reviews* 2014, **13**(4-5):463-466.
 48. Laass MW, Roggenbuck D, Conrad K: **Diagnosis and classification of Crohn's disease.** *Autoimmunity reviews* 2014, **13**(4-5):467-471.
 49. Shizuma T: **Coexistence of Primary Biliary Cirrhosis and Inflammatory Bowel Disease,** vol. 03; 2014.
 50. Yang Y, Owyang C, Wu GD: **East Meets West: The Increasing Incidence of Inflammatory Bowel Disease in Asia as a Paradigm for Environmental Effects on the Pathogenesis of Immune-Mediated Disease.** *Gastroenterology* 2016, **151**(6):e1-e5.
 51. Benchimol EI, Mack DR, Guttman A, Nguyen GC, To T, Mojaverian N, Quach P, Manuel DG: **Inflammatory bowel disease in immigrants to Canada and their children: a population-based cohort study.** *The American journal of gastroenterology* 2015, **110**(4):553-563.

52. Murray KF: **Hepatobiliary associations with inflammatory bowel disease AU - Knight, Crystal.** *Expert Review of Gastroenterology & Hepatology* 2009, **3**(6):681-691.
53. Thorpe ME, Scheuer PJ, Sherlock S: **Primary sclerosing cholangitis, the biliary tree, and ulcerative colitis.** *Gut* 1967, **8**(5):435-448.
54. Ahmad J, Slivka A: **Hepatobiliary disease in inflammatory bowel disease.** *Gastroenterology clinics of North America* 2002, **31**(1):329-345.
55. Lever E, Balasubramanian K, Condon S, Wat BY: **Primary biliary cirrhosis associated with ulcerative colitis.** *The American journal of gastroenterology* 1993, **88**(6):945-947.
56. McCann P, Pramanik A: **Dysphagia and unexpected myasthenia gravis associated with primary biliary cirrhosis, ulcerative colitis and vitiligo.** *Journal of the American Geriatrics Society* 2004, **52**(8):1407-1408.
57. Monsen U, Sorstad J, Hellers G, Johansson C: **Extracolonic diagnoses in ulcerative colitis: an epidemiological study.** *The American journal of gastroenterology* 1990, **85**(6):711-716.
58. Schifter T, Lewinski UH: **Primary biliary cirrhosis and systemic lupus erythematosus. A rare association.** *Clin Exp Rheumatol* 1997, **15**(3):313-314.
59. Trivedi PJ, Corpechot C, Pares A, Hirschfield GM: **Risk stratification in autoimmune cholestatic liver diseases: Opportunities for clinicians and trialists.** *Hepatology (Baltimore, Md)* 2016, **63**(2):644-659.
60. Hohenester S, Oude-Elferink RP, Beuers U: **Primary biliary cirrhosis.** *Seminars in immunopathology* 2009, **31**(3):283-307.
61. Momah N, Lindor KD: **Primary biliary cirrhosis in adults.** *Expert Rev Gastroenterol Hepatol* 2014, **8**(4):427-433.
62. Jang HJ, Kim GS, Eun CS, Kae SH, Jang WY, Lee J: **Development of primary biliary cirrhosis in a patient with Crohn's disease: a case report and review of the literature.** *Digestive diseases and sciences* 2005, **50**(12):2335-2337.
63. Sisman G, Erzin Y, Bal K: **Primary biliary cirrhosis developing in a patient with Crohn's disease during the course of infliximab treatment: the first case in the literature.** *Journal of Crohn's & colitis* 2013, **7**(9):e397-398.
64. Elmore S: **Apoptosis: a review of programmed cell death.** *Toxicologic pathology* 2007, **35**(4):495-516.
65. Thompson CB: **Apoptosis in the pathogenesis and treatment of disease.** *Science* 1995, **267**(5203):1456-1462.
66. Allan A, Bristol JB, Williamson RC: **Crypt cell production rate in ulcerative proctocolitis: differential increments in remission and relapse.** *Gut* 1985, **26**(10):999-1003.
67. Hall PA, Coates PJ, Ansari B, Hopwood D: **Regulation of cell number in the mammalian gastrointestinal tract: the importance of apoptosis.** *Journal of cell science* 1994, **107** (Pt 12):3569-3577.
68. Danese S, Fiocchi C: **Etiopathogenesis of inflammatory bowel diseases.** *World journal of gastroenterology* 2006, **12**(30):4807-4812.
69. Souza HS, Tortori CJ, Castelo-Branco MT, Carvalho AT, Margallo VS, Delgado CF, Dines I, Elia CC: **Apoptosis in the intestinal mucosa of patients with inflammatory bowel disease: evidence of altered expression of FasL and perforin cytotoxic pathways.** *International journal of colorectal disease* 2005, **20**(3):277-286.

70. Peppelenbosch MP, van Deventer SJH: **T cell apoptosis and inflammatory bowel disease.** *Gut* 2004, **53**(11):1556-1558.
71. Staels B, Fonseca VA: **Bile acids and metabolic regulation: mechanisms and clinical responses to bile acid sequestration.** *Diabetes care* 2009, **32** Suppl 2(Suppl 2):S237-S245.
72. Roostae A, Benoit YD, Boudjadi S, Beaulieu J-F: **Epigenetics in Intestinal Epithelial Cell Renewal.** *Journal of cellular physiology* 2016, **231**(11):2361-2367.
73. Renes IB, Verburg M, Van Nispen DJ, Taminau JA, Buller HA, Dekker J, Einerhand AW: **Epithelial proliferation, cell death, and gene expression in experimental colitis: alterations in carbonic anhydrase I, mucin MUC2, and trefoil factor 3 expression.** *International journal of colorectal disease* 2002, **17**(5):317-326.
74. Sommerfeld A, Reinehr R, Haussinger D: **Bile acid-induced epidermal growth factor receptor activation in quiescent rat hepatic stellate cells can trigger both proliferation and apoptosis.** *The Journal of biological chemistry* 2009, **284**(33):22173-22183.
75. Sommerfeld A, Reinehr R, Häussinger D: **Bile acid-induced epidermal growth factor receptor activation in quiescent rat hepatic stellate cells can trigger both proliferation and apoptosis.** *The Journal of biological chemistry* 2009, **284**(33):22173-22183.
76. Cheng K, Raufman JP: **Bile acid-induced proliferation of a human colon cancer cell line is mediated by transactivation of epidermal growth factor receptors.** *Biochemical pharmacology* 2005, **70**(7):1035-1047.
77. Fang Y, Han SI, Mitchell C, Gupta S, Studer E, Grant S, Hylemon PB, Dent P: **Bile acids induce mitochondrial ROS, which promote activation of receptor tyrosine kinases and signaling pathways in rat hepatocytes.** *Hepatology (Baltimore, Md)* 2004, **40**(4):961-971.
78. Dvorak K, Payne CM, Chavarria M, Ramsey L, Dvorakova B, Bernstein H, Holubec H, Sampliner RE, Guy N, Condon A *et al.* **Bile acids in combination with low pH induce oxidative stress and oxidative DNA damage: relevance to the pathogenesis of Barrett's oesophagus.** *Gut* 2007, **56**(6):763-771.
79. Hegyi P, Maleth J, Walters JR, Hofmann AF, Keely SJ: **Guts and Gall: Bile Acids in Regulation of Intestinal Epithelial Function in Health and Disease.** *Physiological reviews* 2018, **98**(4):1983-2023.
80. Laukens D, Devisscher L, Van den Bossche L, Hindryckx P, Vandenbroucke RE, Vandewynckel YP, Cuvelier C, Brinkman BM, Libert C, Vandenabeele P *et al.* **Tauroursodeoxycholic acid inhibits experimental colitis by preventing early intestinal epithelial cell death.** *Lab Invest* 2014, **94**(12):1419-1430.
81. Chiang JYL: **Regulation of bile acid synthesis: pathways, nuclear receptors, and mechanisms.** *Journal of hepatology* 2004, **40**(3):539-551.
82. Yousef I, Mignault D, Tuchweber B: **Effect of complete sulfation of bile acids on bile formation: Role of conjugation and number of sulfate groups.** 1992, **15**(3):438-445.
83. Ward JBJ, Lajczak NK, Kelly OB, O' Dwyer AM, Giddam AK, Gabhann JN, Franco P, Tambuwala MM, Jefferies CA, Keely S *et al.* **Ursodeoxycholic acid and lithocholic acid exert anti-inflammatory actions in the colon.** 2017, **312**(6):G550-G558.
84. Sanchez Pozzi EJ, Crocenzi FA, Pellegrino JM, Catania VA, Luquita MG, Roma MG, Rodriguez Garay EA, Mottino AD: **Ursodeoxycholate reduces ethinylestradiol glucuronidation in the rat: role in prevention of estrogen-induced cholestasis.** *The*

- Journal of pharmacology and experimental therapeutics* 2003, **306**(1):279-286.
85. Alnouti Y: **Bile Acid Sulfation: A Pathway of Bile Acid Elimination and Detoxification.** *Toxicological Sciences* 2009, **108**(2):225-246.
 86. Javitt NB, Emerman S: **Effect of sodium tauroolithocholate on bile flow and bile acid excretion.** *The Journal of clinical investigation* 1968, **47**(5):1002-1014.
 87. Straub RH, Cutolo M: **Glucocorticoids and chronic inflammation.** *Rheumatology* 2016, **55**(suppl_2):ii6-ii14.
 88. Mizoguchi K, Ishige A, Takeda S, Aburada M, Tabira T: **Endogenous Glucocorticoids Are Essential for Maintaining Prefrontal Cortical Cognitive Function.** 2004, **24**(24):5492-5499.
 89. Oakley RH, Cidlowski JA: **The biology of the glucocorticoid receptor: new signaling mechanisms in health and disease.** *The Journal of allergy and clinical immunology* 2013, **132**(5):1033-1044.
 90. Tomlinson JW, Stewart PM: **Cortisol metabolism and the role of 11beta-hydroxysteroid dehydrogenase.** *Best practice & research Clinical endocrinology & metabolism* 2001, **15**(1):61-78.
 91. Hardy RS, Raza K, Cooper MS: **Endogenous glucocorticoids in inflammation: contributions of systemic and local responses.** *Swiss medical weekly* 2012, **142**:w13650.
 92. Braun TP, Marks DL: **The regulation of muscle mass by endogenous glucocorticoids.** *Frontiers in physiology* 2015, **6**:12-12.
 93. Aronson D: **Cortisol — Its Role in Stress, Inflammation, and Indications for Diet Therapy.** *Today' s Dietitian* 2009, **11**:38.
 94. Shibata S, Fujita T: **The kidneys and aldosterone/mineralocorticoid receptor system in salt-sensitive hypertension.** *Current hypertension reports* 2011, **13**(2):109-115.
 95. Funder JW: **Mineralocorticoid receptors in the central nervous system.** *The Journal of steroid biochemistry and molecular biology* 1996, **56**(1-6 Spec No):179-183.
 96. Kino T: **Glucocorticoid Receptor.** *Endotext* 2017.
 97. Gomez-Sanchez E, Gomez-Sanchez CE: **The multifaceted mineralocorticoid receptor.** *Comprehensive Physiology* 2014, **4**(3):965-994.
 98. Barnes PJ: **Anti-inflammatory actions of glucocorticoids: molecular mechanisms.** *Clinical science (London, England : 1979)* 1998, **94**(6):557-572.
 99. Coutinho AE, Chapman KE: **The anti-inflammatory and immunosuppressive effects of glucocorticoids, recent developments and mechanistic insights.** *Molecular and cellular endocrinology* 2011, **335**(1):2-13.
 100. Becker DE: **Basic and clinical pharmacology of glucocorticosteroids.** *Anesthesia progress* 2013, **60**(1):25-32.
 101. van der Velden VH: **Glucocorticoids: mechanisms of action and anti-inflammatory potential in asthma.** *Mediators of inflammation* 1998, **7**(4):229-237.
 102. Rhen T, Cidlowski JA: **Antiinflammatory Action of Glucocorticoids — New Mechanisms for Old Drugs.** 2005, **353**(16):1711-1723.
 103. Moghadam-Kia S, Werth VP: **Prevention and treatment of systemic glucocorticoid side effects.** *International journal of dermatology* 2010, **49**(3):239-248.
 104. Buttgereit F, Burmester GR, Straub RH, Seibel MJ, Zhou H: **Exogenous and endogenous glucocorticoids in rheumatic diseases.** *Arthritis and rheumatism* 2011, **63**(1):1-9.

105. Schacke H, Berger M, Rehwinkel H, Asadullah K: **Selective glucocorticoid receptor agonists (SEGRAs): novel ligands with an improved therapeutic index.** *Molecular and cellular endocrinology* 2007, **275**(1-2):109-117.
106. Schacke H, Docke WD, Asadullah K: **Mechanisms involved in the side effects of glucocorticoids.** *Pharmacology & therapeutics* 2002, **96**(1):23-43.
107. Pratt WB, Morishima Y, Murphy M, Harrell M: **Chaperoning of glucocorticoid receptors.** *Handbook of experimental pharmacology* 2006(172):111-138.
108. Echeverría PC, Mazaira G, Erlejman A, Gomez-Sanchez C, Pilipuk GP, Galigniana MD: **Nuclear Import of the Glucocorticoid Receptor-hsp90 Complex through the Nuclear Pore Complex Is Mediated by Its Interaction with Nup62 and Importin β .** 2009, **29**(17):4788-4797.
109. Kirschke E, Goswami D, Southworth D, Griffin PR, Agard DA: **Glucocorticoid receptor function regulated by coordinated action of the Hsp90 and Hsp70 chaperone cycles.** *Cell* 2014, **157**(7):1685-1697.
110. Buckingham JC: **Glucocorticoids: exemplars of multi-tasking.** *British journal of pharmacology* 2006, **147** Suppl 1:S258-268.
111. Hayashi R, Wada H, Ito K, Adcock IM: **Effects of glucocorticoids on gene transcription.** *European journal of pharmacology* 2004, **500**(1-3):51-62.
112. Dostert A, Heinzel T: **Negative glucocorticoid receptor response elements and their role in glucocorticoid action.** *Current pharmaceutical design* 2004, **10**(23):2807-2816.
113. Savory JG, Préfontaine GG, Lamprecht C, Liao M, Walther RF, Lefebvre YA, Haché RJ: **Glucocorticoid receptor homodimers and glucocorticoid-mineralocorticoid receptor heterodimers form in the cytoplasm through alternative dimerization interfaces.** *Molecular and cellular biology* 2001, **21**(3):781-793.
114. Herrlich P: **Cross-talk between glucocorticoid receptor and AP-1.** *Oncogene* 2001, **20**(19):2465-2475.
115. D Heitzer M, Wolf I, Sanchez E, Witchel S, B DeFranco D: **Glucocorticoid receptor physiology,** vol. 8; 2008.
116. Inaba H, Pui CH: **Glucocorticoid use in acute lymphoblastic leukaemia.** *The Lancet Oncology* 2010, **11**(11):1096-1106.
117. Liu T, Zhang L, Joo D, Sun S-C: **NF- κ B signaling in inflammation.** *Signal transduction and targeted therapy* 2017, **2**:17023.
118. Dolcet X, Llobet D, Pallares J, Matias-Guiu X: **NF- κ B in development and progression of human cancer.** *Virchows Archiv : an international journal of pathology* 2005, **446**(5):475-482.
119. Maneechotesuwan K, Yao X, Ito K, Jazrawi E, Usmani OS, Adcock IM, Barnes PJ: **Suppression of GATA-3 nuclear import and phosphorylation: a novel mechanism of corticosteroid action in allergic disease.** *PLoS medicine* 2009, **6**(5):e1000076-e1000076.
120. Baeuerle PA, Henkel T: **Function and activation of NF-kappa B in the immune system.** *Annual review of immunology* 1994, **12**:141-179.
121. Urban MB, Baeuerle PA: **The role of the p50 and p65 subunits of NF-kappa B in the recognition of cognate sequences.** *The New biologist* 1991, **3**(3):279-288.
122. Huxford T, Malek S, Ghosh G: **Structure and mechanism in NF-kappa B/I kappa B signaling.** *Cold Spring Harbor symposia on quantitative biology* 1999, **64**:533-540.

123. Moynagh PN: **The NF- κ B pathway**. 2005, **118**(20):4589-4592.
124. Sun SC: **CYLD: a tumor suppressor deubiquitinase regulating NF-kappaB activation and diverse biological processes**. *Cell death and differentiation* 2010, **17**(1):25-34.
125. Sun S-C: **The non-canonical NF- κ B pathway in immunity and inflammation**. *Nature reviews Immunology* 2017, **17**(9):545-558.
126. Oeckinghaus A, Ghosh S: **The NF-kappaB family of transcription factors and its regulation**. *Cold Spring Harbor perspectives in biology* 2009, **1**(4):a000034-a000034.
127. Li ZW, Chu W, Hu Y, Delhase M, Deerinck T, Ellisman M, Johnson R, Karin M: **The IKKbeta subunit of IkappaB kinase (IKK) is essential for nuclear factor kappaB activation and prevention of apoptosis**. *The Journal of experimental medicine* 1999, **189**(11):1839-1845.
128. Lawrence T: **The nuclear factor NF-kappaB pathway in inflammation**. *Cold Spring Harbor perspectives in biology* 2009, **1**(6):a001651-a001651.
129. Senftleben U, Cao Y, Xiao G, Greten FR, Krahn G, Bonizzi G, Chen Y, Hu Y, Fong A, Sun SC *et al*: **Activation by IKKalpha of a second, evolutionary conserved, NF-kappa B signaling pathway**. *Science* 2001, **293**(5534):1495-1499.
130. Chen X, Kandasamy K, Srivastava RK: **Differential roles of RelA (p65) and c-Rel subunits of nuclear factor kappa B in tumor necrosis factor-related apoptosis-inducing ligand signaling**. *Cancer research* 2003, **63**(5):1059-1066.
131. Calzado MA, Bacher S, Schmitz ML: **NF-kappaB inhibitors for the treatment of inflammatory diseases and cancer**. *Current medicinal chemistry* 2007, **14**(3):367-376.
132. Camandola S, Mattson MP: **NF-kappa B as a therapeutic target in neurodegenerative diseases**. *Expert opinion on therapeutic targets* 2007, **11**(2):123-132.
133. O'Sullivan B, Thompson A, Thomas R: **NF-kappa B as a therapeutic target in autoimmune disease**. *Expert opinion on therapeutic targets* 2007, **11**(2):111-122.
134. Balaji S, Ahmed M, Lorence E, Yan F, Nomie K, Wang M: **NF- κ B signaling and its relevance to the treatment of mantle cell lymphoma**. *Journal of Hematology & Oncology* 2018, **11**(1):83.
135. Gronemeyer H, Gustafsson JA, Laudet V: **Principles for modulation of the nuclear receptor superfamily**. *Nature reviews Drug discovery* 2004, **3**(11):950-964.
136. Chivers JE, Gong W, King EM, Seybold J, Mak JC, Donnelly LE, Holden NS, Newton R: **Analysis of the Dissociated Steroid RU24858 Does Not Exclude a Role for Inducible Genes in the Anti-Inflammatory Actions of Glucocorticoids**. 2006, **70**(6):2084-2095.
137. Newton R: **Molecular mechanisms of glucocorticoid action: what is important?** 2000, **55**(7):603-613.
138. Belvisi MG, Wicks SL, Battram CH, Bottoms SE, Redford JE, Woodman P, Brown TJ, Webber SE, Foster ML: **Therapeutic benefit of a dissociated glucocorticoid and the relevance of in vitro separation of transrepression from transactivation activity**. *Journal of immunology (Baltimore, Md : 1950)* 2001, **166**(3):1975-1982.
139. Humphrey EL, Williams JH, Davie MW, Marshall MJ: **Effects of dissociated glucocorticoids on OPG and RANKL in osteoblastic cells**. *Bone* 2006, **38**(5):652-661.
140. Capper CP, Rae JM, Auchus RJ: **The Metabolism, Analysis, and Targeting of Steroid Hormones in Breast and Prostate Cancer**. *Hormones & cancer* 2016, **7**(3):149-164.
141. Rauner M, Hofbauer LC: **Minireview: Live and Let Die: Molecular Effects of Glucocorticoids on Bone Cells**. *Molecular Endocrinology* 2009, **23**(10):1525-1531.

142. Coghlan MJ, Jacobson PB, Lane B, Nakane M, Lin CW, Elmore SW, Kym PR, Luly JR, Carter GW, Turner R *et al.* **A novel antiinflammatory maintains glucocorticoid efficacy with reduced side effects.** *Molecular endocrinology (Baltimore, Md)* 2003, **17**(5):860-869.
143. Rosen J, Miner JN: **The search for safer glucocorticoid receptor ligands.** *Endocrine reviews* 2005, **26**(3):452-464.
144. Heathcote EJ: **Management of primary biliary cirrhosis. The American Association for the Study of Liver Diseases practice guidelines.** *Hepatology (Baltimore, Md)* 2000, **31**(4):1005-1013.
145. Biancone L, Michetti P, Travis S, Escher JC, Moser G, Forbes A, Hoffmann JC, Dignass A, Gionchetti P, Jantschek G *et al.* **European evidence-based Consensus on the management of ulcerative colitis: Special situations.** *Journal of Crohn's & colitis* 2008, **2**(1):63-92.
146. Farraye FA, Odze RD, Eaden J, Itzkowitz SH, McCabe RP, Dassopoulos T, Lewis JD, Ullman TA, James T, 3rd, McLeod R *et al.* **AGA medical position statement on the diagnosis and management of colorectal neoplasia in inflammatory bowel disease.** *Gastroenterology* 2010, **138**(2):738-745.
147. Ward JBJ, Lajczak NK, Kelly OB, O'Dwyer AM, Giddam AK, Ni Gabhann J, Franco P, Tambuwala MM, Jefferies CA, Keely S *et al.* **Ursodeoxycholic acid and lithocholic acid exert anti-inflammatory actions in the colon.** *American journal of physiology Gastrointestinal and liver physiology* 2017, **312**(6):G550-g558.
148. Ikegami T, Matsuzaki Y, Fukushima S, Shoda J, Olivier JL, Bouscarel B, Tanaka N: **Suppressive effect of ursodeoxycholic acid on type IIA phospholipase A2 expression in HepG2 cells.** *Hepatology (Baltimore, Md)* 2005, **41**(4):896-905.
149. Tanaka H, Makino I: **Ursodeoxycholic acid-dependent activation of the glucocorticoid receptor.** *Biochemical and biophysical research communications* 1992, **188**(2):942-948.
150. Tanaka H, Makino Y, Miura T, Hirano F, Okamoto K, Komura K, Sato Y, Makino I: **Ligand-independent activation of the glucocorticoid receptor by ursodeoxycholic acid. Repression of IFN-gamma-induced MHC class II gene expression via a glucocorticoid receptor-dependent pathway.** *Journal of immunology (Baltimore, Md : 1950)* 1996, **156**(4):1601-1608.
151. Weitzel C, Stark D, Kullmann F, Scholmerich J, Holstege A, Falk W: **Ursodeoxycholic acid induced activation of the glucocorticoid receptor in primary rat hepatocytes.** *European journal of gastroenterology & hepatology* 2005, **17**(2):169-177.
152. Copaci I, Micu L, Iliescu L, Voiculescu M: **New therapeutic indications of ursodeoxycholic acid.** *Romanian journal of gastroenterology* 2005, **14**(3):259-266.
153. Sharma R, Prichard D, Majer F, Byrne A-M, Kelleher D, Long A, Gilmer JF: **Ursodeoxycholic Acid Amides As Novel Glucocorticoid Receptor Modulators.** *Journal of medicinal chemistry* 2011, **54**(1):122-130.
154. Festa C, Renga B, D'Amore C, Sepe V, Finamore C, De Marino S, Carino A, Cipriani S, Monti MC, Zampella A *et al.* **Exploitation of cholane scaffold for the discovery of potent and selective farnesoid X receptor (FXR) and G-protein coupled bile acid receptor 1 (GP-BAR1) ligands.** *Journal of medicinal chemistry* 2014, **57**(20):8477-8495.
155. Beuers U, Trauner M, Jansen P, Poupon R: **New paradigms in the treatment of hepatic cholestasis: from UDCA to FXR, PXR and beyond.** *Journal of hepatology* 2015, **62**(1

- Suppl):S25-37.
156. Pellicciari R, Gioiello A, Macchiarulo A, Thomas C, Rosatelli E, Natalini B, Sardella R, Pruzanski M, Roda A, Pastorini E *et al.* **Discovery of 6 α -ethyl-23(S)-methylcholic acid (S-EMCA, INT-777) as a potent and selective agonist for the TGR5 receptor, a novel target for diabetes.** *Journal of medicinal chemistry* 2009, **52**(24):7958-7961.
 157. Majer F: **Synthetic photophysical and biological studies into new tools for investigating bile acid disposition and toxicity.** *School of Pharmacy and Pharmaceutical Sciences, Trinity College Dublin* 2013:323.
 158. Gavin JK: **Chemical Biology Studies on Ursodeoxycholic Acid and Azo Prodrugs.** *School of Pharmacy and Pharmaceutical Sciences, Trinity College Dublin* 2016:196-224.
 159. Liu Y, Peterson DA, Kimura H, Schubert D: **Mechanism of cellular 3-(4,5-dimethylthiazol-2-yl)-2,5-diphenyltetrazolium bromide (MTT) reduction.** *J Neurochem* 1997, **69**(2):581-593.
 160. Markaki AE: **AlamarBlue Assay for Assessment of Cell Proliferation using the FLUOstar OPTIMA.**
 161. Ward JBJ, Lajczak NK, Kelly OB, O' Dwyer AM, Giddam AK, Ní Gabhann J, Franco P, Tambuwala MM, Jefferies CA, Keely S *et al.* **Ursodeoxycholic acid and lithocholic acid exert anti-inflammatory actions in the colon.** *American Journal of Physiology-Gastrointestinal and Liver Physiology* 2017, **312**(6):G550-G558.
 162. Kim SJ, Ko W-K, Jo M-J, Arai Y, Choi H, Kumar H, Han I-B, Sohn S: **Anti-inflammatory effect of Tauroursodeoxycholic acid in RAW 264.7 macrophages, Bone marrow-derived macrophages, BV2 microglial cells, and spinal cord injury.** *Scientific Reports* 2018, **8**(1):3176.
 163. Vang S, Longley K, Steer CJ, Low WC: **The Unexpected Uses of Urso- and Tauroursodeoxycholic Acid in the Treatment of Non-liver Diseases.** *Global advances in health and medicine* 2014, **3**(3):58-69.
 164. Romero-Ramírez L, Nieto-Sampedro M, Yanguas-Casás N: **Tauroursodeoxycholic acid: more than just a neuroprotective bile conjugate.** *Neural regeneration research* 2017, **12**(1):62-63.
 165. Butler JJS: **The behavior of antigens and antibodies immobilized on a solid phase.** 1992, **1**:208-259.
 166. O'Connor K: **The ELISA Guidebook, Volume 149, Methods in Molecular Biology.** John R. Crowther, vol. 291; 2001.
 167. Lajczak NK, Saint-Criq V, O' Dwyer AM, Perino A, Adorini L, Schoonjans K, Keely SJ: **Bile acids deoxycholic acid and ursodeoxycholic acid differentially regulate human β -defensin-1 and -2 secretion by colonic epithelial cells.** 2017, **31**(9):3848-3857.